COMPARISON OF BACKWARD AND FORWARD CONSTRUCTION STAGE ANALYSIS PROCEDURES OF CABLE STAYED BRIDGES

A THESIS SUBMITTED TO
THE GRADUATE SCHOOL OF NATURAL AND APPLIED SCIENCES
OF
MIDDLE EAST TECHNICAL UNIVERSITY

BY

SERKAN ÖZEN

IN PARTIAL FULFILLMENT OF THE REQUIREMENTS
FOR
THE DEGREE OF MASTER OF SCIENCE
IN
CIVIL ENGINEERING

DECEMBER 2023

Approval of the thesis:

COMPARISON OF BACKWARD AND FORWARD CONSTRUCTION STAGE ANALYSIS PROCEDURES OF CABLE STAYED BRIDGES

submitted by **SERKAN ÖZEN** in partial fulfillment of the requirements for the degree of **Master of Science** i**n Civil Engineering, Middle East Technical University** by,

Prof. Dr. Halil Kalıpçılar
Dean, Graduate School of **Natural and Applied Sciences** _____

Prof. Dr. Erdem Canbay
Head of the Department, **Civil Engineering** _____

Prof. Dr. Özgür Kurç
Supervisor, **Civil Engineering, METU** _____

Examining Committee Members:

Prof. Dr. Afşin Sarıtaş
Civil Engineering, METU _____

Prof. Dr. Özgür Kurç
Civil Engineering, METU _____

Prof. Dr. Yalın Arıcı
Civil Engineering, METU _____

Prof. Dr. Alp Caner
Civil Engineering, METU _____

Assist. Prof. Dr. Feyza Soysal Albostan
Civil Engineering, Çankaya University _____

Date: 01.12.2023

I hereby declare that all information in this document has been obtained and presented in accordance with academic rules and ethical conduct. I also declare that, as required by these rules and conduct, I have fully cited and referenced all material and results that are not original to this work.

Name Last name : Özen, Serkan

Signature :

ABSTRACT

COMPARISON OF BACKWARD AND FORWARD CONSTRUCTION STAGE ANALYSIS PROCEDURES OF CABLE STAYED BRIDGES

Özen, Serkan
Master of Science, Civil Engineering
Supervisor: Prof. Dr. Özgür Kurç

December 2023, 137 pages

In recent years, many cable-stayed bridges have been designed and built worldwide. This type of bridge design necessitates an especially good understanding of structural analysis. Firstly, the bridge is designed according to the finished configuration, and cable forces are determined. Afterwards, construction stage analysis is done to find cable forces in each construction stage. In the end, these determined cable forces in each construction stage should satisfy the desired cable forces, internal forces of the girder and pylons, and desired shape of the whole structure at the finished configuration. The analysis to determine these forces can be done in two different ways, one is backward, and the other one is forward analysis. Backward analysis starts from the finished configuration and goes back to the first stage by dismantling the structure piece by piece. In the backward analysis time dependent material properties can only be taken into account partially, and therefore they should be calculated and inserted into the analysis manually. In the forward construction stage analysis, the bridge is analyzed starting from the initial configuration and continues exactly as it is in the actual construction process. Time-dependent properties can be taken into account with small time steps in this analysis type more correctly. This thesis will investigate the forward and backward analysis of an actual cable-stayed

bridge with a concrete superstructure being constructed recently in Türkiye. The differences and similarities of the results of these two different analysis methods are compared by two different software, Midas Civil and Larsa 4D were utilized for structural analysis and their differences are also discussed .

Keywords: Cable Stayed Bridge, Concrete Deck Section, Construction Stage Analysis, Backward and Forward Analysis, Time-Dependent Material Properties

ÖZ

EĞİK ASKILI KÖPRÜLERİN İLERİYE VE GERİYE DOĞRU İNŞAAT AŞAMALARI ANALİZ PROSEDÜRLERİNİN KARŞILAŞTIRILMASI

Özen, Serkan
Yüksek Lisans, İnşaat Mühendisliği
Tez Yöneticisi: Prof. Dr. Özgür Kurç

Aralık 2023, 137 sayfa

Son yıllarda tüm dünyada çok sayıda gergin eğik askılı köprü tasarlanmakta ve inşa edilmektedir. Bu tür köprü tasarımı, özellikle yapısal analizin iyi anlaşılmasını gerektirir. İlk olarak, bitmiş konfigürasyona göre köprü tasarlanır ve kablo kuvvetleri belirlenir. Daha sonra her inşaat aşamasındaki kablo kuvvetlerini bulmak için inşaat aşaması analizi yapılır. Sonunda, her inşaat aşamasında belirlenen bu kablo kuvvetleri, istenen kablo kuvvetlerini, üstyapı ve pilonların iç kuvvetlerini ve bitmiş konfigürasyonda tüm yapının istenen şeklini sağlamalıdır. Bu inşaat aşaması analizi, biri geriye doğru, diğeri ileriye doğru analiz olmak üzere iki farklı şekilde yapılabilir. Geriye doğru analiz, bitmiş konfigürasyondan başlar ve yapıyı parça parça sökerek ilk aşamaya geri döner. Geriye doğru analizde zamana bağlı malzeme özellikleri dikkate alınamaz ve bu nedenle manuel olarak hesaplanmalı ve analize dahil edilmelidir. İleriye doğru inşaat aşaması analizinde, köprü ilk konfigürasyondan başlayarak analiz edilir ve aynen gerçek yapım sürecinde olduğu gibi devam eder. Zamana bağlı özellikler bu analiz türünde küçük zaman adımları ile daha doğru bir şekilde hesaba katılabilir. Bu tezde, Türkiye'de yakın zamanda inşa edilmekte olan gerçek bir betonarme üstyapılı gergin eğik askılı köprü ileriye ve geriye doğru analizi

incelenecek ve bu iki analiz yönteminin sonuçlarının farklılık ve benzerlikleri iki farklı analiz programı Midas Civil ve Larsa 4D kullanılarak karşılaştırılacaktır ve ayrıca bu iki program arasındaki farklara da değinilecektir.

Anahtar Kelimeler: Kablo Askılı Köprü, Betonarme Köprü Üstyapısı, İnşaat Aşaması Analizi, Geriye Doğru Ve İleriye Doğru Analiz, Zamana Bağlı Malzeme Özellikleri

To my family,

To my wife,

To my beloved son Yüksel Yavuz and

To my daughter Zeynep

ACKNOWLEDGMENTS

I want to express my deepest gratitude to my supervisor Prof. Dr. Özgür Kurç, for his guidance, great help, advice, criticism, encouragement, and insight throughout the research.

I want to thank my father and mother for all their support throughout my life.

I want to thank my wife, whom I love and who was always with me through this study and my life. Thank you for all your support, my precious.

Lastly, sorry, my son Yüksel Yavuz for the time I could not spend with you during my thesis studies. I dedicate this thesis to you.

TABLE OF CONTENTS

ABSTRACT v

ÖZ vii

ACKNOWLEDGMENTS x

TABLE OF CONTENTS xi

LIST OF TABLES xv

LIST OF FIGURES xvi

LIST OF ABBREVIATIONS xxii

LIST OF SYMBOLS xxiii

1 INTRODUCTION 1

1.1 Literature Review 2

1.2 Objective and Scope 5

2 CABLE STAYED BRIDGES 9

2.1 History of Cable Stayed Bridges 9

2.2 Cable Stayed Bridge Types 12

2.3 Elements of Cable Stayed Bridges 19

2.3.1 Stay Cables 19

2.3.1.1 Parallel Strand Cables 20

2.3.2 Cable Anchorages 21

3 ANALYSIS OF CABLE STAYED BRIDGES 25

3.1 General Dimensioning Rules for CSB 25

3.1.1 The Ratio of Side Span to Main Span 25

3.1.2 The Ratio of Tower to Main Span and Stiffness of Towers 27

3.2 Preliminary Basic Calculations and Flow of Forces in CSB 27
3.2.1 Flow of Forces in A Cable Stayed Bridge 28
3.2.2 Preliminary Basic Calculations 29
3.3 Cable Force Determination (Final Stage) 32
3.3.1 Concrete Deck Bridges 32
3.3.2 Steel Deck Bridges 34
3.3.3 Composite Deck Bridges 35
3.4 Construction Stage Analysis Procedures 36
3.4.1 Backward Construction Stage Analysis 36
3.4.2 Forward Construction Stage Analysis 40
3.4.3 Construction Stage Analysis of Composite Deck Bridges 41
3.5 Static Analysis of Cables 46
4 CONCRETE CABLE-STAYED STRUCTURE 53
4.1 Comparison of Larsa4D and Midas Civil 53
4.1.1 Analysis of a Cable 53
4.1.2 Geometric Nonlinearity With Large Displacement 55
4.1.3 Match Cast Approach 56
4.2 Information About the Structure 57
4.3 Desired Final Configuration of the Structure 58
4.4 Analysis of the Structure 59
4.4.1 Backward Construction Stage Analysis 59
4.4.2 Forward Construction Stage Analysis 60
4.4.3 Linear Truss Element 62

4.4.3.1 Comparison of Analysis Methods Results (Without Time-Dependent Material Properties) (Linear Truss Element) 62
4.4.3.2 Comparison of Analysis Methods Results (With Time-Dependent Material Properties) (Linear Truss Element) 66
4.4.4 Ernst Truss Element 70
4.4.4.1 Comparison of Analysis Methods Results (Without Time-Dependent Material Properties) (Ernst Truss Element) 71
4.4.4.2 Comparison of Analysis Methods Results (With Time-Dependent Material Properties) (Ernst Truss Element) 74
4.4.5 Cable Element 78
4.4.5.1 Comparison of Analysis Methods Results (Without Time-Dependent Material Properties) (Catenary Cable Element) 79
4.4.5.2 Comparison of Analysis Methods Results (With Time-Dependent Material Properties) (Catenary Cable Element) 82
4.5 Effects of Time Step Size on Time-Dependent Material Properties and Their Impact on the Results 88
4.6 Comparison of Different Cable Element Type Results 90
5 CONCRETE CABLE-STAYED BRIDGE 93
5.1 Information About the Structure 93
5.2 Desired Final Configuration of the Structure 95
5.3 Analysis of the Structure 96
5.3.1 Backward Construction Stage Analysis 96
5.3.2 Forward Construction Stage Analysis 99
5.3.3 Comparison of Backward and Forward Construction Stage Analysis 100
6 SUMMARY AND CONCLUSIONS 107

REFERENCES 113

APPENDICES 115

A. Node Numbering of Basic Concrete Cable-Stayed Structure 116

B. Calculation of Modulus of Elasticity, Development of Strength and Modulus of Elasticity with Time, Creep Coefficient and Shrinkage Strain of Concrete Cable-Stayed Structure 117

C. Calculation of Temperature Loading Values of Concrete Cable-Stayed Structure To Take into Account Time-Dependent Material Properties 124

D. Cross Sectional Properties of Girder and Cables 125

E. Calculation of Modulus of Elasticity, Development of Strength and Modulus of Elasticity with Time, Creep Coefficient and Shrinkage Strain of Concrete Cable-Stayed Bridge 130

F. Calculation of Temperature Loading Values of Concrete Cable-Stayed Bridge To Take into Account Time-Dependent Material Properties in Backward Analysis for One Day Duration 137

LIST OF TABLES

TABLES

Table 2.1 Number of Cable Stayed Bridges Until 2000 (Svensson, 2012) 12
Table 4.1 Properties of Cables (Vu et al., 2012)..... 54
Table 4.2 Comparison of Displacement Results..... 55
Table 4.3 Comparison of Analysis Results (20 Elements) 56
Table 4.4 Comparison of Analysis Results (1 Element)..... 56
Table 4.5 Comparison of Analysis Results..... 57
Table 4.6 Cross Sectional Properties of Girder and Cables..... 58
Table 4.7 Material Properties of Girder and Cables 58
Table 5.1 Material Properties of Pylon, Superstructure and Cable..... 95

LIST OF FIGURES

FIGURES

Figure 1.1. Optimal Bridge Types and Span Lengths in Feet (http://hotrails.net/2014/09/) 1
Figure 1.2. Distribution of Forces in Cable Stayed Bridges (Svensson, 2012) 2
Figure 2.1 Eye Bar Supported Bridge Drawing By Verantius, 1617 (Svensson, 2012) 9
Figure 2.2 Kings Meadow Bridge, 1817 (Svensson, 2012) 10
Figure 2.3 Brooklyn Bridge (https://www.nyc.gov) 11
Figure 2.4 Development of Main Span Lengths of Cable Stayed Bridges Through Years (Svensson, 2012) 11
Figure 2.5 Cost Versus Center Span Length of Bridge Types (Svensson, 2012) 13
Figure 2.6 Critical Flutter Wind Speed Comparison (Svensson, 2012) 13
Figure 2.7 Fan, Harp and Semi Fan Type Cable Arrangements Respectively (Leonhardt & Zellner, 1980) 14
Figure 2.8 Two Cables Plane Pylon Shapes (Leonhardt & Zellner, 1980) 15
Figure 2.9 One Cable Plane Pylon Shapes (Leonhardt & Zellner, 1980) 15
Figure 2.10 Steel Cross Sections (Svensson, 2012) 17
Figure 2.11 Concrete Cross Sections (Svensson, 2012) 18
Figure 2.12 Steel Composite Cross Sections (Svensson, 2012) 19
Figure 2.13 Seven Wire Strand (Gimsing & Georgakis, 2012) 20
Figure 2.14 Mechanical Properties of Cable Stays (Svensson, 2012) 20
Figure 2.15 Typical Strand Cable (DSI) 21
Figure 2.16 Strand Wedge and Typical Layout Section of Strands in A Cable (Svensson, 2012) 21
Figure 2.17 Anchorage of Cables to Concrete Pylon with Prestressing Tendons and to the Girder (Leonhardt & Zellner, 1980) 22
Figure 2.18 Anchorage of Steel Beam by Web Extension and Anchorage of Cable to Pylon with Steel Beam (Svensson, 2012) 23

Figure 2.19 Typical Layout of a Pendulum (Svensson, 2012)..... 23
Figure 3.1 Diagram for Determining Optimum Ratio of Side to Main Span (Leonhardt & Zellner, 1980)..... 26
Figure 3.2 Quantity of Cable Steel as a Function of Relative Height of Tower (Leonhardt & Zellner, 1980)..... 27
Figure 3.3 Structural Behavior of a Classical Cable Stayed Bridge with Three Spans (Virlogeux, 2001)..... 29
Figure 3.4 Structural Behavior of a Classical Cable Stayed Bridge with Intermediate Supports in Side Spans (Virlogeux, 2001)..... 30
Figure 3.5 Normal Forces in a Hinged System (Svensson, 2012)..... 31
Figure 3.6 Largest Normal Forces in Beam and Pylon and Approximation of Largest Beam Forces (Svensson, 2012)..... 32
Figure 3.7 Beam on Continuous Supports Approach (El Shenawy, 2013)..... 33
Figure 3.8 Cable Forces and Their Effects on Creep (El Shenawy, 2013)..... 34
Figure 3.9 Run of Moments of Steel and Concrete Deck Sections (Svensson, 2012)..... 35
Figure 3.10 Dismantling of Symmetric Bridge (Svensson, 2012)..... 38
Figure 3.11 Dismantling by Using Derrick (Svensson, 2012)..... 39
Figure 3.12 Cases of Cable Tensioning (Schlaich, 2001)..... 42
Figure 3.13 Creep and Shrinkage of the Composite Section (El Shenawy, 2013) 43
Figure 3.14 Initial Force Determination (Schlaich, 2001)..... 45
Figure 3.15 General Definitions of a Stay Cable (Gimsing & Georgakis, 2011).. 46
Figure 3.16 Force Deflection Curves of Truss and Cable Element (Gimsing & Georgakis, 2011)..... 47
Figure 3.17 Tangent and Secant Stiffness (Gimsing & Georgakis, 2011)..... 47
Figure 3.18 Cable and Equivalent Beam Forces and Reactions (Gimsing & Georgakis, 2011)..... 48
Figure 3.19 Change of Effective Elasticity Modulus with Respect to Cable Horizontal Length and Sag, (Leonhardt & Zellner, 1980)..... 49

Figure 3.20 Real and Idealized Equivalent Truss Stay Cable Element (Gimsing & Georgakis, 2011) 51
Figure 3.21 Error Introduced in to the Calculations by Using T instead of N_t (Gimsing & Georgakis, 2011) 51
Figure 4.1 Cable Element Geometric Properties and Loading Positions (Vu et al., 2012) 54
Figure 4.2 Beam Element Bent About Its Tip (Roark & Young, 1975) 55
Figure 4.3 General Dimensions of the Structure 57
Figure 4.4 Target Moment Diagram of the Structure at Time Infinity 59
Figure 4.5 Backward Construction Stage Analysis Steps 60
Figure 4.6 Casting Types of the Newly Erected Segment (Midas Civil) 61
Figure 4.7 Forward Construction Stage Analysis Steps 61
Figure 4.8 Cable 1 Tension Force Change (Truss Element) 62
Figure 4.9 Cable 2 Tension Force Change (Truss Element) 63
Figure 4.10 Cable 3 Tension Force Change (Truss Element) 63
Figure 4.11 Cable 4 Tension Force Change (Truss Element) 64
Figure 4.12 Backward, Forward Analysis and Target Moment Diagram (Truss Element) 65
Figure 4.13 Backward and Forward Analysis Moment Diagram (P-Δ) (Truss Element) 66
Figure 4.14 Cable 1 Tension Force Change with Time-Dependent Material (Truss Element) 67
Figure 4.15 Cable 2 Tension Force Change with Time-Dependent Material (Truss Element) 67
Figure 4.16 Cable 3 Tension Force Change with Time-Dependent Material (Truss Element) 68
Figure 4.17 Cable 4 Tension Force Change with Time-Dependent Material (Truss Element) 68
Figure 4.18 Backward, Forward Analysis and Target Moment Diagram with Time-Dependent Material (Truss Element) 69

Figure 4.19 Backward, Forward Analysis and Target Moment Diagram with Time-Dependent Material at Time Infinity t=25000 days (Truss Element) 70
Figure 4.20 Cable 1 Tension Force Change (Ernst Truss Element) 71
Figure 4.21 Cable 2 Tension Force Change (Ernst Truss Element) 72
Figure 4.22 Cable 3 Tension Force Change (Ernst Truss Element) 72
Figure 4.23 Cable 4 Tension Force Change (Ernst Truss Element) 73
Figure 4.24 Backward and Forward Analysis Moment Diagram (Ernst Truss Element) 74
Figure 4.25 Cable 1 Tension Force Change with Time-Dependent Material (Ernst Truss Element) 75
Figure 4.26 Cable 2 Tension Force Change with Time-Dependent Material (Ernst Truss Element) 75
Figure 4.27 Cable 3 Tension Force Change with Time-Dependent Material (Ernst Truss Element) 76
Figure 4.28 Cable 4 Tension Force Change with Time-Dependent Material (Ernst Truss Element) 76
Figure 4.29 Backward, Forward Analysis and Target Moment Diagram with Time-Dependent Material Effects (Ernst Truss Element) 77
Figure 4.30 Backward, Forward Analysis and Target Moment Diagram with Time-Dependent Material at Time Infinity t=25000 days (Ernst Truss Element) 78
Figure 4.31 Cable 1 Tension Force Change (Catenary Cable Element) 80
Figure 4.32 Cable 2 Tension Force Change (Catenary Cable Element) 80
Figure 4.33 Cable 3 Tension Force Change (Catenary Cable Element) 81
Figure 4.34 Cable 4 Tension Force Change (Catenary Cable Element) 81
Figure 4.35 Backward and Forward Analysis Moment Diagram (Catenary Cable Element) 82
Figure 4.36 Cable 1 Tension Force Change with Time-Dependent Material (Catenary Cable Element) 83
Figure 4.37 Cable 2 Tension Force Change with Time-Dependent Material (Catenary Cable Element) 83

Figure 4.38 Cable 3 Tension Force Change with Time-Dependent Material (Catenary Cable Element) 84
Figure 4.39 Cable 4 Tension Force Change with Time-Dependent Material (Catenary Cable Element) 84
Figure 4.40 Backward, Forward Analysis Moment Diagram with Time-Dependent Material (Catenary Cable Element) 85
Figure 4.41 Backward, Forward Analysis and Target Moment Diagram with Time-Dependent Material at Time Infinity t=25000 days (Catenary Cable Element) 86
Figure 4.42 Backward, Forward Analysis Deformation Graph at Construction Finish (Catenary Cable Element) 87
Figure 4.43 Backward, Forward Analysis Deformation Graph at Time Infinity (Catenary Cable Element) 87
Figure 4.44 Creep Coefficient For 0.5 day and 1 day 88
Figure 4.45 Shrinkage Strain For 0.5 day and 1 day 89
Figure 4.46 Moment Diagrams For 0.5 Day, 1 Day and 10 Days' Time Steps 90
Figure 4.47 Forward Analysis with Time-Dependent Material Properties at Finish of Construction, for Linear Truss, Ernst Truss and Elastic Catenary Element 91
Figure 4.48 Forward Analysis and Target Moment Diagram with Time-Dependent Material Properties at Time Infinity t=25000 days, for Linear Truss, Ernst Truss and Elastic Catenary Element 92
Figure 5.1 General View of the Bridge 93
Figure 5.2 General Dimensions of the Structure 94
Figure 5.3 Balanced Cantilever Construction of the Bridge 94
Figure 5.4 Target Moment Diagram of the Bridge Superstructure 96
Figure 5.5 Backward Construction Stage Analysis Procedure 97
Figure 5.6 Moment Diagram at Which Temperature Given in Backward Direction 98
Figure 5.7 Moment Diagram at which Key Segment Was Dismantled in Backward Direction 99
Figure 5.8 Moment Diagram Before Support Was Jacked Down 100

Figure 5.9 Moment Diagram After Support Was Jacked Down 101
Figure 5.10 Moment Diagram After Key Segment Closed 102
Figure 5.11 Moment Diagram at Time Infinity 103
Figure 5.12 Moment Diagram at Time Infinity for 1 Day and 7 Days 104
Figure 5.13 Change of Tension Force in Cable (460) During Construction Stages 105
Figure 5.14 Change of Deflection At The Tip of The Pylon During Construction Stages 106

LIST OF ABBREVIATIONS

ABBREVIATIONS

CSB: Cable Stayed Bridge

LIST OF SYMBOLS

SYMBOLS

$\Delta\sigma$ = Allowable fatigue stress range

f_u= Ultimate tensile strength of cable

E= Modulus of elasticity

H= Height of the section

B= Width of the section

Asy = Shear area in global y direction

Asz = Shear area in global z direction

Ixx = Moment of inertia about x axis

Iyy = Moment of inertia about y axis

Izz = Torsional moment of inertia

R_H( ) = Horizontal reaction force at cable ends

H(x) = Horizontal force in cable element

R_v( ) = Vertical reaction force at cable ends

H = Constant horizontal force in cable element

k(x) = sag of the cable curve

M(x) = Moment diagram with respect to x coordinate

h = Vertical distance between ends of the cable

a = Horizontal distance between ends of the cable

CHAPTER 1

INTRODUCTION

Starting with the Industrial Revolution, people needed to transport the produced goods to distant places, often traversing long paths filled with obstacles such as valleys, lakes, and mountains. Consequently, they began constructing bridges with longer spans compared to historical bridge designs. Initially, bridges were built with numerous short spans. However, this approach proved to be time-consuming and expensive due to the need to construct many spans with short lengths. In response, bridge design evolved over time. Thanks to advancements in computational and construction methods, engineers started designing bridges with fewer, larger spans. Throughout this period, various bridge construction methods were developed to address different objectives, primarily utilizing concrete and steel as the primary construction materials. The optimal span lengths for different bridge types and the materials used can be explored in Figure 1.1.

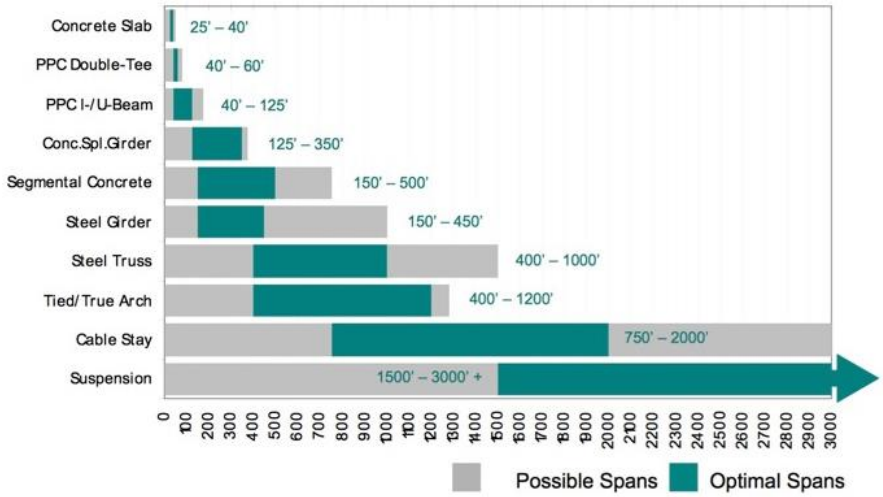

Figure 1.1. Optimal Bridge Types and Span Lengths in Feet (http://hotrails.net/2014/09/)

Cable-stayed bridges are particularly favored for spanning long obstacles like deep valleys, rivers, and lakes. This is because they allow for span lengths of up to 1000m without requiring excessive intermediate piers. Cable-stayed bridges consist of key components: stay cables, pylons, and the deck. Recent technological developments have led to the construction of very slender decks, which are susceptible to wind-induced vibrations. However, with the availability of wind tunnel laboratories worldwide, these decks can be precisely designed based on results obtained from tests, such as the Rüzgem Test Center at METU. The flow of forces in cable-stayed bridges is depicted in Figure 1.2, where towers and the deck serve as compression elements, while cables function as tension elements.

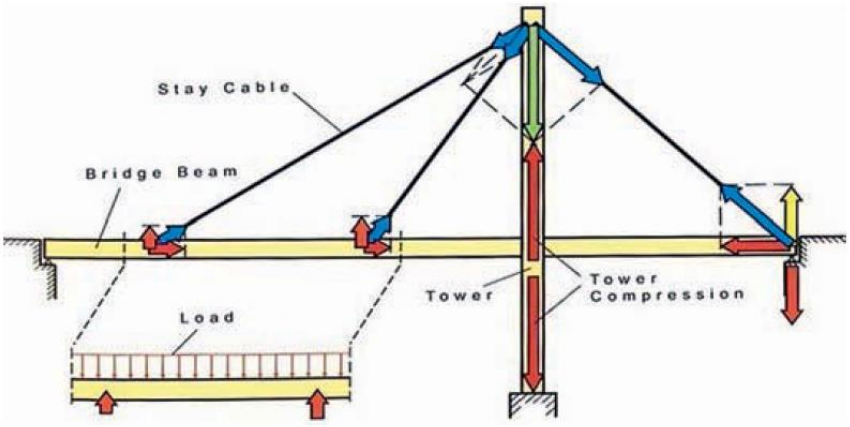

Figure 1.2. Distribution of Forces in Cable Stayed Bridges (Svensson, 2012)

Three types of decks can be designed for cable-stayed bridges: concrete, steel, and composite. Although all these types will be explained in the thesis, particular emphasis is placed on bridges with concrete decks.

1.1 Literature Review

(Leonhardt & Zellner, 1980) asserted that closely spaced cable stays minimize the depth and bending stiffness of longitudinal deck girders, which are primarily

governed by buckling safety and curvature line considerations. In light of these factors, bending and shear forces become secondary, while tension and compression predominate. The paper highlighted that opting for high cable stresses leads to improved dynamic behavior. When cables are stressed to approximately 0.45fu, as indicated by the Ernst formula, they exhibit significant rigidity in the axial direction. This phenomenon will be further elucidated in the subsequent sections, reinforcing its significance in the overall design.

(Svensson et al., 1986) In 1982, a composite girder-type bridge was selected as the preferred option for the Sunshine Skyway Bridge, marking a novel choice at the time for cable-stayed bridges. The superstructure consisted of steel plate girders and precast slabs. During the design of this bridge, engineers proposed beam-on-rigid-support approach in the final stage, particularly due to the presence of a concrete part in the girder. This method enabled the effective management of internal forces and deflections arising from creep and shrinkage. Moreover, the design of the bridge exclusively employed backward analysis procedures. In line with the solution strategy presented in this paper, two approaches—backward and forward analysis—are compared using the beam-on-rigid-supports approach. This comparative analysis aims to evaluate the effectiveness and merits of each method based on the results obtained from the proposed solution strategy.

(Schlaich, 1998) introduced an innovative construction design method for composite girder cable-stayed bridges. This method involves a two-step tensioning process designed to minimize the impact of unwanted locked-in moments, ensuring the desired end shape of the bridge and an optimal dead load configuration of the deck. However, subsequent research by other scholars revealed that this method exhibited sensitivity to the relative inertia ratios of steel and concrete sections, as well as eccentricity ratios of steel-only and composite girder properties. In response to these findings, researchers proposed additional stressing operations for cables. The analysis of these supplementary stressing operations is addressed in the subsequent sections, focusing on their implications for cable structures and cable-stayed bridges.

(Virlogeux, 2001) explained the force distribution in classical three-span cable-stayed bridges comprehensively in his paper titled "Bridges with Multiple Cable-Stayed Spans." Additionally, he provided detailed insights into the design principles and force transfer mechanisms of multiple cable-stayed bridges, shedding light on the fundamental behavior of such structures. The explanations presented in this paper serve as the foundation for understanding all cable-stayed structures, as further discussed in the subsequent sections.

(Janjic et al., 2002) proposed the unit force method as a means to derive an optimal solution sequence for the tensioning of stay cables. This method successfully incorporated various factors, including large displacements, cable sag, creep, and shrinkage, providing a comprehensive approach. The authors introduced a computer program designed to facilitate these intricate calculations. Through this method, accurate final tensioning forces for the cables were computed based on predetermined bending moments for both the deck and the pylon. A closely related approach, employed in the determination of stressing values for the cables, is presented in the thesis, with the exception of time-dependent material properties.

(Wang et al., 2002) introduced a finite element computation procedure specifically tailored for the shape finding of cantilevered cable-stayed bridges. They developed two computational procedures, namely backward and forward analysis. Through their study, it was deduced that the successful determination of the final desired configuration is crucial for both forward and backward analyses. While forward analysis yielded multiple solutions for the final configuration, backward analysis resulted in a unique solution. One notable advantage of forward analysis over backward analysis was its effective handling of time-dependent effects. These comparisons and findings are further examined in the thesis, with a more in-depth evaluation using both small and large-scale examples.

(Arici et al., 2010) proposed a procedure which allows engineers to design cable stayed concrete bridges by reducing and avoiding creep effects instead of calculating them with the refined models from the beginning of construction. The chosen

approach follows the influence matrix method in order to reach a pattern close to that of a continuous beam on rigid supports for each stage and the final one. Besides refined analysis as used in the forward analysis a basic approach such that converting creep and shrinkage effects into temperature loading was implemented in this research.

(Pipinato et al., 2012) developed a procedure for the finite element computation of cable-stayed bridges, with a specific focus on comparing various methods. The study compared partial and full cantilever methods and investigated the distinctions between linear and nonlinear analyses. However, the primary objective was to compare backward and forward analysis methods. The findings indicated that both forward and backward analyses could be employed to derive the desired bending moment diagram and deflected shape. Notably, in forward analysis, each phenomenon manifested its effects only in successive stages without influencing pre-stages. The study emphasized that nonlinear theory yielded more accurate results compared to linear theory. The comprehensive comparison between nonlinear and linear theories was conducted through the use of forward and backward analysis in a small cable-stayed structure in subsequent chapters.

(Song et al., 2018) investigated the optimization of cable forces using the counterweight method. In their finite element model, they conducted an in-depth analysis of geometrical nonlinearity and developed an optimization algorithm that took into account girder bending moment diagrams and bearing reactions. However, their study did not address the management of creep effects in concrete girders. Different from this study time dependent effects were considered with geometric nonlinearities in this study.

1.2 Objective and Scope

The main objective of this thesis is to perform a comparative analysis of construction stage results using two distinct approaches: backward and forward analysis. This

focus on a comparative assessment sets the current study apart from Svensson's (2012) work, as it directly compares these two approaches. By evaluating and contrasting the outcomes of backward and forward analyses, the thesis seeks to offer insights into the strengths and weaknesses of each method within the context of construction stage analysis for cable-stayed bridges. The ultimate goal is to equip engineers with essential knowledge for applying these two distinct methods in practical bridge projects and interpreting their results accurately.

In the forward construction stage analysis, calculations follow the real steps in the construction site but in the backward analysis calculations are done in the reverse direction by dismantling the bridge.

Generally, backward analysis are used to determine the cable forces and these forces are used in forward analysis as input. But at the times when computers are not widely used and computational power was low, bridges were designed by backward method. Nowadays engineers prefer mainly forward analysis procedures which takes into account the time dependent material properties in small time steps and with greater accuracy.

In this thesis, time dependent material affects will be applied in the reverse direction as static loads and cable forces, deflection of girder and pylons will be calculated. Then forward analysis will be done and results of both analysis will be compared to each other. In order to achieve this target, a real bridge that is already being designed in Türkiye is taken as the benchmark bridge. The purpose of selecting a real bridge is to obtain results and compare them in real bases.

Initially, a primary model is developed using computer programs such as Midas Civil and Larsa 4D. Cable forces will be determined based on criteria outlined by backward analysis. Two separate construction stage analysis models will then be created for use in backward and forward analyses. Pylon deflections, girder moments, deflections, and cable forces will be recorded for each construction stage analysis approach and subjected to comparative analysis. It is anticipated that

accurate backward analysis will yield results that closely align with those obtained through forward analysis.

Firstly, a brief overview of the history and evolution of cable-stayed bridges were introduced. Various types of cable-stayed bridges, including those constructed from concrete, steel, or composite materials, were defined. The components composing cable-stayed bridges, such as cables, anchorages, and pendulums, were explained.

Then, the works done over a long period of time for cable-stayed bridges were covered. General dimensioning rules, preliminary basic calculations, cable force determination, construction stage analysis procedures, and static analysis of cables were explained based on the available literature.

Furthermore, a basic structure was chosen to investigate the behavior of cable stayed bridges in principle. Different types of elements were employed to represent cable components. Backward and forward analyses were carried out using each element type, considering both time-dependent material properties and their absence. The obtained results were compared.

In order to verify results of the previous topic, a real cable stayed concrete bridge was chosen as a benchmark bridge and backward analysis were conducted. Cable stay forces from these analysis were then used in the forward analysis directly and girder bending moment diagrams were compared to each other.

Lastly, summary of each chapter were represented and findings were evaluated based on the results.

CHAPTER 2

CABLE STAYED BRIDGES

In this chapter of the thesis, a brief history on how cable stayed bridges evolved in time, their types and important elements that constitue these type of bridges were explained.

2.1 History of Cable Stayed Bridges

Early examples of cable stayed bridges goes back to 1600s (Svensson, 2012). Faustus Verantius's design drawings shows the early designs in Figure 2.1.

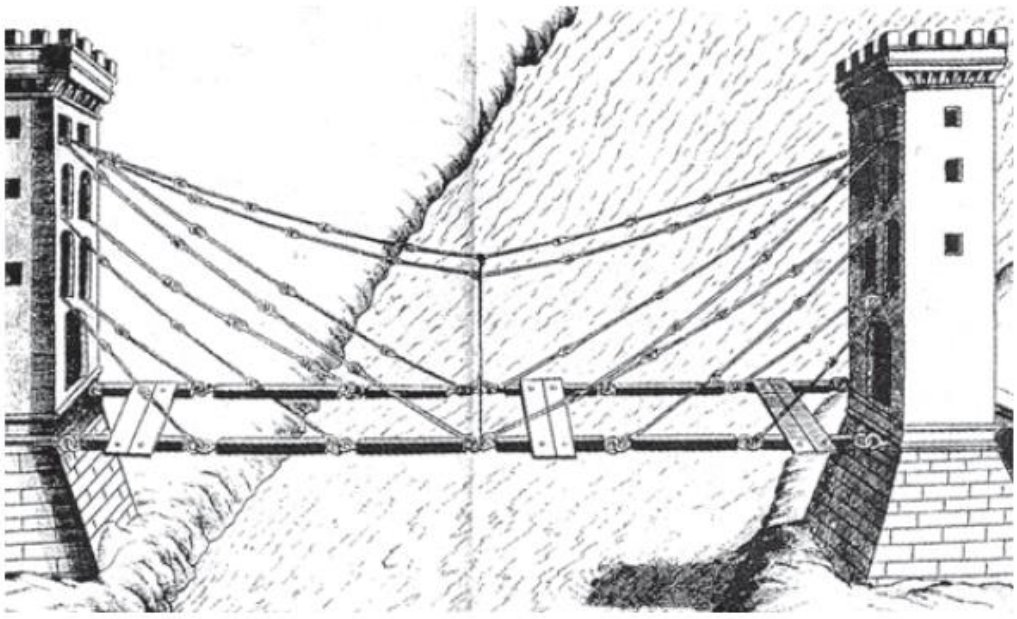

Figure 2.1 Eye Bar Supported Bridge Drawing By Verantius, 1617 (Svensson, 2012)

The first built bridge was the Kings Meadow Bridge with inclined ties in England in 1817 as shown in Figure 2.2. But this bridge partially collapsed between years 1922-1923 and was strengthened with additional stays. However, the bridge was completely destroyed in 1954 due to a flood. (Svensson, H., 2012)

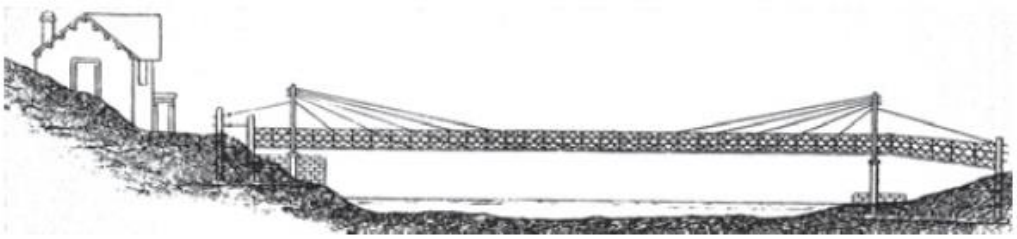

Figure 2.2 Kings Meadow Bridge, 1817 (Svensson, 2012)

The reason behind these failures were that designers at those times did not understand the structural behavior, and cables were not designed properly, and construction material qualities and strengths were not suitable. These failures were reported by French engineer Navier and suggested to use suspension bridges rather than cable stayed ones. These statements by Navier made bridge engineers prefer suspension bridge type. (Troitsky, 1977)

But John Roebling, one of the greatest bridge engineers in 19th century developed the fabrication of parallel wire cables and stated that use of stay cables strengthened the suspension bridges against wind induced oscillations and heavy live loads. His first successful design was Niagara Falls Bridge. But his highest success as bridge engineer was Brooklyn Bridge in New York (Figure 2.3). At those times there were no tools to calculate the forces in such highly indeterminate structures but he designed the bridge with great intelligence. It was the milestone in cable stayed bridge design although this bridge was a hybrid one which contains both suspension and stay cables. After these accomplishments in design WWII was the turning point in cable stayed bridge construction. In Germany modern cable stayed bridges were designed starting with the Rhine River Bridges and spread all over the World after WWII. The span ranges and total number of cable-stayed bridges built until the year

2000 can be observed in Figure 2.4 and Table 2.1 below, respectively (Svensson, 2012).

Figure 2.3 Brooklyn Bridge (https://www.nyc.gov)

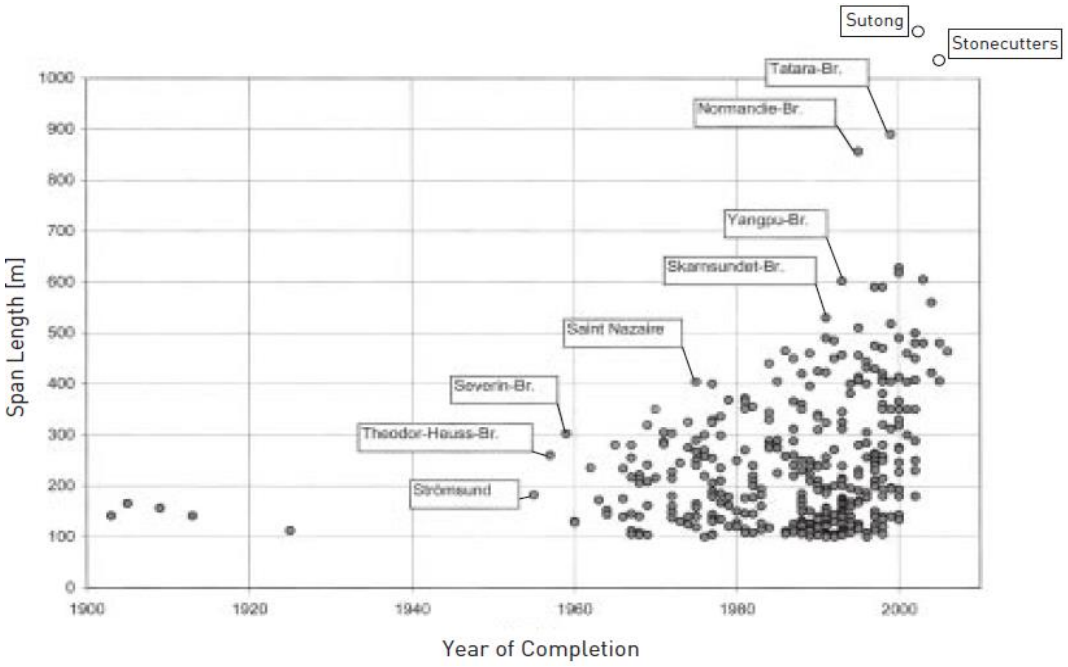

Figure 2.4 Development of Main Span Lengths of Cable Stayed Bridges Through Years (Svensson, 2012)

Table 2.1 Number of Cable Stayed Bridges Until 2000 (Svensson, 2012)

	1900 – 1950	1960	1970	1980	1990	2000	Σ
Japan				1	8	12	21
China						17	17
Germany		2	5	6	2		15
USA				2	7	4	13
Netherlands				2	1	2	5
France				2		2	4
USSR				1	1	2	4
Great Britain				1	1	2	4
other				3	9	21	33
Σ	0	2	5	18	29	62	116

2.2 Cable Stayed Bridge Types

Cable stayed bridges are economical between spans 100m and 1000m as shown in Figure 2.5. They have three distinct advantages. Firstly, because closely spaced stay cables are used, they can minimize the bending moments that occur from dead load and live loads at the superstructure. Secondly, these bridges have same flow of forces during construction which simplifies the erection. Thirdly, cable stayed bridges are stiffer than the suspension bridges. This situation can be best explained by the Figure 2.6 which shows how the critical wind speed for flutter increases for this bridge type compared to suspension bridges. (Svensson, 2012)

There are three distinct cable arrangements in cable-stayed bridges: fan, harp, and semi-fan types. The fan-type arrangement is challenging to construct due to the convergence of all cables at the top of the pylon, leading to construction difficulties arising from cable congestion. The harp arrangement is easy to construct but less effective than the fan type because cables are not steep. Semi fan type is between fan and harp system. It is easy to construct than fan type because all cables are distributed

over the pylon and more effective than harp type in load carrying because of steeper stay cable angles. These different configurations can be seen in Figure 2.7.

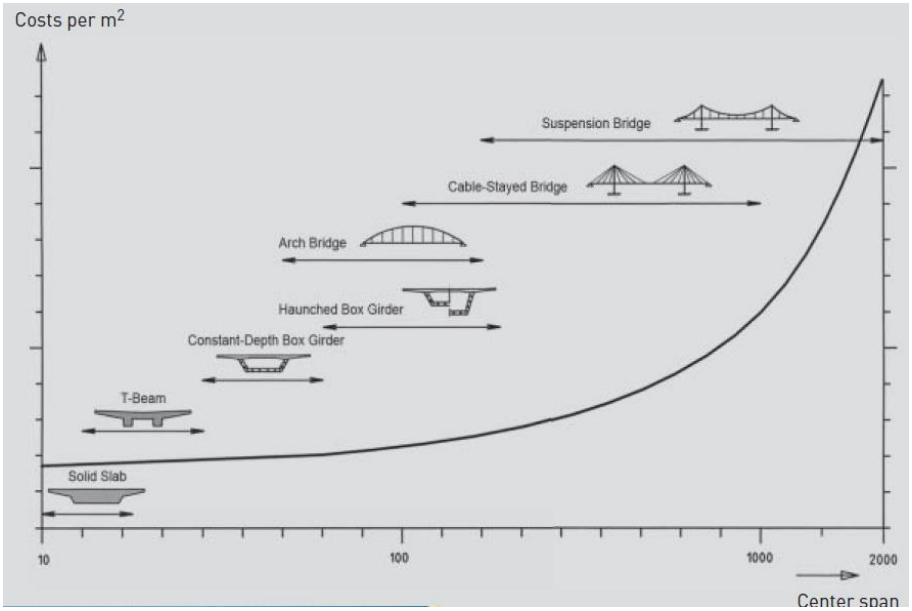

Figure 2.5 Cost Versus Center Span Length of Bridge Types (Svensson, 2012)

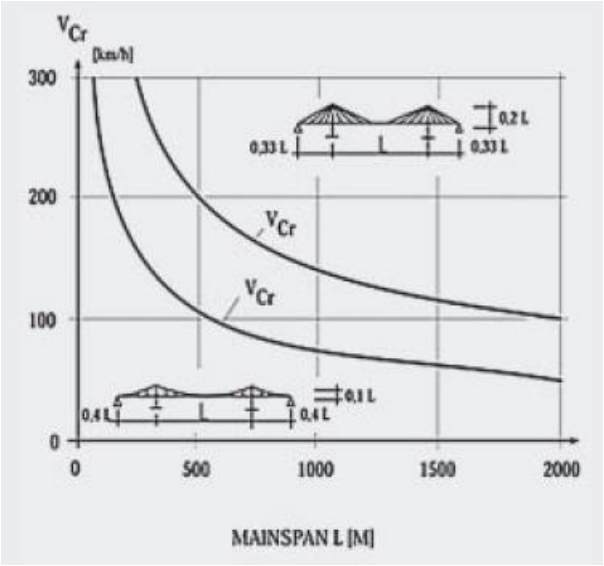

Figure 2.6 Critical Flutter Wind Speed Comparison (Svensson, 2012)

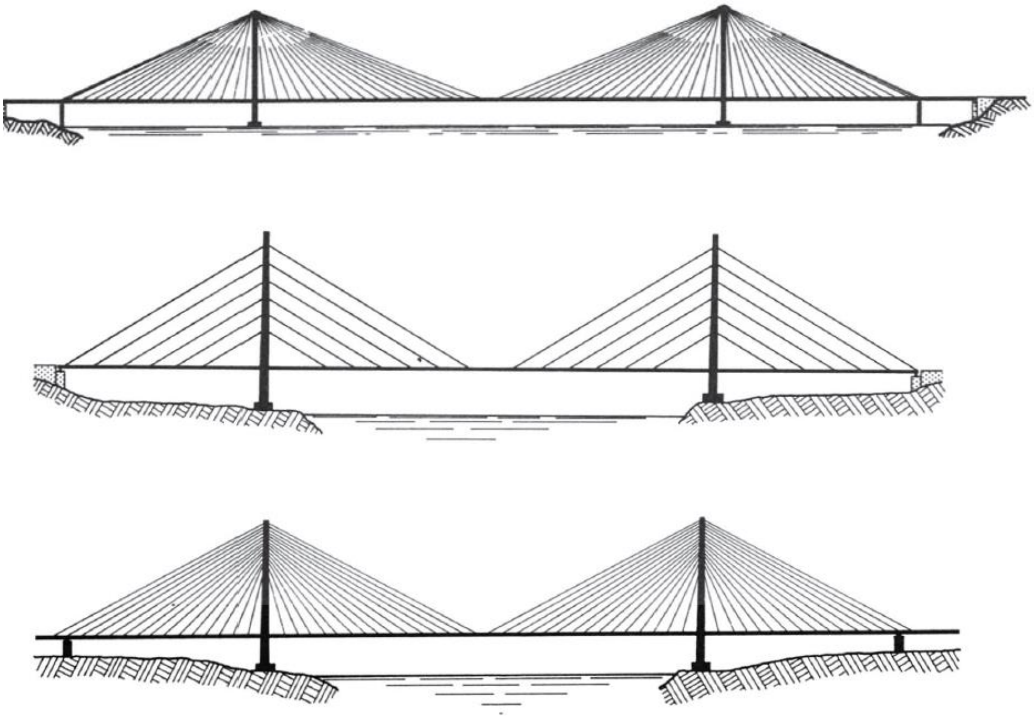

Figure 2.7 Fan, Harp and Semi Fan Type Cable Arrangements Respectively (Leonhardt & Zellner, 1980)

There are different shapes for pylon that can be preferred in the design. In addition, steel or concrete materials can be chosen for the towers. Towers are mainly in compression therefore; it is better to choose concrete as base material which performs better under compression. Chosen number of cable planes also affects the tower shape besides material. It is generally better to use two cable planes in design because it increases the rotational stiffness of the whole bridge. Therefore, “H” and “A” shaped pylons can be used for two planes of cable. Two legs of “H” shaped pylons can be joined together with transverse beams which increases torsional stiffness. In an “A” shaped tower, because two legs come closer at the top and connected with a cross beam, and backstays start to act like a closed frame, so rotational stiffness of the whole bridge increases. This benefits both in designing according to eccentric live loads and increasing the aerodynamic stability. Besides, one cable plane can be chosen, too. This situation affects the superstructure type because if one cable plane is used, the torsional rigidity of the structure becomes very

low and torsionaly rigid type of deck should be chosen like closed box section. Some examples for pylon shapes are shown in Figure 2.8 and Figure 2.9.

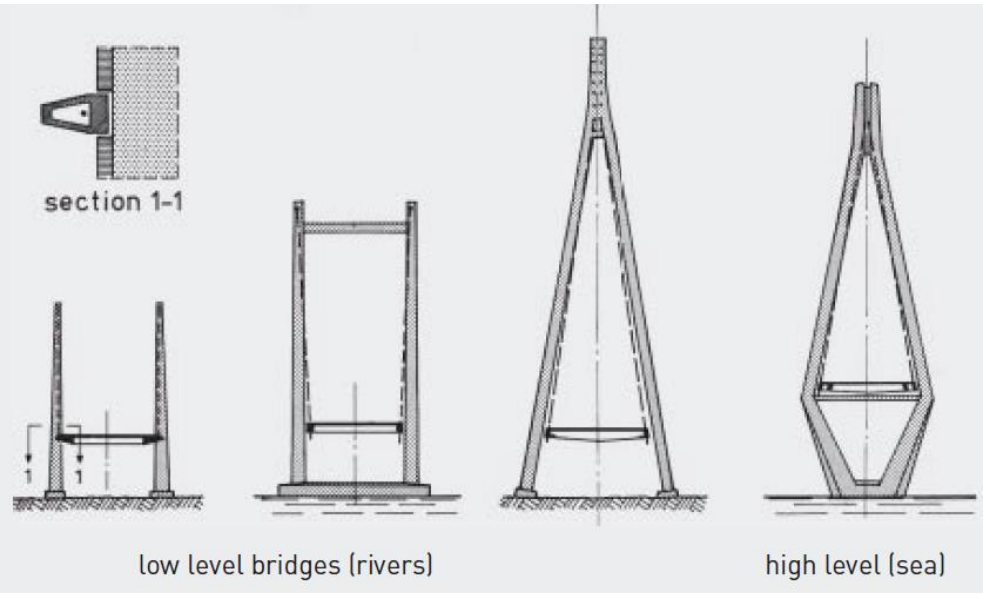

Figure 2.8 Two Cables Plane Pylon Shapes (Leonhardt & Zellner, 1980)

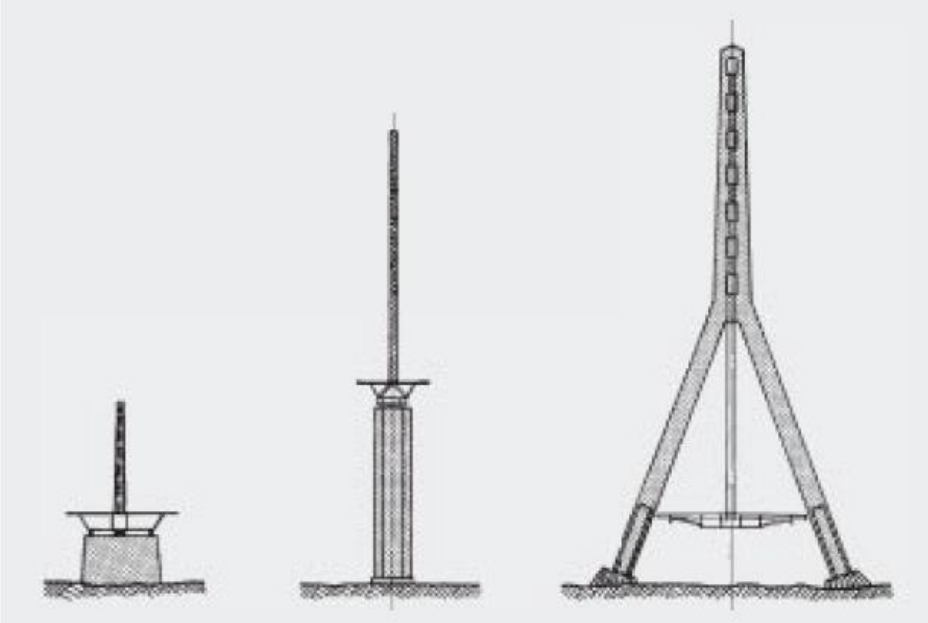

Figure 2.9 One Cable Plane Pylon Shapes (Leonhardt & Zellner, 1980)

Steel, concrete and composite cross sections can be used as deck type in cable stayed bridges based on economy and design requirements.

For steel (orthotropic) cross sections with one cable plane, torsionaly rigid closed sections are used against eccentric heavy live loads and wind loads. For two cable planes both open and closed sections can be chosen because cables provide the necessary torsional rigidity.

For concrete sections if two cables plane is chosen, open, box and solid cross sections can be used. In case of one cable plane, box girder should be used to satisfy the rotational rigidity. Also, most probably transverse post tensioning should also be used against high tension stresses in the concrete.

For composite sections, only two cables plane should be used because if one cable plane is chosen, the concrete slab is exposed to tension in the transverse direction. And post tensioning cannot be used in composite sections because all post tensioning can be transferred to the steel part which is not desirable. Therefore, the only solution is to use two cable planes in this type of girder cross section. (Leonhardt & Zellner, 1980) Typical cross section drawings for these three types of superstructures can be found in the Figure 2.10, Figure 2.11 and Figure 2.12.

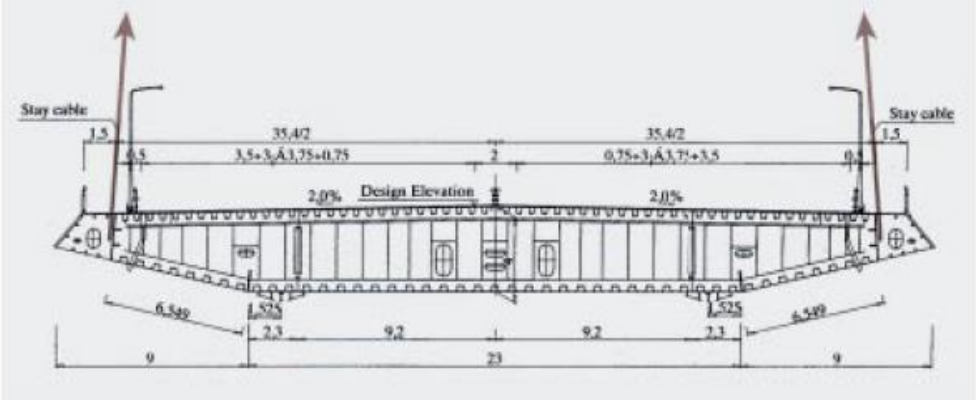

a) Closed Cross Section (Two Cable Plane)

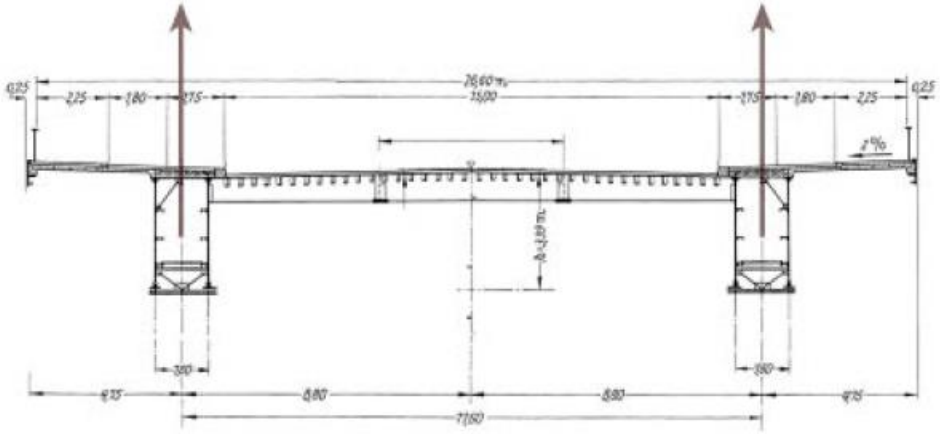

b) Open Cross Section (Two Cable Plane)

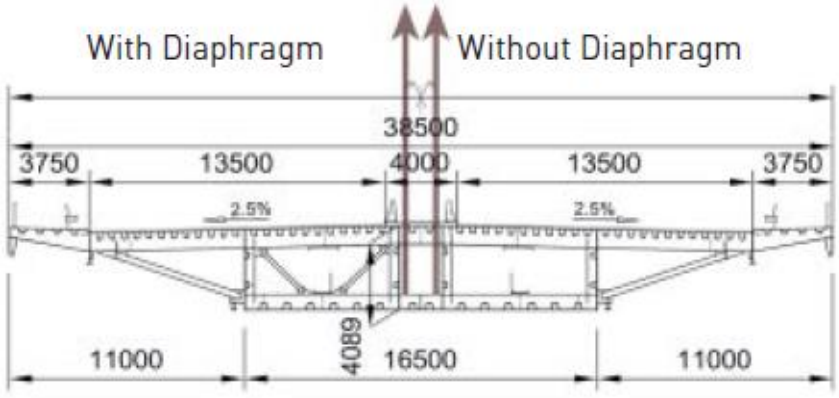

c) Closed Cross Section (One Cable Plane)

Figure 2.10 Steel Cross Sections (Svensson, 2012)

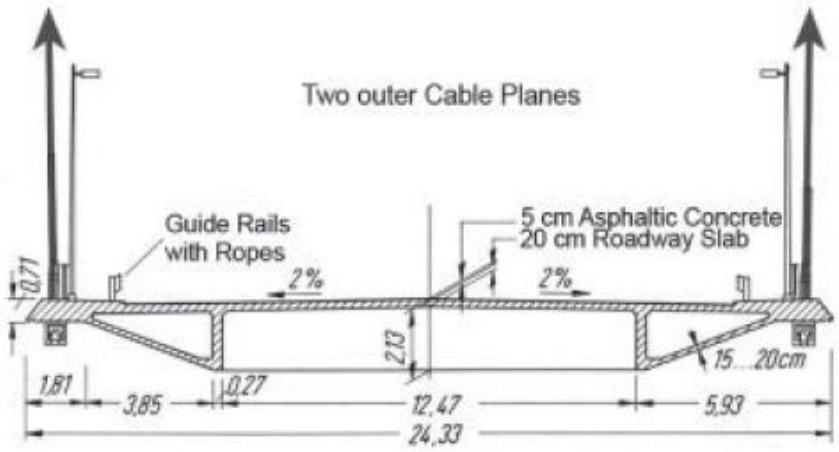

a) Open Cross Section (Two Cable Plane)

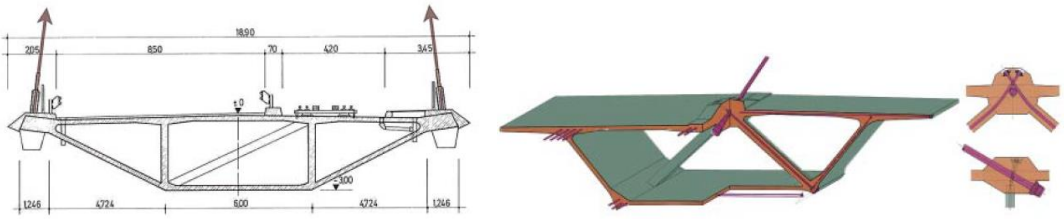

b) Closed Cross Section (Two and One Cable Plane)

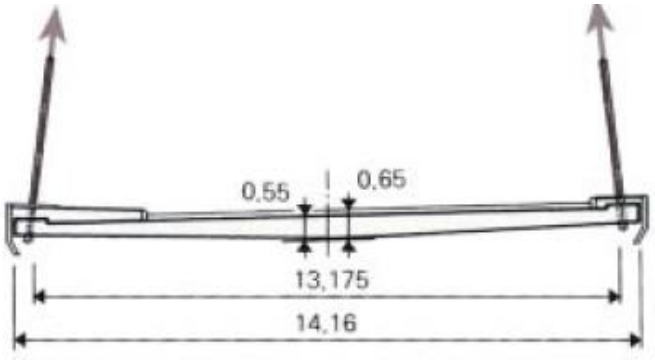

c) Solid Cross Section (Two Cable Plane)

Figure 2.11 Concrete Cross Sections (Svensson, 2012)

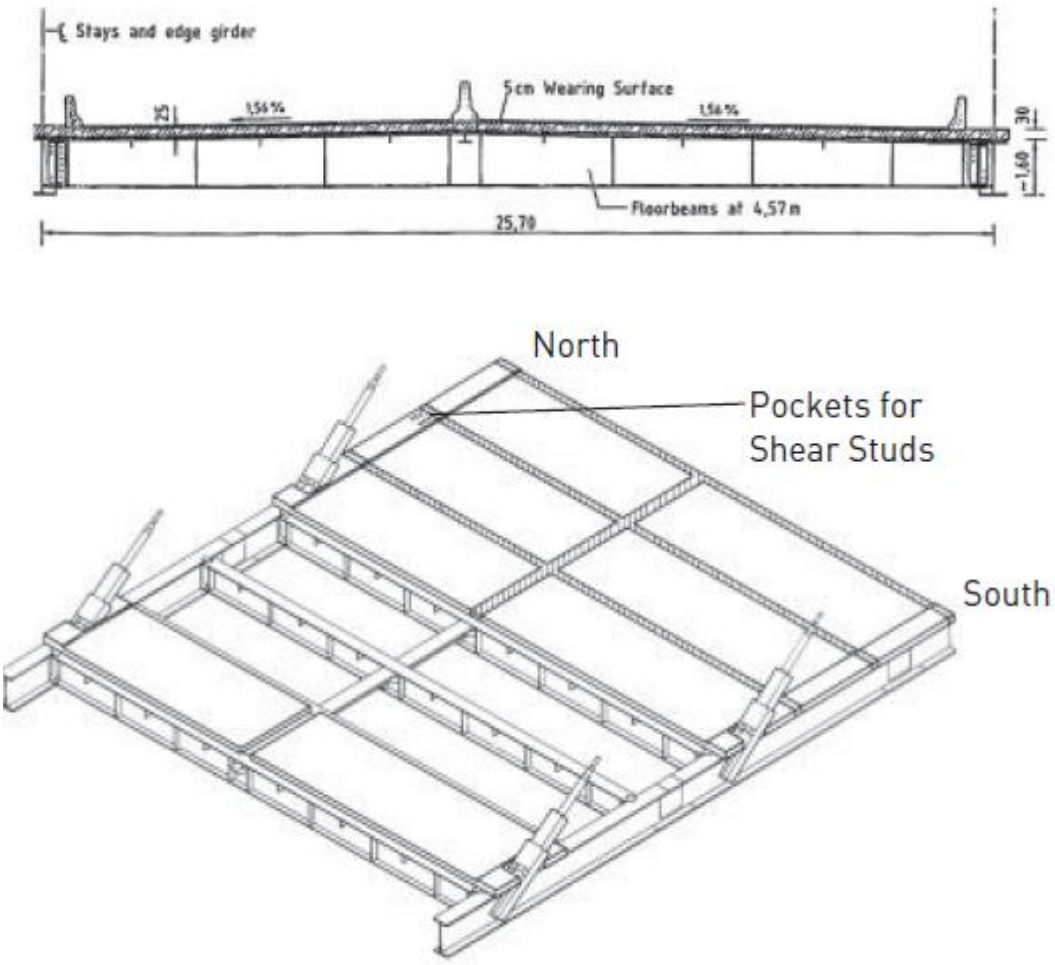

Figure 2.12 Steel Composite Cross Sections (Svensson, 2012)

2.3 Elements of Cable Stayed Bridges

2.3.1 Stay Cables

Stay cables are the main and most important elements of the cable stayed bridge. Their performance governs the behavior of the complete bridge , not only in the final stage but also during the construction. These cables consist of steel wires that are characterized by larger tensile strength than ordinary steels. Typical seven wire strand can be seen in Figure 2.13. In modern construction three types of cables are

used. These are locked coil ropes, parallel wire cable and parallel strand cable. Their mechanical properties can be found in Figure 2.14. Generally throughout the World parallel strand cables are used commonly therefore, in this thesis only their properties will be explained in the following sections.

Figure 2.13 Seven Wire Strand (Gimsing & Georgakis, 2012)

Characteristics	Modern locked coil rope	Parallel wire cable	Parallel strand cable
	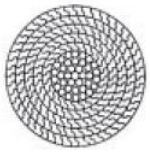		
$E \cdot 10^{-6}$ [N/mm^2]	0.170	0.205	0.195
f_u [N/mm^2]	1470	1670	1870
$\Delta\sigma$ [N/mm^2]	150	200	200

Figure 2.14 Mechanical Properties of Cable Stays (Svensson, 2012)

2.3.1.1 Parallel Strand Cables

These cables are comprised of 7 wire strands with 15mm diameter with a tensile strength of 1860 Mpa. There are some advantages of parallel strand cables. Firstly, installation is done strand by strand, therefore transportation weights are small. These strands can be changed individually instead of changing all cable strands. Also cement grout or wax is not required.

The system of parallel cable strand is shown in Figure 2.15. The strands run parallel to each other. They spread outer and clamped with wedges at the anchor block. These wedges cover the strand ends and prevent them from slipping into the inside as shown in Figure 2.16. Bearing plate and ring nut are the two important components of this system. Bearing plate transfers forces to anchorages and ring nut is used to elongate the cables mainly.

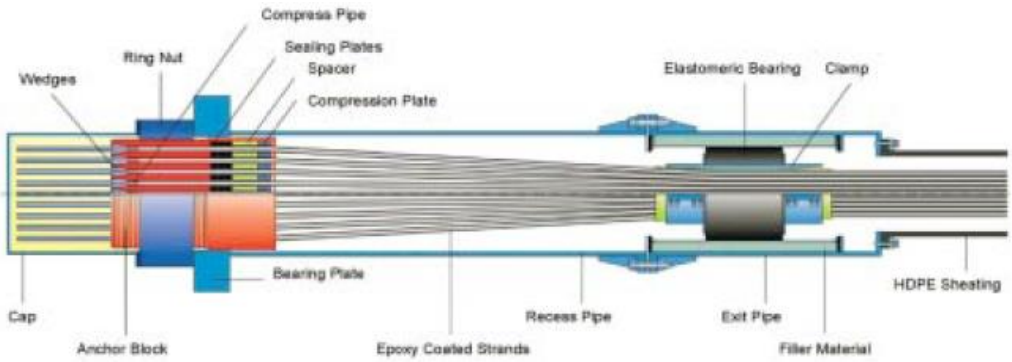

Figure 2.15 Typical Strand Cable (DSI)

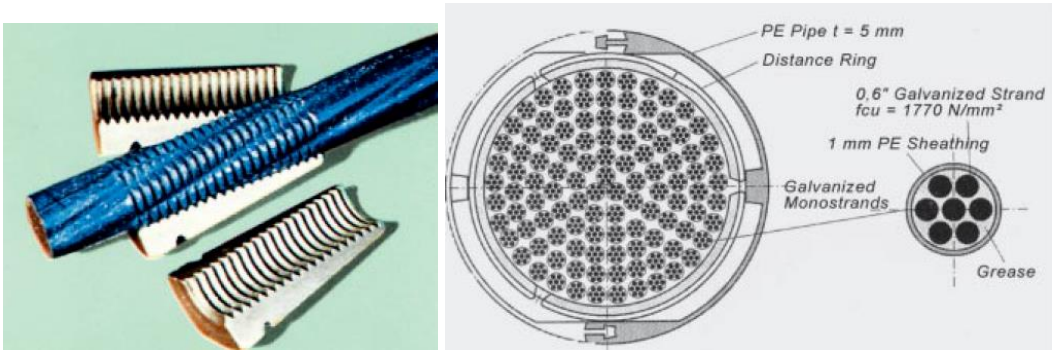

Figure 2.16 Strand Wedge and Typical Layout Section of Strands in A Cable (Svensson, 2012)

2.3.2 Cable Anchorages

Cable stays should transfer their forces to the bridge girder and pylon. Therefore, different type of anchorages are designed to transfer these large forces to the structure. One of these anchorages is at the pylons. Cables can directly give tension

load to concrete pylon but at these locations because of high tension prestressing is used. Anchorage of cable to concrete deck and pylon is shown in Figure 2.17. In the steel decks, anchorages can be designed by extending the web, and cables can be anchored to the pylons by steel beams, as shown in Figure 2.18. These steel beams are designed as if they carry all tension forces and transfer interface shear to concrete directly. Lastly but as crucial as the other parts of the bridge, where backstay cables are tied vertically to hold down piers, is tie down cables with anchorages or what is called traditionally tie down pendulums. If backstay cables can not be anchored vertically to a support, static load scheme can not be considered complete. Backstays carry the unbalanced dead and live load, and hold-down cables are needed to anchor these huge loads to a stable point. Also, a gap in the longitudinal direction that is enough to compensate for movements of thermal or other actions should be left for proper design, as shown in Figure 2.19.

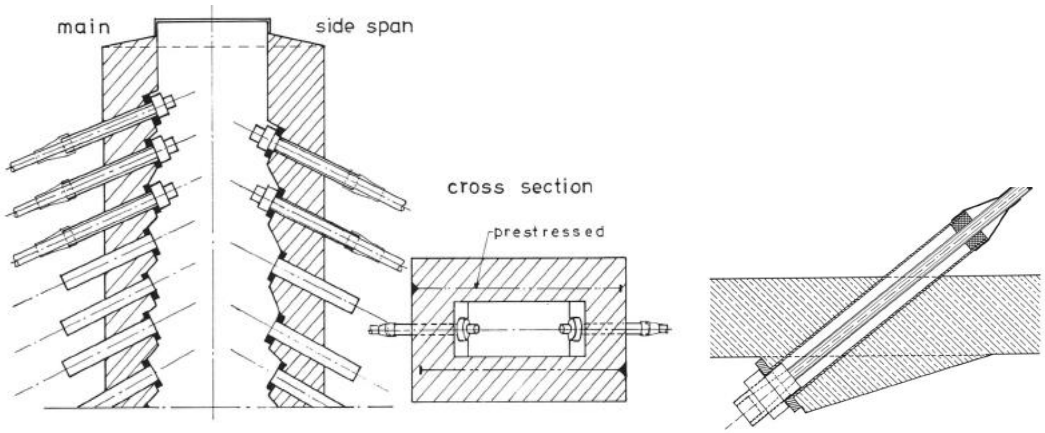

Figure 2.17 Anchorage of Cables to Concrete Pylon with Prestressing Tendons and to the Girder (Leonhardt & Zellner, 1980)

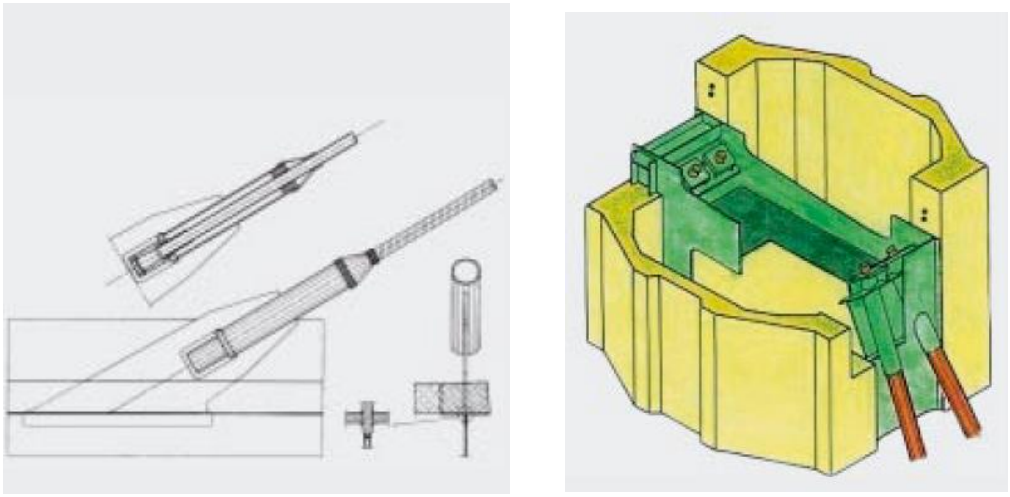

Figure 2.18 Anchorage of Steel Beam by Web Extension and Anchorage of Cable to Pylon with Steel Beam (Svensson, 2012)

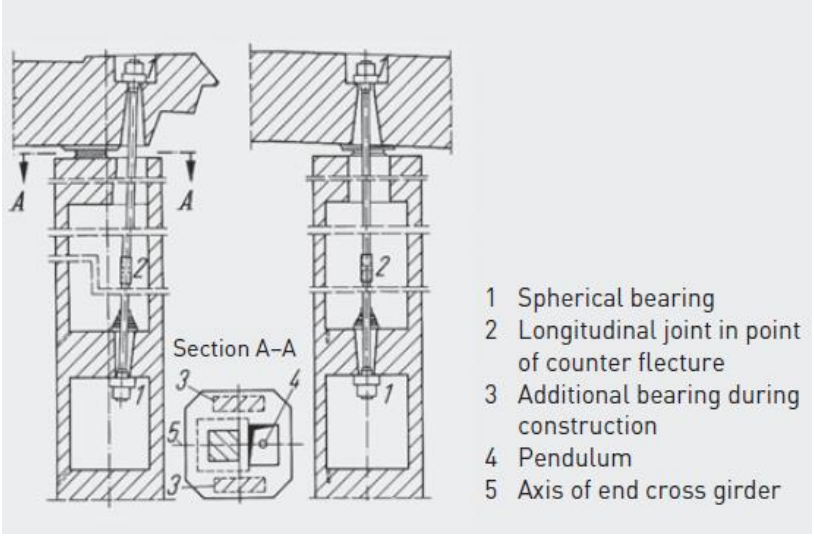

Figure 2.19 Typical Layout of a Pendulum (Svensson, 2012)

CHAPTER 3

ANALYSIS OF CABLE STAYED BRIDGES

General dimensioning rules, basic hand calculations for preliminary design (flow of forces), cable stay force determination and construction stage analysis procedures of cable stayed bridges are explained in this chapter of the thesis. The primary objectives of this chapter are to offer the reader a concise overview of the calculation methods for forces in cable-stayed bridges, to present cable statics in an accessible manner, and most importantly, to thoroughly explore the analysis procedures for both the backward and forward construction stages. Additionally, it consolidates scattered information found in the literature, presenting it in an easily understandable format.

3.1 General Dimensioning Rules for CSB

To design cable stayed bridge, engineers need to determine preliminary dimensions, make assumptions and finalize the design after many iterations of trial and error. Determining the ratio of height of the pylon to main span and side span to main span ratios are critical first steps in designing the cable stayed bridges.

3.1.1 The Ratio of Side Span to Main Span

The ratio between the side span and main span length influences back stays cable stresses. Live load in main span increases back stay cable stresses but loads in the side span decreases them. These changes in stresses can be adjusted with proper side to main span ratio. For instance, if ratio of side to main span is above 0.4, more steel is needed and slag amount can increase. In cable stayed bridges it is interesting to note that back stay cables seem to carry compression if side span is loaded. This

means not compression but reduction in tension forces. Also, these cables are subjected to largest tension and compression forces in the bridge. Therefore, fatigue becomes an important parameter in determining the span ratios. In addition, this ratio influences value of vertical anchor forces at anchor piers. This force decreases with increasing ratios. Based on these observations span ratio should be chosen carefully for economic and safe design. For this purpose, a chart is given in Figure 3.1 where vertical axis shows the live load to dead load ratio and horizontal axis shows the main span length. Vertical curve shows the points where assumed fatigue stress of 200 MPa is reached under %40 live load. Therefore, for concrete bridges ratio of 0.4, for railway bridges 0.3 can be chosen for design purposes. (Leonhardt & Zellner, 1980)

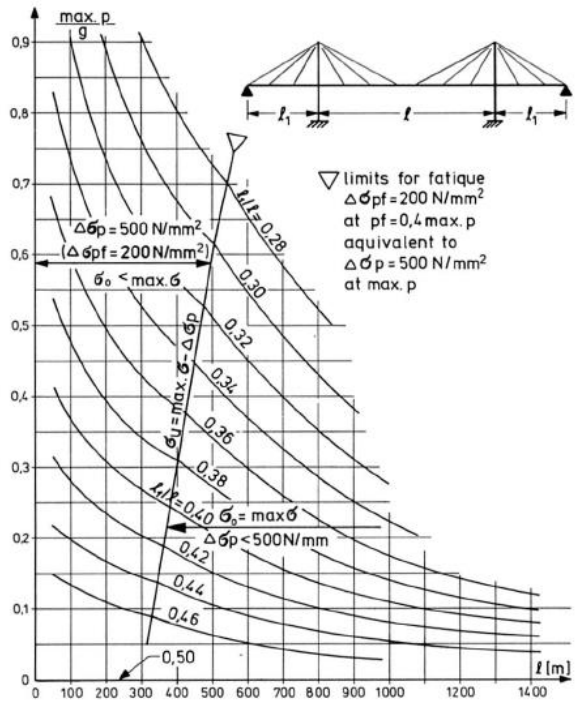

Figure 3.1 Diagram for Determining Optimum Ratio of Side to Main Span (Leonhardt & Zellner, 1980)

3.1.2 The Ratio of Tower to Main Span and Stiffness of Towers

Amount of cable steel and compressive forces in the bridge deck are strongly influenced by the tower height. The higher the tower the smaller will be the cable steel quantity and compressive forces. But tower cannot be too high because material quantities of pylons increase. Figure 3.2 can be used as reference for choosing optimum height of the towers.

In the longitudinal direction choosing tower stiffness lower has benefit against live loads. For instance, if the main span is full with live load, there will be large moments in the tower which has high bending stiffness. It will not be able to transfer the load to backstays which are the main load carrying elements. Therefore, it will not be an economical choice. And as shown in the below the figure 0.2 to 0.25 is a good ratio.

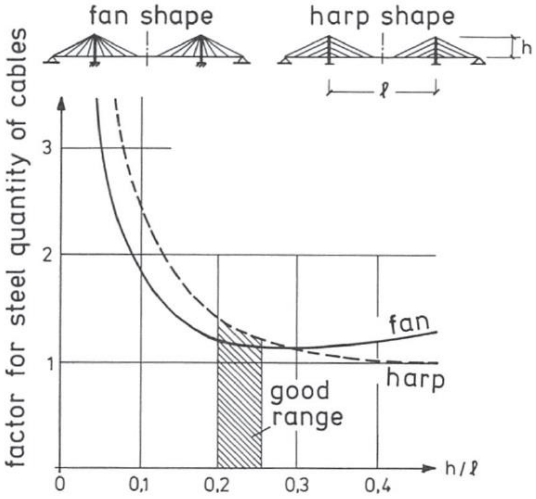

Figure 3.2 Quantity of Cable Steel as a Function of Relative Height of Tower (Leonhardt & Zellner, 1980)

3.2 Preliminary Basic Calculations and Flow of Forces in CSB

CSBs are highly indeterminate structures both in construction and final stages. Therefore, hand calculations can be very cumbersome. But it is possible to simplify

the calculations and to get very close solutions to the computer results. Also, by this way flow of forces in this bridge type can be understood clearly. In the literature a lot of simplified calculation ways can be found but the easiest to understand and to apply to the real bridges is given by Holger Svensson in the book, “Cable Stayed Bridges, 40 Years of Experience Worldwide”. These calculations can only be used for the final stage of the bridge. For construction stage analysis a computer is definitely needed because geometric nonlinearity should be considered.

3.2.1 Flow of Forces in A Cable Stayed Bridge

(Virlogeux, 2001) explains how forces flow in a highly indeterminate cable stayed bridges in the following paragraphs. Firstly, classical three span bridge was investigated. When the main span is loaded tension in the cables increases in this region. Mid span deflects downwards and because of this load towers move to each other. But side span cable tensions do not deviate too much because of the upward deflection of this span. All the horizontal load that is caused by midspan loading is carried by the backstay cables. Because of this reason tower tip laterally deflects and high bending moments occur in the pylon.

If the side span is loaded it deflects downwards with the increase in the tension of the cables. But in back stays tension decreases. And the main span deflects upward. Figure 3.3 best explains this situation. Therefore, back stays are exposed to very large tension variations and are very prone to fatigue problems.

To improve this behavior a basic technique is to use intermediate supports in the side span. If mid span is loaded, all cable stays anchored in the side span start to behave like back stays. Also, other cables carry more tension than the previous configuration because they are now close to intermediate side piers. Midspan and side span deflections decrease. If side spans are loaded, very small tensions occur in these cable stays because now intermediate piers carry the applied load. This situation

increases the fatigue behavior of the back stays. Figure 3.4 explains the load transfer mechanism visually.

3.2.2 Preliminary Basic Calculations

Holger Svensson in his book, “Cable Stayed Bridges, 40 Years of Experience Worldwide” suggests some preliminary calculations for bridges as explained in the following texts. The deformation characteristics of the bridge are influenced mainly by stay cables. For slender deck bridges, pylon and deck stiffness affect deformations only %5. Therefore, it can be assumed that loads are mainly carried by normal forces, rather than moments in the beam and towers. These normal forces can be calculated in good approximation if the anchor points of the cables are treated as hinges. By this way a statically determinate equal system which shows good coherence with the real one can be established in order to find all the axial forces in the bridge.

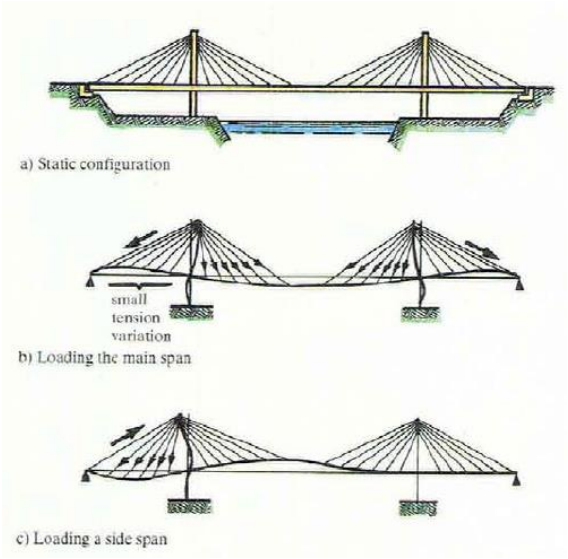

Figure 3.3 Structural Behavior of a Classical Cable Stayed Bridge with Three Spans (Virlogeux, 2001)

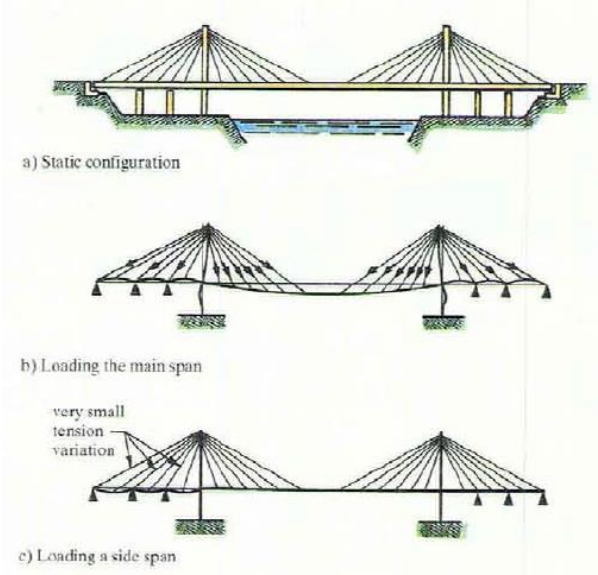

Figure 3.4 Structural Behavior of a Classical Cable Stayed Bridge with Intermediate Supports in Side Spans (Virlogeux, 2001)

Best way to explain these assumptions is to show them in a figure. As reference to Figure 3.5, a point load in the main span creates tension both in the forestay and backstay. Forestay force can be determined by multiplying the force with the reverse of sine of the angle. Backstay vertical force can be found by taking moments according to the pylon. One important parameter to find live load moments of the girder is the deflection of the deck and this can be calculated by Force Method as shown in the "b" part of the figure. By applying a load in the main span, pylon and bridge deck remains under compression. If this load is applied to the side span, tension in the forestay can be found by dividing load to sine of the angle. By taking moments at the pylon vertical component of the backstay is found. This force is compressive, cables cannot carry compression which means that reduction in the tension of the cable occurs. Girder, on the left of the applied load, becomes in tension. Pylon normal forces can be found by applying force equilibrium in the vertical axis.

To find the maximum tension force in the backstay cable, main span should be fully loaded. In addition side span is loaded along the full length in order to obtain the minimum tension force in the backstay cable. These two values are used in the

fatigue calculations of the backstays. Also, pylon is exposed to large normal forces and to calculate the buckling safety, maximum axial load should be determined carefully and this load can be found by summing two cases described above as shown in Figure 3.6. Maximum axial load in the girder can be found by parabolic approximation. The maximum force will be at the pylon location and it will be used for the calculation of second order effects and to find the safety against buckling. The formula is,

$$N = \frac{DL+LL}{2h}(l^2 - x^2) \qquad (3\text{-}1)$$

where:

DL= Uniformly distributed dead load

LL= Uniformly distributed live load

h= Height of pylon above deck

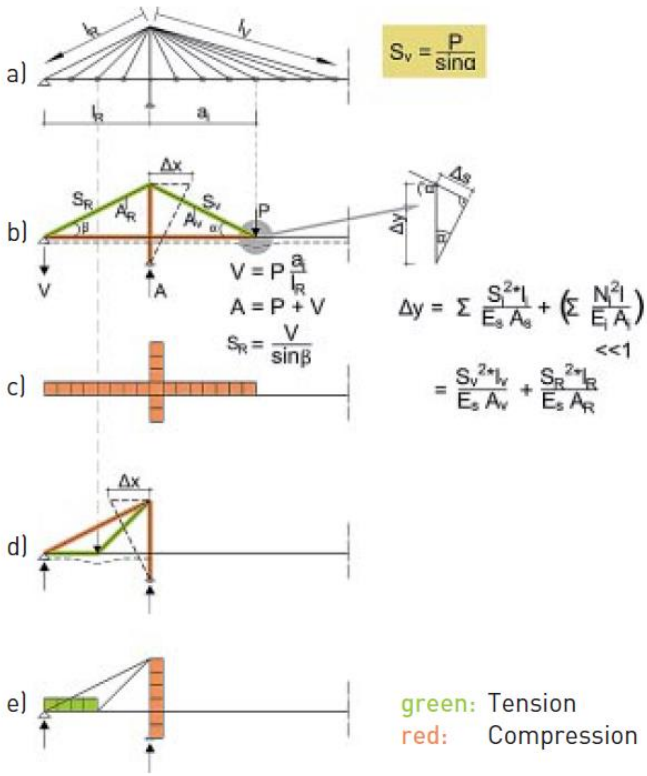

Figure 3.5 Normal Forces in a Hinged System (Svensson, 2012)

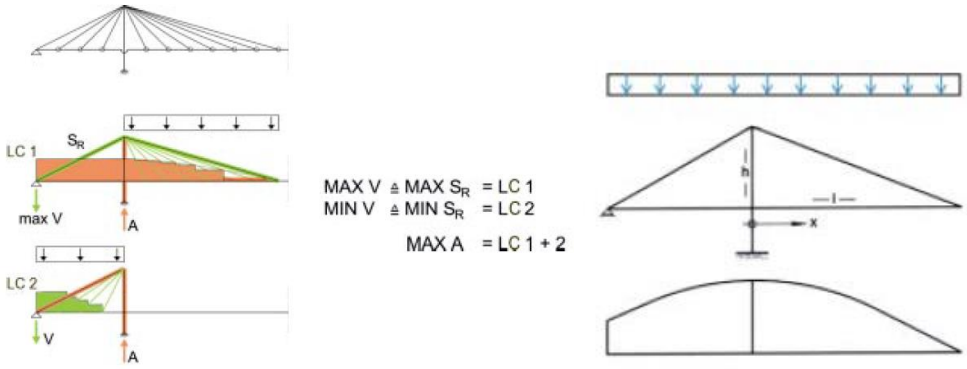

Figure 3.6 Largest Normal Forces in Beam and Pylon and Approximation of Largest Beam Forces (Svensson, 2012)

Live load bending moments in the girder can be found by the beam on elastic foundation approximation. Positive bending moments give good results but negative ones give conservative results compared to computer outputs. Detailed explanation on this topic can be found in (Svensson, 2012).

3.3 Cable Force Determination (Final Stage)

In this section, determination of cable forces is explained. Cable forces can be chosen according to bridge superstructure type and construction materials. These superstructures can be classified as concrete, steel and composite.

Cable forces are determined according to the final bridge configuration. They can be calculated for different needs and purposes. For instance, they can be stressed to values in order to give deck and pylon specific moment diagram or to give zero deflection to the deck.

3.3.1 Concrete Deck Bridges

Concrete is a material which creeps and shrinks. Also, it is weak in tension but very strong in compression. Therefore, care should be given while designing decks with concrete. Bridge engineers prefer to choose cable forces of cable stayed bridges

under dead load at time infinity after all creep and shrinkage taken place, as if there are fixed supports at the cable anchorage points at the deck level. So, deck can be thought as a continuous beam on rigid supports. Vertical reactions at these supports can be calculated and if divided by the sine of each cable inclination, cable forces are found. It is straightforward but there is another very important logic behind this assumption. Because concrete is a material that creeps, moments in the deck will not be exposed to creep if cable forces are chosen as the support reactions of a continuous rigidly supported beam (Svensson, 2012). If cable forces had been chosen lower, then the deck would have deflected downwards because of creep of moments and cable forces and deck moments would be different from target values. Or if they had been chosen higher, then these forces will creep the deck upwards and again deck moments and cable forces would change. The only way to come up with a good and stable solution is to choose cable forces as if there are rigid supports at the anchor points. Figure 3.7 and Figure 3.8 explains this topic.

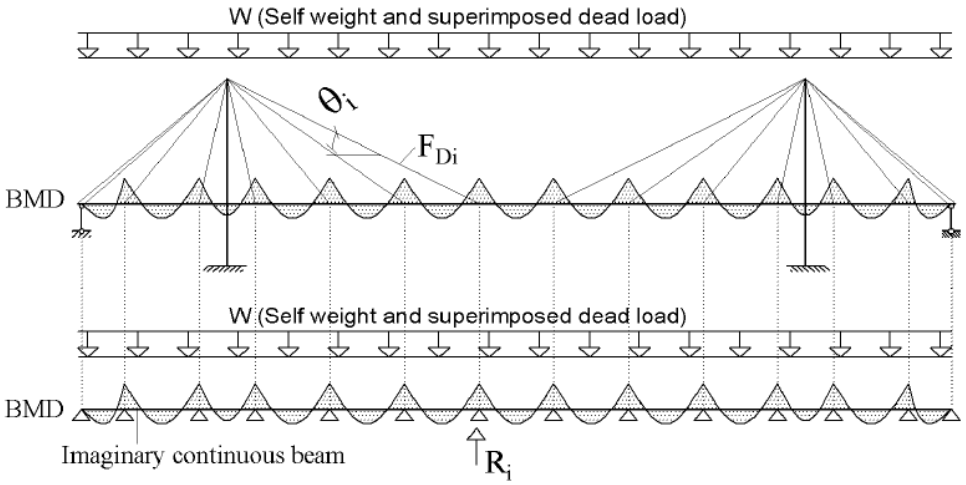

Figure 3.7 Beam on Continuous Supports Approach (El Shenawy, 2013)

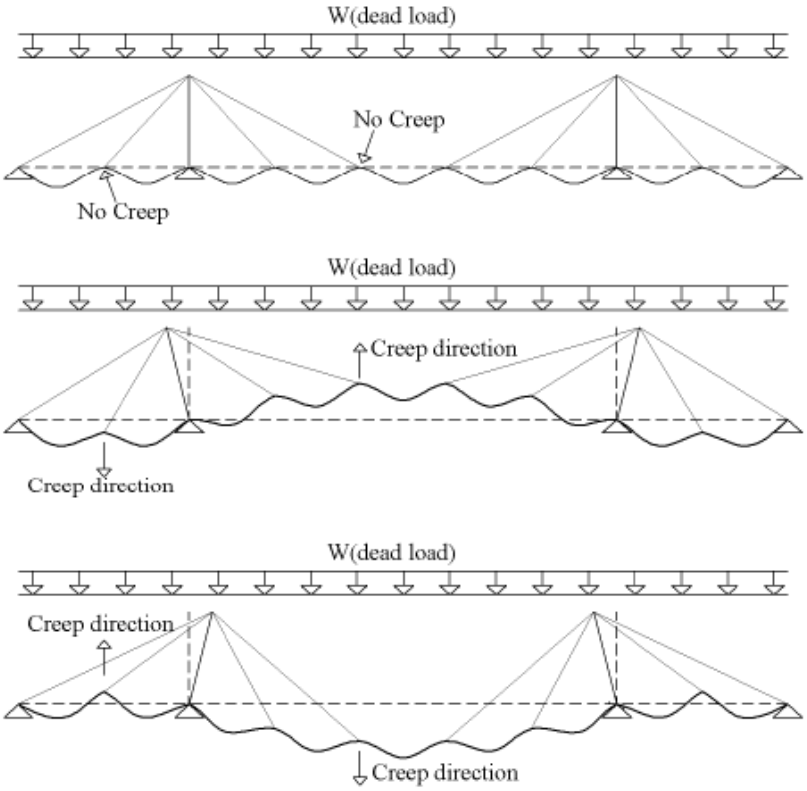

Figure 3.8 Cable Forces and Their Effects on Creep (El Shenawy, 2013)

3.3.2 Steel Deck Bridges

Calculation of desired cable forces for steel deck bridges can change according to engineers' choice. In the literature some engineers choose to design them as if they are like concrete decks (rigid support approach). Holger Svensson choses to design them in such a way that superstructure will have least amount of material. In order to achieve this design target cable forces are chosen larger and more negative bending moment is given to the steel deck. This can be applied because steel does not creep or shrink as concrete. But in this case cable steel quantities increase. If this design philosophy is used, after live loading, moment in the deck will be small. Graphical illustration of this explanation and steel, concrete moment diagrams can be found in Figure 3.9.

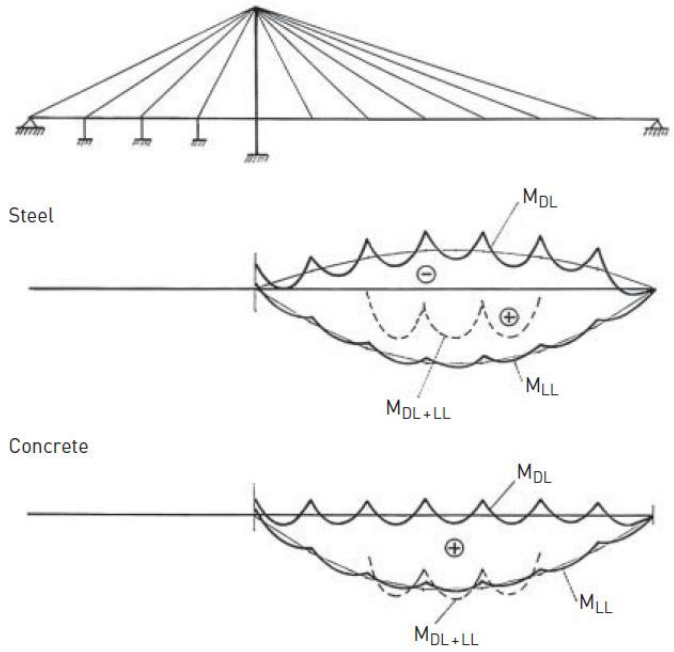

Figure 3.9 Run of Moments of Steel and Concrete Deck Sections (Svensson, 2012)

3.3.3 Composite Deck Bridges

Composite deck bridges consist of two materials one is concrete and the other one is steel. Concrete part is generally used as slab and steel part is used as main and cross girder. As stated before, concrete is a material which shows creep and shrinkage characteristics. Therefore, for composite decks at time infinity, cable forces are determined as the deck is rigidly supported at anchor points as explained in concrete deck bridges at Section 3.3.1. Otherwise, concrete creep and shrinkage will cause change in moments and neither desired forces nor desired profile will be achieved. In addition, after bridge is constructed, concrete slab will creep and shrinkage will occur, this should be considered while adjusting cable forces, otherwise desired results will not be achieved.

3.4 Construction Stage Analysis Procedures

Cable stayed bridges are designed according to the final stage at time infinity where creep and shrinkage finished. All dimensions and final cable forces are determined according to this phase. But these dimensions should also be checked for each construction stage. Also, boundary conditions can change many times during the construction and additional loadings act to the members like crane weight etc. In order to achieve the correct cable forces, internal forces and desired profile of the deck, careful and detailed construction stage analysis should be done. In the literature there are two different methods in achieving this target. These are backward and forward construction stage analysis. In the following sections they will be explained in detail.

3.4.1 Backward Construction Stage Analysis

(Svensson, 2012) states that for construction stages, it is better to start analysis from the final stage and to dismantle the bridge backwards. Loads and deformations are added to the final situation with negative values. At the end no remaining force must be left as residual.

Firstly, creep and shrinkage values should be calculated and applied with negative sign to the bridge. This can be achieved by equivalent cross-sectional forces or temperature loads. Then superimposed dead loads are removed. Exactly at this point the bridge is at the stage where the construction and all adjustments are finished. Afterwards, dismantling operations of the bridge superstructure start. This can be done by floating crane or derrick. Initially dismantling by floating crane will be explained then dismantling by derrick will be given also. It will be beneficial to follow the steps shown in Figure 3.10.

Firstly, creep, shrinkage and superimposed dead load are eliminated from the bridge and all conditions are taken back to time zero where the real construction finished.

Secondly, dead load of the middle element is removed from the system. In order to dismantle this element, M, N and V (moment, axial and shear) forces should be zero. To achieve this target three cables on the left and right must be lengthened. After trials when these values are zero, segment can be removed by opening the joints.

Thirdly, first cables are lengthened until the cable forces are zero or they are cut directly. Then dead load of the cantilever segment is removed from the model and joints are separated.

Operations described in the third step is repeated until all the bridge is dismantled including pylons and side span piers, if any.

This analysis has very important conclusions. For instance, before cutting the cable, obtained load in the cable is the tensioning force of that cable that should be applied in order to reach the desired forces and deformations at the final stage. After cut and before cut, change in elevation of the deck can be obtained and deformation control can be done on site with these values.

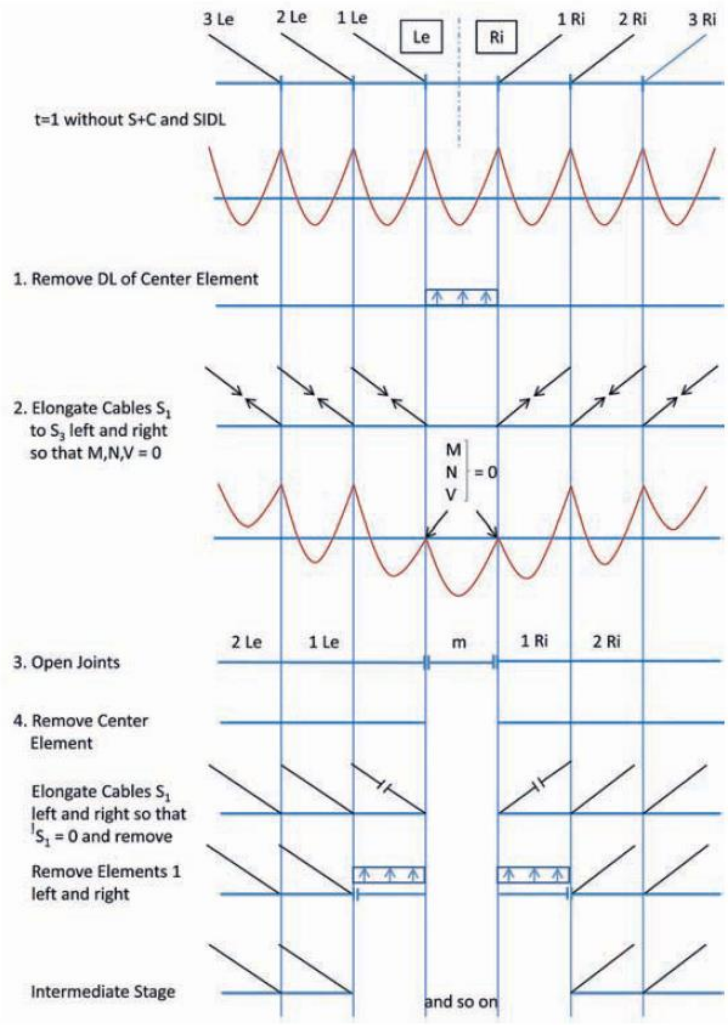

Figure 3.10 Dismantling of Symmetric Bridge (Svensson, 2012)

When derrick is used instead of floating crane, because operations are going backwards its weight should be added to the structure. Tensioned cable or cables are cut then, element is completely supported by derrick and equal weight is applied, this weight goes to derrick by axial load and force couple. Afterwards, deck segment is removed from the system, derrick is moved to the new position and the procedure goes until all the segments are dismantled and derrick is removed. But most importantly, all moment, shear and axial loads should be zero at the end.

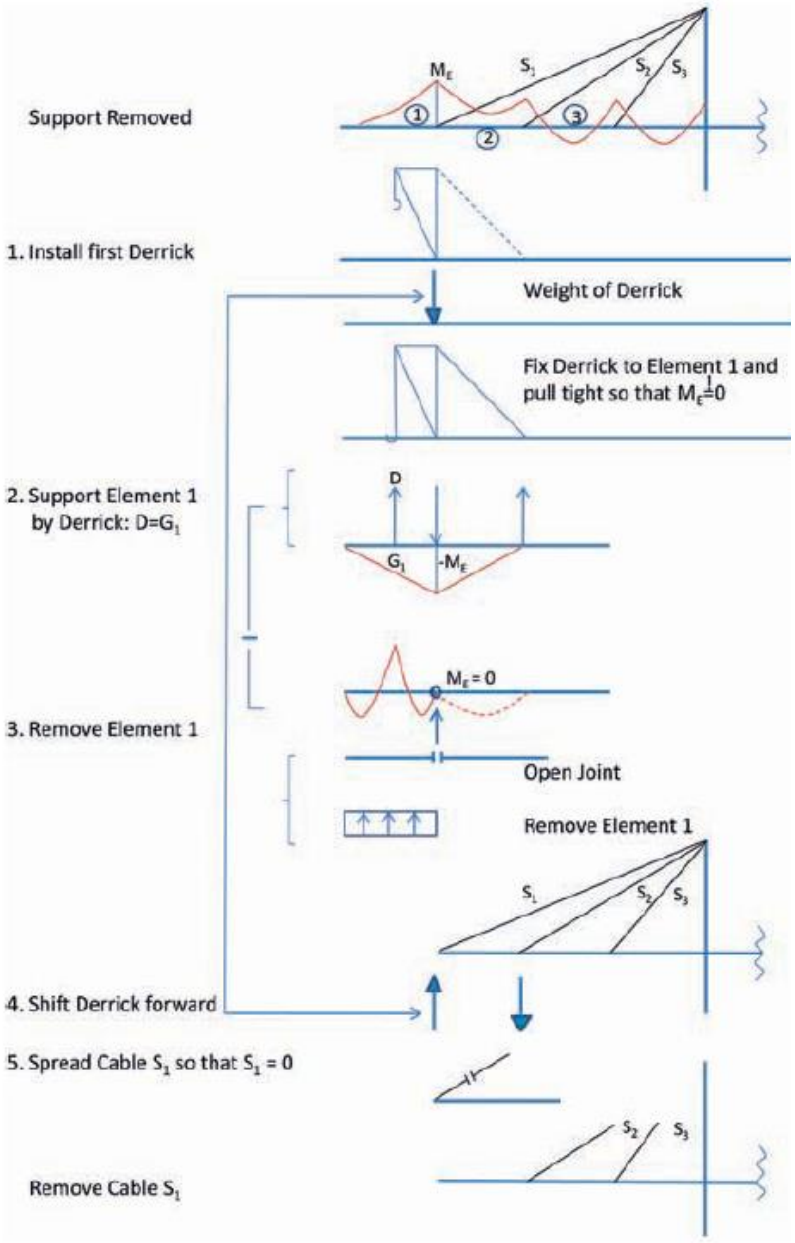

Figure 3.11 Dismantling by Using Derrick (Svensson, 2012)

3.4.2 Forward Construction Stage Analysis

Forward construction stage analysis simulates the real construction sequence. Time dependent effects can be considered precisely. Finding cable tension forces is not easy as backward analysis which gives directly the required tensions. Therefore, some designers use backward analysis first and find the cable tensions. Then they do forward analysis with time dependent properties with these cable forces. In this thesis it will be investigated how different will be the results between backward and forward analysis.

Up to this point different construction stage analysis were defined and explained. In the backward analysis engineer can find the required cable pretension at each stage by dismantling the structure. But in the forward analysis engineer does not know exactly the required cable prestresses.

There is a concept known as tensioning to length. In concrete and steel deck bridges final cable forces had been determined. In this stage cable lengths are the elongated ones which means tension forces stretched the cables to longer lengths. If this elongation is calculated and a shorter cable is installed in construction stages, after completion of the bridge, both the desired cable forces and deflection profile will be achieved. For this purpose, following formula can be used to determine the unstressed length of the cable, $L_{ui.}$(El Shenawy, 2013)

$$L_{ui} = \frac{L_i}{1+\varepsilon_i} = \frac{L_i}{\left(1+\left(\frac{F_{di}}{E_S\, A_{si}}\right)\right)} \qquad (3\text{-}2)$$

L_i = the stressed length of the stay cable i, in the completed structure configuration, at time infinity.

F_{di} = desired cable force at final stage under dead load.

ε_i = elastic strain of the cable under load F_{di}

A_{si} = cross sectional area of the stay cable

In the real construction, unstressed length is calculated and the cable is put on the ground with zero stress and determined unstressed length is marked. Then installed cable is tensioned up to this mark and at the end of the construction, desired final end cable forces are reached. In addition, this adjustment can be achieved in force basis, too. The required elongation is calculated and converted to equal prestress load and this load is applied to the cable.

3.4.3 Construction Stage Analysis of Composite Deck Bridges

Tensioning to length approach explained in the above text can be successfully applied to the concrete and steel bridges. But for composite deck section bridges, the situation is different because there are two materials in the deck and concrete creeps and shrinks. (Schlaich, 2001) suggests a procedure in order to be applied for composite deck bridges. But this procedure has some limitations too as they will be explained in the following paragraphs. Three cases will be explained as Case-A, Case-B and Case-C. In all these cases, continuous beam on rigid supports approach will be used and cables will be tensioned to the unstressed length.

In Case-A, steel portion of the deck is erected first and the cable is tensioned to the unstressed length determined from the final stage. After this operation concrete panels are placed and concrete is poured to the connections. In this case because only steel portion is given all the tension, deck tip deflects up and the desired profile will not be reached at the final stage. Furthermore, in tension operation there will be locked in curvature in the steel part and after concrete casting this curvature will cause the concrete creep when steel part straightens. And because there is locked in moments, desired bending diagram will not be obtained as shown in Figure 3.12.

In Case-B steel part is attached first, then concrete part is cast, cable is installed and tensioned to the determined length. In this case there will be locked in negative moments in the steel part only. Because of this curvature, the deck profile will go

down. Neither deck profile nor desired cable forces and bending moments will be reached.

In Case-C, two step tensioning procedure is applied in order to eliminate the problems in the previous cases. First, steel section which is cantilevering, is applied to the weight of the concrete part and cable is tensioned such that two curvatures in the steel will be equal to each other and no additional creep of concrete will take place. After the deck becomes composite, cable is tensioned to the determined length. By this way desired deck profile and moment diagram will be reached.

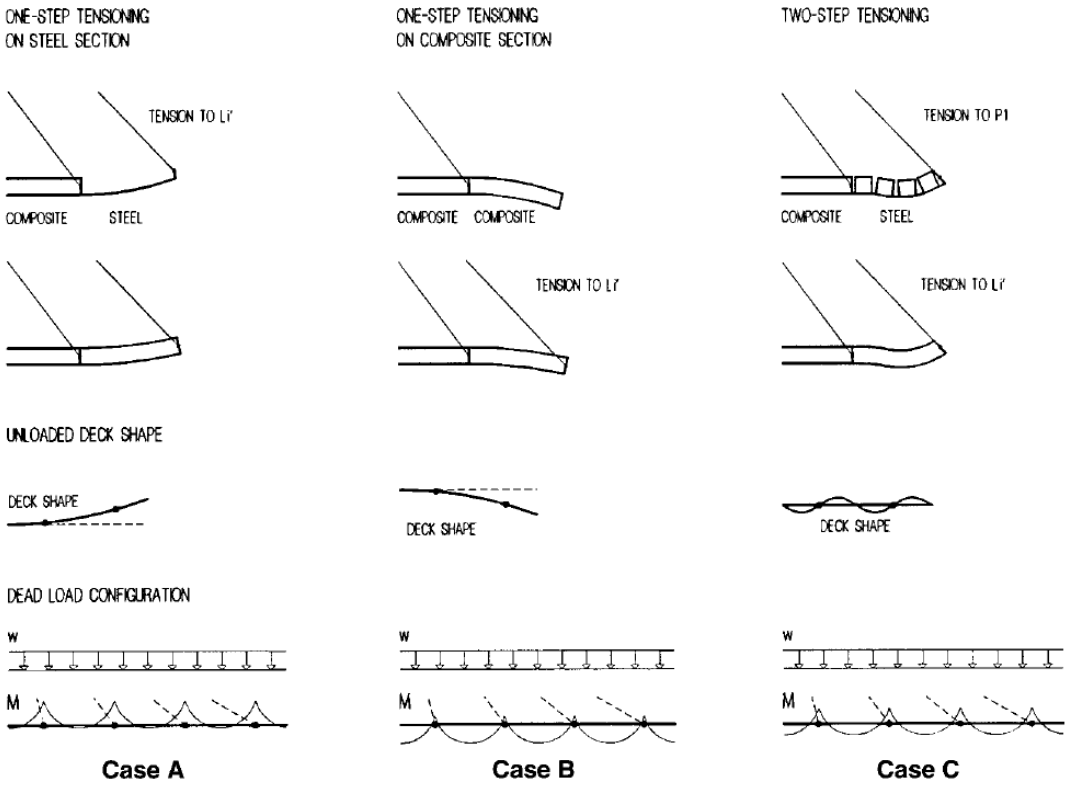

Figure 3.12 Cases of Cable Tensioning (Schlaich, 2001)

It was understood that Case-C also does not solve all the problems in the design. Because achieving the desired results depends strongly on the moment of inertia ratios and difference between centroids of steel only and composite deck section. Therefore, a new method was suggested. Detailed explanation on this topic can be

found in (El Shenawy, 2013). When moment of inertia of steel only to composite section is high and difference between eccentricity of centroids is small, this procedure is giving good results for both internal forces and deck profile, otherwise it is not possible to obtain the targeted values. Before going in to the details of the proposed new method, identifying different creep and shrinkage types would be beneficial. Concrete in composite deck bridges creep in two types. In the first one creep does not develop if the girder is analyzed as if it is a continuously, rigidly supported deck by the cables. This situation was explained in Section 3.3.1.

But for composite bridges there is another type of creep and shrinkage that will mainly occur after the bridge is constructed. This creep is caused by the axial loads of the cables, and under this compression, concrete creeps and these strains create additional axial and bending moments in the section with the shrinkage strains as shown in Figure 3.13. These additional forces due to creep and shrinkage can be considered by stressing and destressing of the cables after construction.

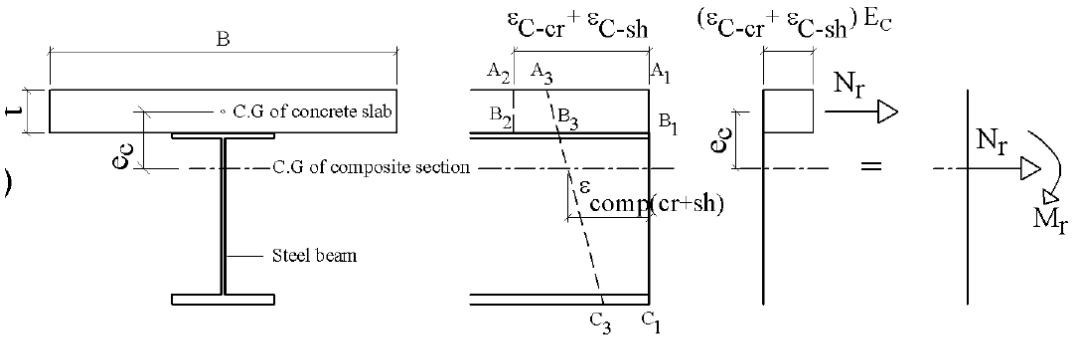

ote: $A_1 B_1$ would move to $A_2 B_2$ if the concrete slab is not restrained by the steel element. Due to the composite action between the concrete slab and the steel element, $A_1 B_1 C_1$ will move to $A_3 B_3 C_3$ under the effect of shrinkage and creep of the concrete slab.

Figure 3.13 Creep and Shrinkage of the Composite Section (El Shenawy, 2013)

Calculation of the normal force and bending moment is as follows,

$$N_{ri} = (\varepsilon_{cr} + \varepsilon_{sh})_i \, E_c \, B \, t \qquad (3\text{-}3)$$

N_{ri} = Normal force due to creep and shrinkage of concrete part.

$(\varepsilon_{cr} + \varepsilon_{sh})_i$ = creep and shrinkage strains of the concrete part.

E_c = Modulus of elasticity of concrete

B = Width of the concrete slab

t = Thickness of the concrete slab

Moment M_{ri} can be found as shown below,

$$M_{ri} = N_{ri}\, e_c \qquad (3\text{-}4)$$

e_c = distance between concrete and composite section centroids.

These forces should be calculated for each deck section and then they should be summed for the entire bridge and applied at the start and finish of the bridge as nodal loads. This will cause change in cable forces and to solve this issue cables will be tensioned or elongated.

Firstly, at time infinity, vertical cable forces will be determined by using continuous girder on rigid supports approach. Cables unstressed lengths will be determined from these forces. Then cable forces to be applied at the first stage of tensioning will be determined. This force can be determined, as there will be no differential settlement between the two ends of the girder as shown in Figure 3.14 and in the below formula.

$$P_1 = 3\,\frac{w\,L}{(8\sin\alpha)}\,\frac{1}{\left(1+\frac{\frac{3}{2}e}{L}\cot\alpha\right)} \qquad (3\text{-}5)$$

w = Uniformly distributed dead weight of the deck

α = Cable inclination angle

e = Distance between centroid of steel and composite section

L = Length of the segment

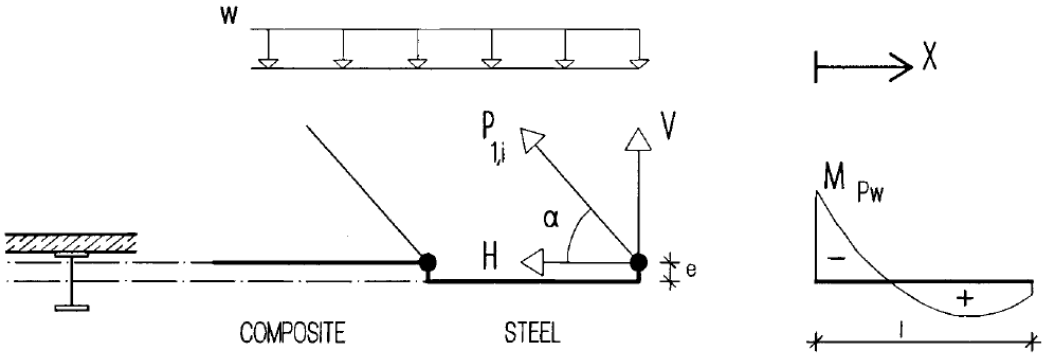

Figure 3.14 Initial Force Determination (Schlaich, 2001)

Construction stages will start with the first tensioning load, then cable will be stressed up to the determined length. All the stages will follow this sequence and final configuration will be reached at the end. Because time dependent properties were defined in the computer model, deflected shape, bending moment diagram and cable forces will change due to creep and shrinkage and will not be equal to the initially calculated final forces at time infinity. Therefore, in the analysis change of cable forces between end of construction and time infinity is calculated. And this difference should be subtracted from the firstly calculated final desired cable forces. Cable forces calculated immediately at the end of the construction should be made equal to the subtracted amount by tensioning or lengthening the cables.

By applying the final desired cable forces to the deck at time infinity, camber values may be found by taking the mirror of the deflected shape of the bridge with respect to the desired profile.

In the forward construction stage analysis two models can be used. In the first model the deck will be considered fully composite and cable tensions will be given in one step. In the second model sections will be steel only section and first tensioning will be applied, after it becomes composite, second tensioning will be given. The procedure will continue in this sequence. First model will be used in order to determine jacking forces and middle section closure forces correctly; same forces will be applied to the second model in order not to lock additional forces to the structure.

3.5 Static Analysis of Cables

The primary load-bearing components in cable-stayed bridges are the stay cables. While the literature comprehensively explains the statics and behavior of these cables, the information is often disorganized and fragmented. In the subsequent text, the most crucial properties will be outlined to facilitate analysis and enhance comprehension of cable behavior.

First of all, some definitions related to the topic will be explained. Chord is the line that connects the two ends of the cable stay as a straight line. Sag is the deformation caused by the self-weight of the cable and is measured from the chord line to the cable itself. Chord force T is the force that acts along the chord. Horizontal force H acts in the global horizontal axis and is constant throughout the cable section. These are described in the below Figure 3.15.

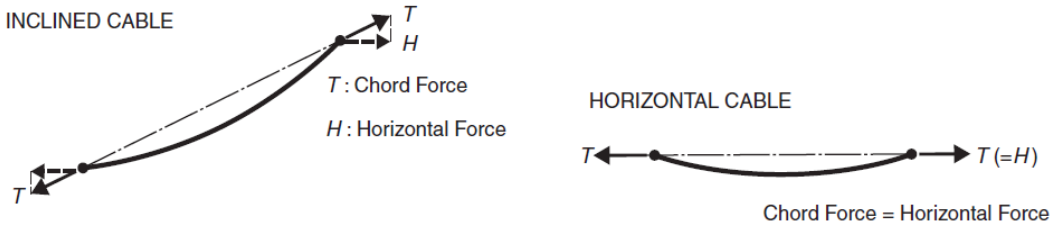

Figure 3.15 General Definitions of a Stay Cable (Gimsing & Georgakis, 2011)

Because sag occurs in cables, they behave different than truss elements. Truss element's rigidity is constant but cable rigidity changes with the amount of sag as shown in the Figure 3.16. Furthermore, from the figure it can be concluded that cable stiffeness is nonlinear and inversely proportional to the sag amount. In order to consider this stifness change in analysis, a linearization of the elasticity modulus can be used as an approximation. Tangent modulus, E_{tan} is defined for this purpose and can be used in permenant dead load conditions. But if transient loads act to the cable, secant approximation E_{sec} gives better results than E_{tan}. this definitions can be followed from Figure 3.17 as shown below.

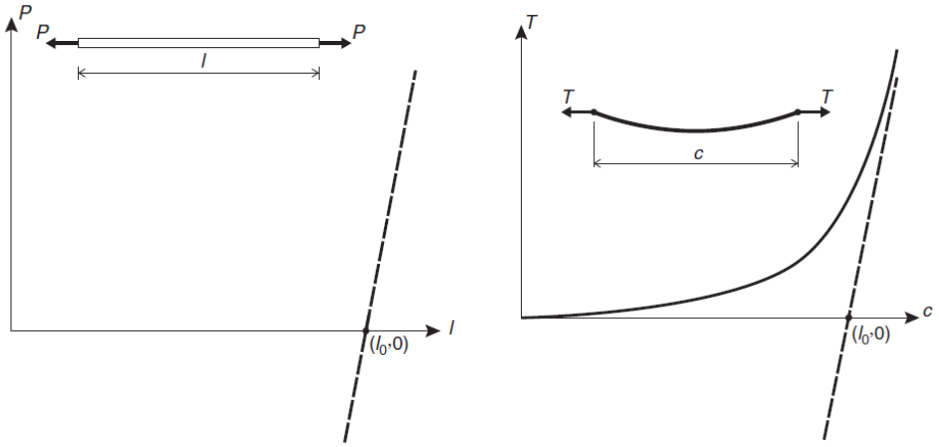

Figure 3.16 Force Deflection Curves of Truss and Cable Element (Gimsing & Georgakis, 2011)

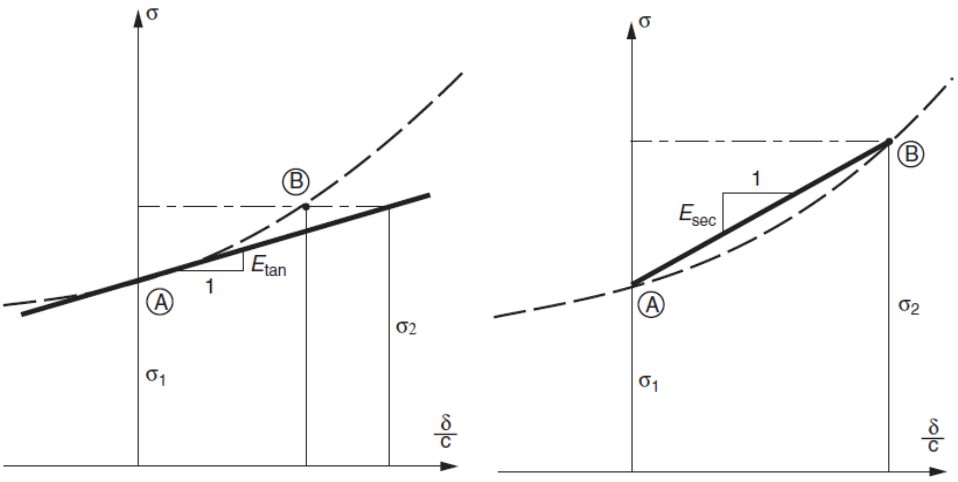

Figure 3.17 Tangent and Secant Stiffness (Gimsing & Georgakis, 2011)

Static analysis of cables can be discussed as follows defined by (Gimsing & Georgakis, 2011). A distributed load is acting perpendicular to the cable. This situation is similar to the simply supported beam with the same loading. Internal forces in the beam can be determined by static equilibrium equations and they can be used in calculation of cable forces, sag and horizontal constant cable force etc. as shown in Figure 3.18.

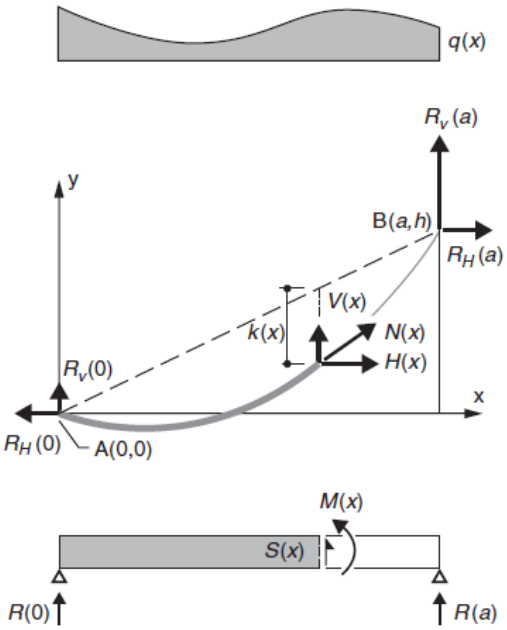

Figure 3.18 Cable and Equivalent Beam Forces and Reactions (Gimsing & Georgakis, 2011)

$$R_h(0) = R_H(a) = H(x) = constant = H \tag{3-6}$$

$$R_v\,(0) = R(0) - H\left(\frac{h}{a}\right) \tag{3-7}$$

$$R_v\,(a) = R(a) - H\left(\frac{h}{a}\right) \tag{3-8}$$

$$V(x) = S(x) + H\left(\frac{h}{a}\right) \tag{3-9}$$

$$y(x) = -\frac{M(x)}{H} + \left(\frac{h}{a}\right)x \tag{3-10}$$

$$k(x) = \frac{M(x)}{H} \tag{3-11}$$

Cable length can be found approximately as,

$$s = a\left\{1 + \left(\frac{8}{3}\right)\left(\frac{h}{a}\right)^2 - \left(\frac{32}{5}\right)\left(\frac{h}{a}\right)^4\right\} \tag{3-12}$$

Tension in the cable can be found as,

$$T = H/\cos\theta \tag{3-13}$$

θ = Tangent angle at a point on the cable

Above discussed cable was the one with vertical distributed loading, in the cables that are tensioned between ends and subjected to its own weight shows catenary equation as given in the following formula (catenary shape equation).

$$y = T/g_{cb}\left[\cosh\left(\frac{\frac{g_{cb}}{T}(x-1)}{2c}\right) - \cosh\left(\frac{g_{cb}}{2T}\right)\right] \tag{3-14}$$

g_{cb}= cable dead load per unit length

Cable stiffness calculation can be done by using two different magnitudes of loads that act along the chord length. Two catenary shape equations are produced by this way. Division of these two equations will give ratio of change in cord length to initial chord length. The formulation will not be given here, but end result after mathematical manipulations for inclined cable is given which is a linearized equivalent cable modulus of elasticity. This formula is named as Ernst formula for cables and shown both graphically in Figure 3.19 and by the following formulation.

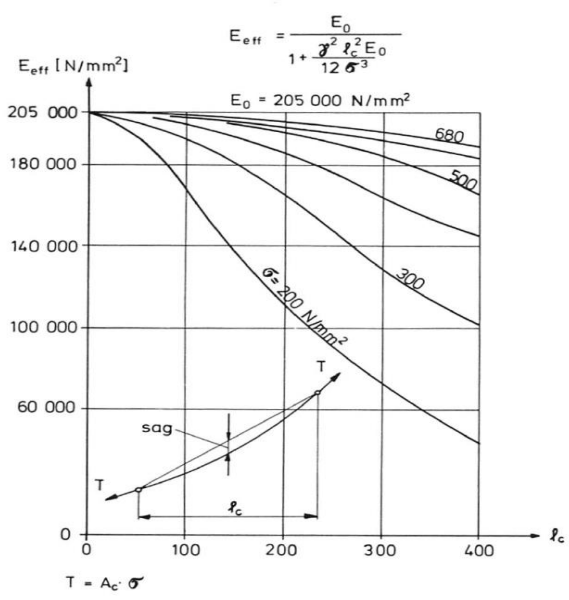

Figure 3.19 Change of Effective Elasticity Modulus with Respect to Cable Horizontal Length and Sag, (Leonhardt & Zellner, 1980)

Ernst formula,

$$E_{eff} = \frac{E_0}{1+\frac{\gamma^2 l_c^2 E_0}{12\sigma^3}} \quad (3\text{-}15)$$

E_0=Elasticity modulus of cable steel

γ=Weight per unit volume of cable

l_c=Horizontal projection length of inclined cable

σ=Tensile stress applied to cable

Ernst formula is used to apply equivalent axial member properties instead of using nonlinear cable elements. If the tensile stress in the cable is increased, sag reduces and effective modulus increases by the cube of stress applied. Therefore, to obtain an axially rigid cable, more axial tensile stress should be given if the cross-sectional area is kept constant. By this way analysis are simplified and calculation time is reduced.

Another version of the above formula can be used when the cable forces change due to different loadings like live load. In this case formula is updated to the form shown below by using secant elasticity modulus.

$$\frac{1}{E_{sec}} = \frac{1}{E} + \frac{\frac{\gamma^2 a^2}{24}(\sigma_1+\sigma_2)}{(\sigma_1^2\sigma_2^2)} \quad (3\text{-}16)$$

where,

σ_1=Initial tensile stress applied to cable

σ_2=Increased or decreased tensile stress applied to cable

By using Ernst formula, the cable with sag can be modeled as straight truss element with an equivalent modulus of elasticity and with same cross-sectional area as shown in Figure 3.20. Also, in the real cable tension force N can be divided into two force components as T and V. V is equal to the half of the weight of the cable. And the largest tension occurs at the top of the cable. When computer model is established

by using equivalent truss element these two vertical forces (half of the dead load) are assigned as point loads as if they are dead loads of the girder. After the analysis has been finished and tensile force T is found, tangential tension force in the cable can be found by the cosine law. Detailed analysis and obtaining ratio of N_t to T can be found in Gimsing & Georgakis, (2011). Based on the Figure 3.21 showing N_t/T ratio, it can be concluded that up to horizontal cable lengths of 200m using T as tensile force instead of N_t introduces error less than one percent. Therefore, tensile force T calculated by using equivalent truss element can be used in the design of the cable instead of N value that is calculated in real catenary element.

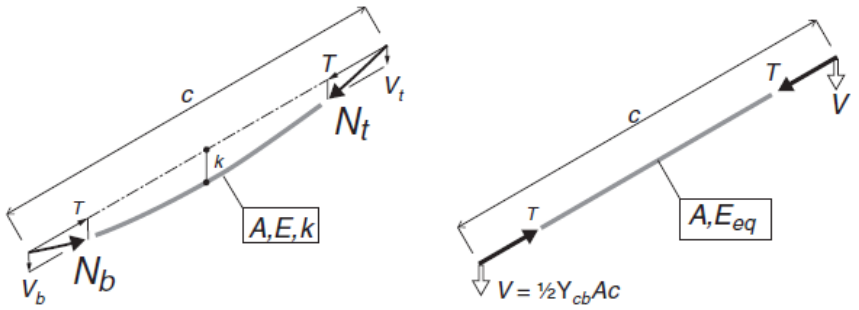

Figure 3.20 Real and Idealized Equivalent Truss Stay Cable Element (Gimsing & Georgakis, 2011)

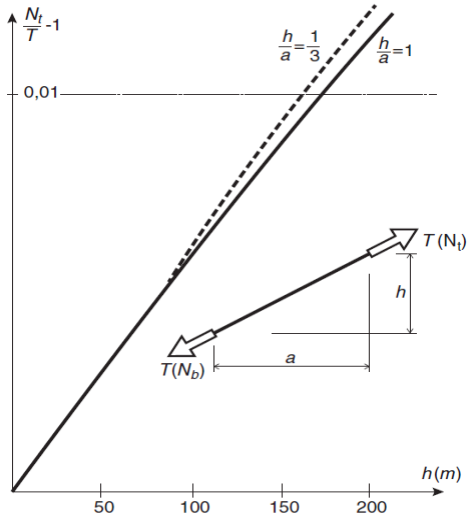

Figure 3.21 Error Introduced in to the Calculations by Using T instead of N_t (Gimsing & Georgakis, 2011)

CHAPTER 4

CONCRETE CABLE-STAYED STRUCTURE

In this chapter of the thesis, a comparison was initially made between two structural analysis programs, namely Larsa 4D and Midas Civil. The comparison involved evaluating the performance of these programs in modeling catenary cable elements, handling geometric nonlinearity with large displacements, and their approach to match casting. Subsequently, a basic concrete cable-stayed structure was analyzed, and the obtained results were assessed. Both computer programs were employed simultaneously for the purpose of this analysis. The results were further compared, focusing on the most advanced analysis using catenary elements to represent the cables, while also considering time-dependent material properties and geometric nonlinearities. Then the study proceeded to evaluate the effects of analysis time step length on the obtained results. This analysis aimed to assess how variations in the time step length could impact the accuracy of the simulation outcomes.

4.1 Comparison of Larsa4D and Midas Civil

In this section, the cable element formulations of the two programs were examined first. Subsequently, an analysis of geometric nonlinearity with large displacements was carried out. Lastly, a comparison was made between the two analysis software regarding one of the most commonly used casting techniques, known as match casting procedure.

4.1.1 Analysis of a Cable

In this section, an analysis was conducted on a cable element with a length of 304.8 meters and a sag of 30.48 meters by using the data from paper (Vu, et al., 2012) . A

point load of 35.586 kN was applied at a distance of 121.94 meters from the left support, as illustrated in Figure 4.1. Additionally, important properties such as cross-sectional area, elastic modulus, self-weight, and unstrained length of the cables can be found in Table 4.1.

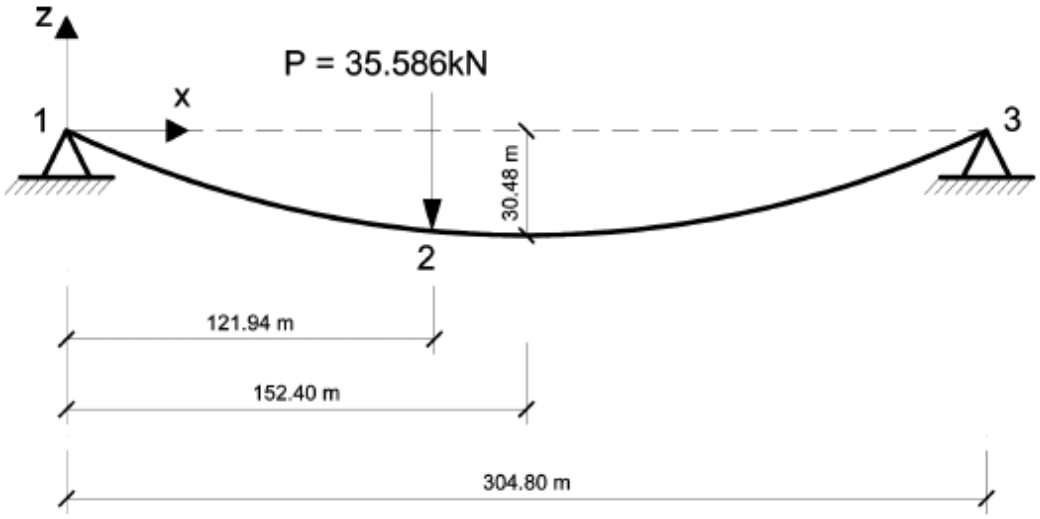

Figure 4.1 Cable Element Geometric Properties and Loading Positions (Vu et al., 2012)

Table 4.1 Properties of Cables (Vu et al., 2012)

Description		Magnitude
Cross-sectional area		5.484 cm^2
Elastic modulus		13,100 KN/cm^2
Self weight		46.120 N/m
Unstrained length	Segment 1-2	125.88 m
	Segment 2-3	186.850 m

A nonlinear analysis was carried out, and the results were presented in Table 4.2, showing the displacements of point 2 for both Midas Civil and Larsa4D. These results were then compared with the benchmark results. The comparison leads to the conclusion that the catenary cable element formulations are consistent between both software programs.

Table 4.2 Comparison of Displacement Results

Displacement (m)	*Larsa 4D*	*Midas Civil*	*Benchmark*
Vertical	5.626 (%0)	5.625 (%0)	5.625
Horizontal	0.859 (%0)	0.858 (%0)	0.859

4.1.2 Geometric Nonlinearity With Large Displacement

In this section of the thesis, a benchmark problem was selected, as defined in Roark & Young, (1975) in their book titled "Formulas for Stress and Strain." A beam element with cross-sectional properties, including an area of 3.83 in^2, a moment of inertia of 11.3 in^4, a length of 100 inches, and an elastic modulus of 29,000 k/in^2, was chosen. This beam was subjected to bending by 180 degrees at the tip of the cantilever, as illustrated in Figure 4.2. First, the structure was divided into 20 elements and then only one element was considered in the analysis and results were compared in Table 4.3 and 4.4 respectively.

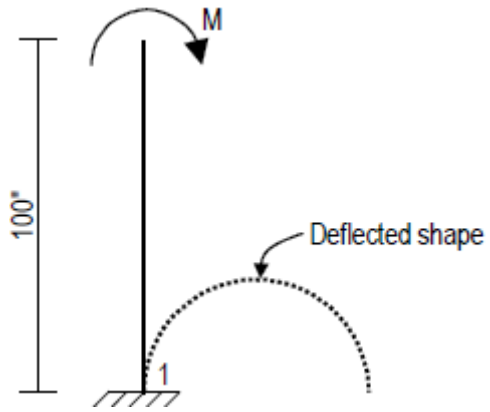

Figure 4.2 Beam Element Bent About Its Tip (Roark & Young, 1975)

According to Table 4.3 (20 elements), it can be concluded that the differences between Larsa 4D and Midas Civil are negligible, to the extent that they would not significantly impact the analysis. However, it's important to note that in real cable-stayed bridges, the span lengths are much longer, and the slenderness ratios are

considerably higher compared to the benchmark problem. As a result, it becomes evident that these differences between computed values will increase to higher levels. When the structure was analyzed as a single undivided element (1 element), the differences in results between Larsa 4D and Midas Civil were more pronounced, as shown in Table 4.4. This study highlights the significance of element division in the analysis.

Table 4.3 Comparison of Analysis Results (20 Elements)

	Larsa 4D	*Midas Civil*	*Benchmark*
Vertical Displacement (in)	100 (%0)	100 (%0)	100
Horizontal Displacement (in)	63.662 (%0)	64.998 (%2.1)	63.662
Moment (k-in)	10295 (%0)	10172 (%1.2)	10295

Table 4.4 Comparison of Analysis Results (1 Element)

	Larsa 4D	*Midas Civil*	*Benchmark*
Vertical Displacement (in)	100 (%0)	100 (%0)	100
Horizontal Displacement (in)	63.789 (%0.2)	65.762 (%3.3)	63.662
Moment (k-in)	10285 (%0.1)	10017 (%2.7)	10295

4.1.3 Match Cast Approach

In this section, the most commonly used casting procedure, the "match cast approach," of the programs with each other was compared. Procedure details can be found in Chapter 4.4.2. Each segment was connected tangentially to the previous one, representing the real construction process. The geometric and sectional properties are the same as the structure defined in Chapter 4.2, but without cables and their pre-tension forces. Each 20m segment was added to the next one following the shape defined in each program's algorithm. Results can be tracked in Table 4.5.

Cables would be tensioned to varying values until reaching their unstressed lengths, which undeniably altered the moment diagrams in the superstructure. Therefore, these three conceptual analyses demonstrated that the accumulation of differences between the two programs in calculating geometric nonlinearity with large displacement and the match cast approach can yield scattered results in a large-scale example.

Table 4.5 Comparison of Analysis Results

	Larsa 4D	*Midas Civil*	*Difference (%)*
Vertical Displacement (m)	20.757	20.749	0.04
Horizontal Displacement (m)	3.143	3.139	0.13
Rotation (rad)	0.35	0.349	0.29

4.2 Information About the Structure

The main dimensions of the structure and cables were taken from the thesis " Form Finding for Cable-Stayed and Extradosed Bridges" (El Shenawy, 2013). The system has four spans with equal lengths of 20m and a total length of 80m. Four cables were attached to the beam structure at every 20m. The location where all the cables are anchored is 40m above the superstructure, as in Figure 4.3. The start of the beam and anchor points of the cables were modeled as fixed supports.

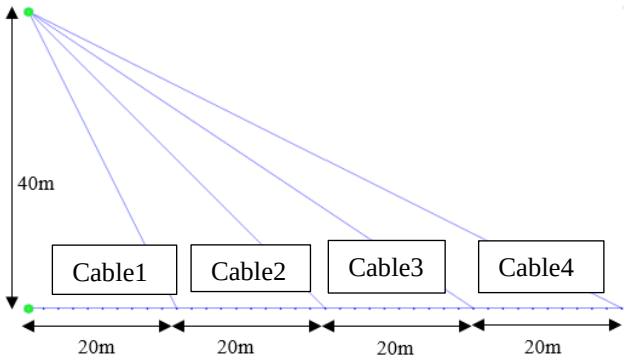

Figure 4.3 General Dimensions of the Structure

The beam and cable have rectangular and solid round sections, respectively. Cross-sectional and material properties are shown in Table 4.6 and Table 4.7. The numbering of nodes can be found in Appendix A.

Table 4.6 Cross Sectional Properties of Girder and Cables

	H(m)	*B(m)*	*Area(m^2)*	*Asy(m^2)*	*Asz(m^2)*	*Ixx(m^4)*	*Iyy(m^4)*	*Izz(m^4)*
Girder	2	1	2	1.67	1.67	4.57e-1	6.67e-1	1.67e-1
Cable1	-	-	7.5e-3	-	-	-	-	
Cable2	-	-	9.15e-3	-	-	-	-	
Cable3	-	-	1.37e-2	-	-	-	-	
Cable4	-	-	5.85e-3	-	-	-	-	

Table 4.7 Material Properties of Girder and Cables

	Unit Weight (kN/m^3)	*Elasticity Modulus (kN/m^2)*	*Thermal Coefficient (1/C)*
Girder	100	35000000	1e-5
Cable1	78	200000000	1e-5
Cable2	78	200000000	1e-5
Cable3	78	200000000	1e-5
Cable4	78	200000000	1e-5

4.3 Desired Final Configuration of the Structure

As explained in Section 3.3.1, cable-stayed bridges with concrete decks usually and preferably are designed as at time infinity, girder would have a moment distribution like at cable anchor points; there are roller supports that are fixed in the gravity direction. This way, creep in that direction is eliminated, and no additional forces are

expected because of time-dependent material properties. Target bending moment diagram is shown in Figure 4.4.

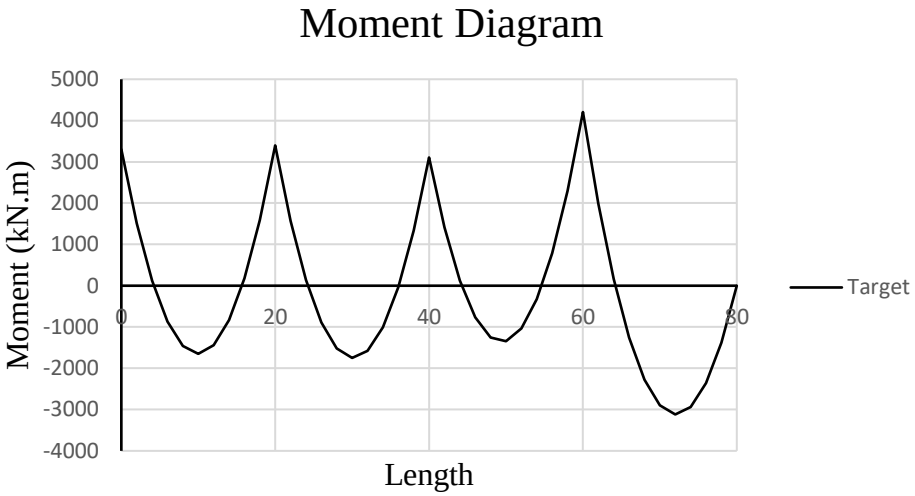

Figure 4.4 Target Moment Diagram of the Structure at Time Infinity

4.4 Analysis of the Structure

Structure was analyzed by using linear Truss, Ernst Truss and Catenary element respectively with and without time-dependent material effects and with and without geometric nonlinearity. Results of these different analysis were compared to each other at the end.

4.4.1 Backward Construction Stage Analysis

Backward procedure is used in cable stayed bridge construction stage analysis. As explained in 3.4.1, this type of analysis consists of dismantling the finished structure in the backward direction. The proces is shown in Figure 4.5.

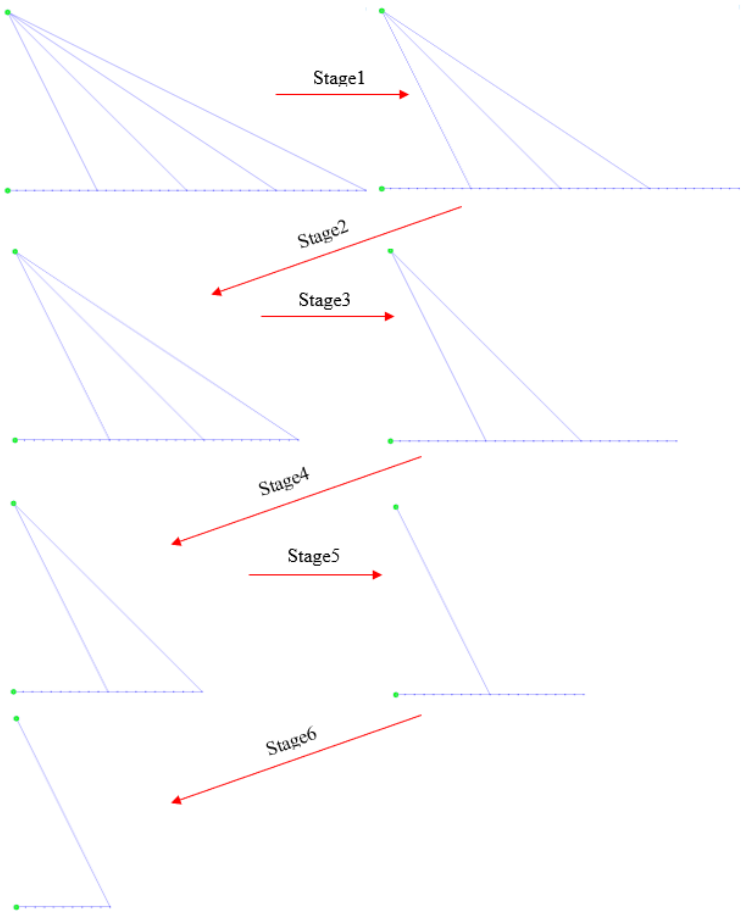

Figure 4.5 Backward Construction Stage Analysis Steps

4.4.2 Forward Construction Stage Analysis

Forward construction stage analysis follows the same sequence as the bridge is constructed at the site, as shown in Figure 4.7. The main difference between modeling these linear models is how the elements are added to each other. Because the structure continuously deforms at each stage in the forward construction method; standard, hinged, or matched cast procedures should be used. In bridge engineering applications, matched cast connection of nodes is used in practice because, in this way, the formwork can be attached to the finished segment tangentially, which is the desired operation as shown in Figure 4.6. Because of this operation on how the parts are connected, backward and forward analysis results for displacements will never

coincide. In analysis, cable forces that are determined from the backward analysis are directly used.

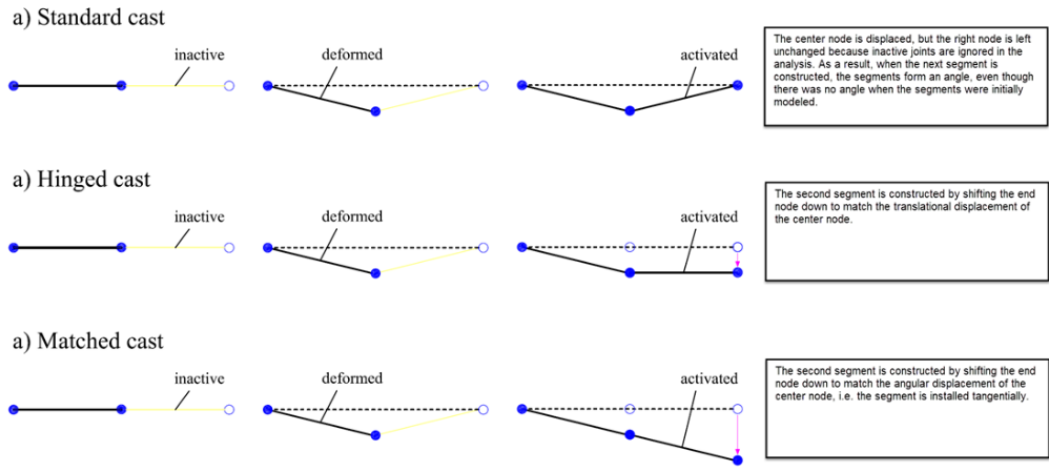

Figure 4.6 Casting Types of the Newly Erected Segment (Midas Civil)

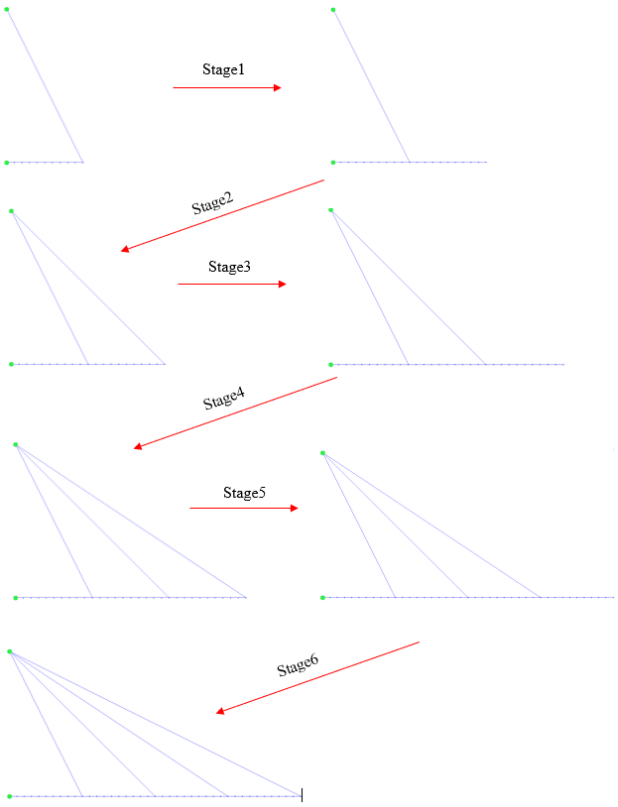

Figure 4.7 Forward Construction Stage Analysis Steps

4.4.3 Linear Truss Element

A truss element is a basic uniaxial tension-compression only element with two nodes in three-dimensional space. This element undergoes only axial deformations. It is used to compare construction stage analysis results with other elements like the Ernst truss and catenary cable element.

4.4.3.1 Comparison of Analysis Methods Results (Without Time-Dependent Material Properties) (Linear Truss Element)

Cable Forces for both methods and change in tension in each cable can be found in Figure 4.8 to Figure 4.11.

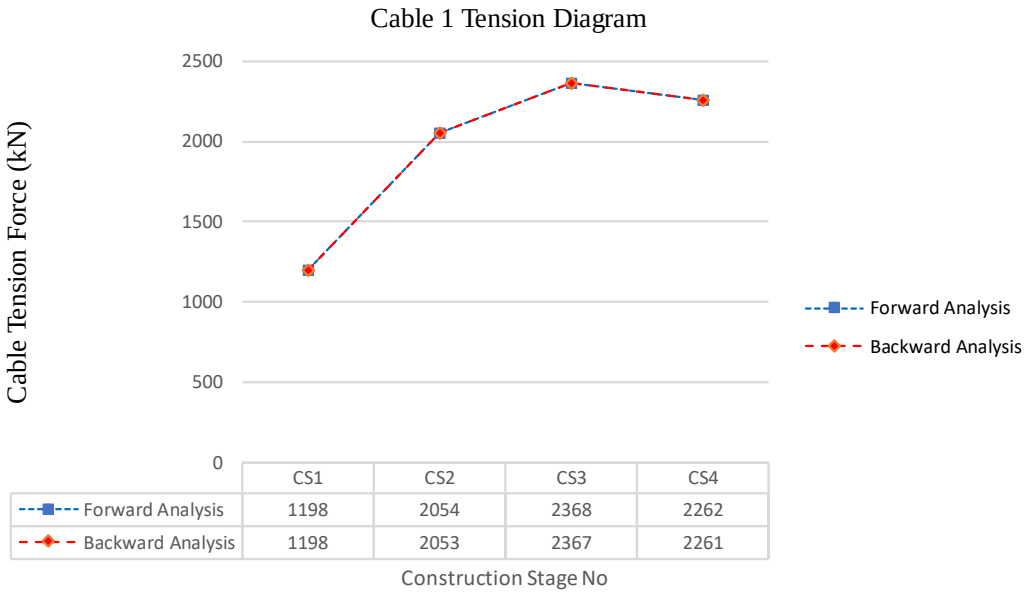

Figure 4.8 Cable 1 Tension Force Change (Truss Element)

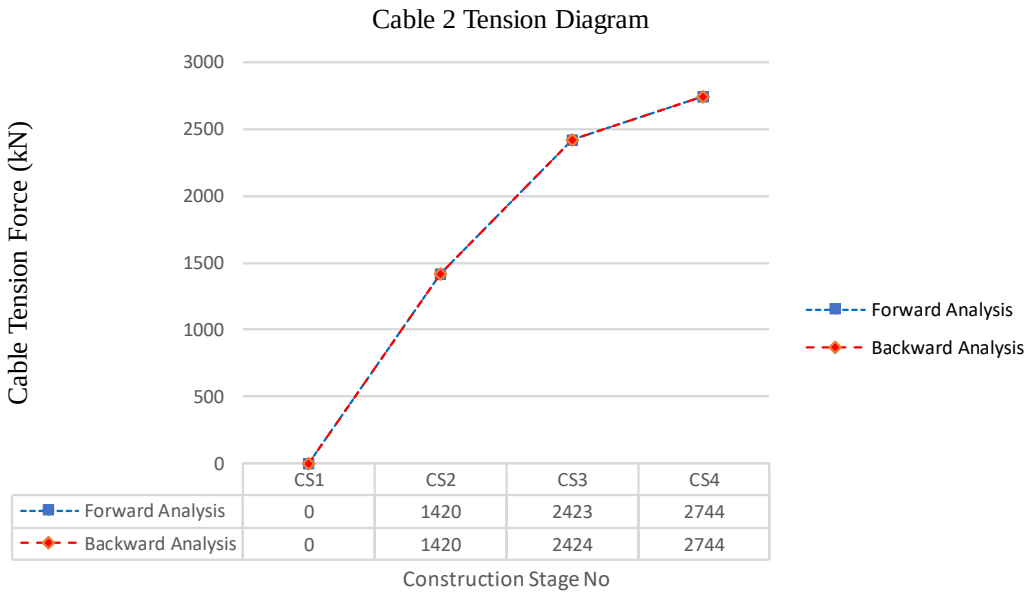

Figure 4.9 Cable 2 Tension Force Change (Truss Element)

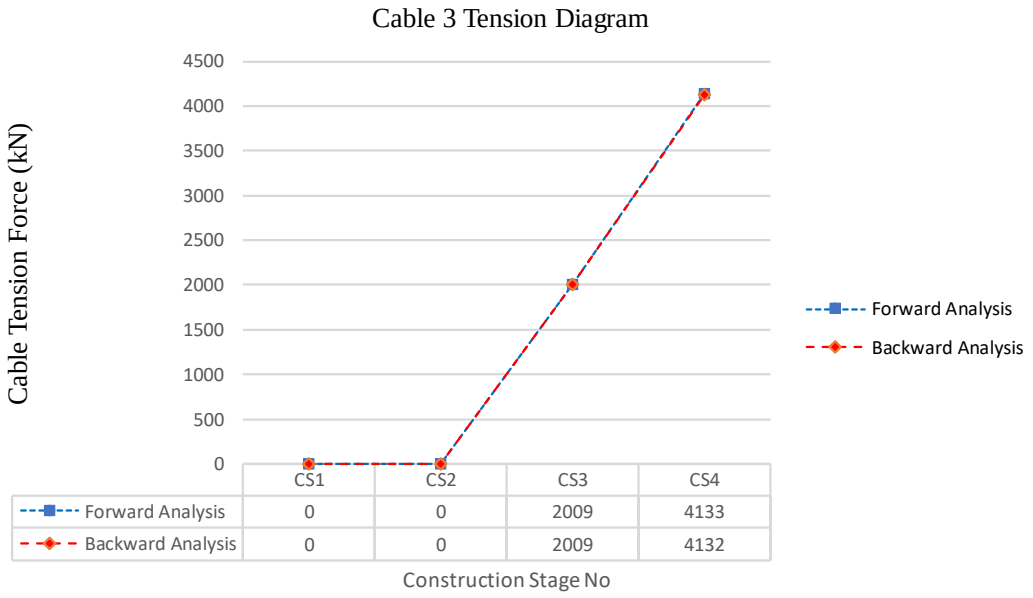

Figure 4.10 Cable 3 Tension Force Change (Truss Element)

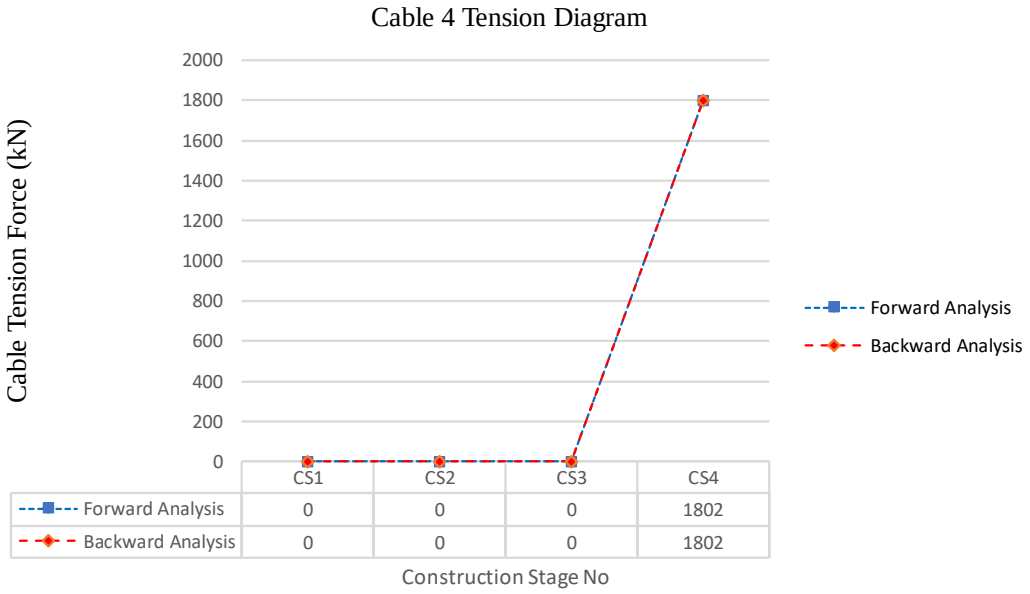

Figure 4.11 Cable 4 Tension Force Change (Truss Element)

As expected, and seen from the above figures there is not a significant difference (less than %0.03) in cable tension forces between backward and forward analysis, because both analyses are linear, cable stiffnesses are not changing during the stages and geometric nonlinearity is not considered. Without P-Δ effects moment diagram is same in both analysis methods at the end. The moment diagram can be seen in Figure 4.12.

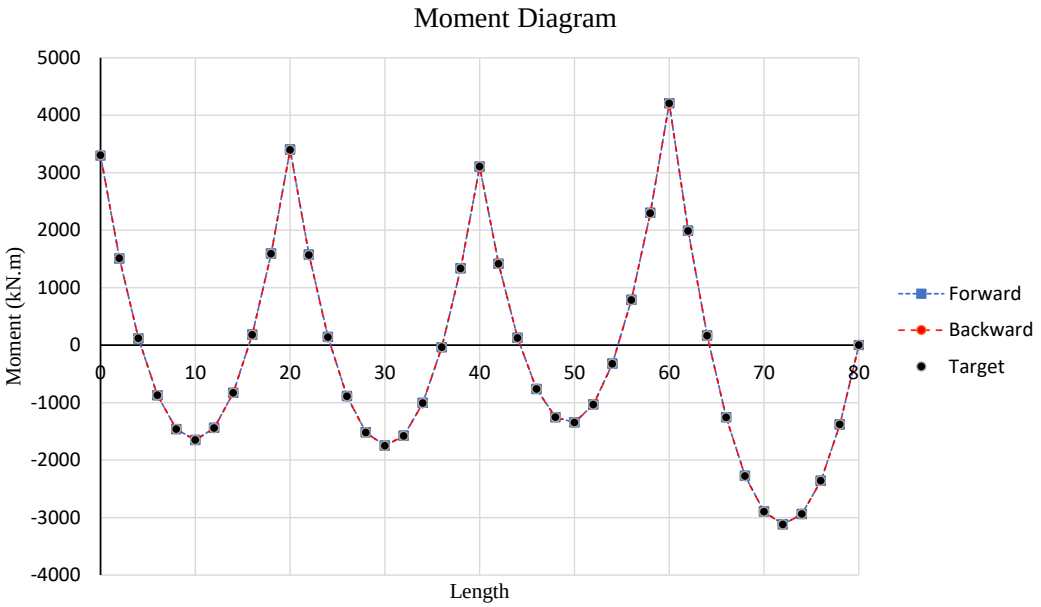

Figure 4.12 Backward, Forward Analysis and Target Moment Diagram (Truss Element)

Therefore, if linear truss elements are used as cable elements, cable forces, and end moment diagrams will not deviate from each other. In Figure 4.13, P-Δ effects were also considered, but only a little difference (%5.5) is observed because in cable-stayed bridges, although more displacements are occurring compared to other bridge types, P-Δ has a limited effect on the results. From bridge engineering design perspective, these changes in the moment diagram are not significant because the load case that creates rigorous nonlinear effects is the moving load case.

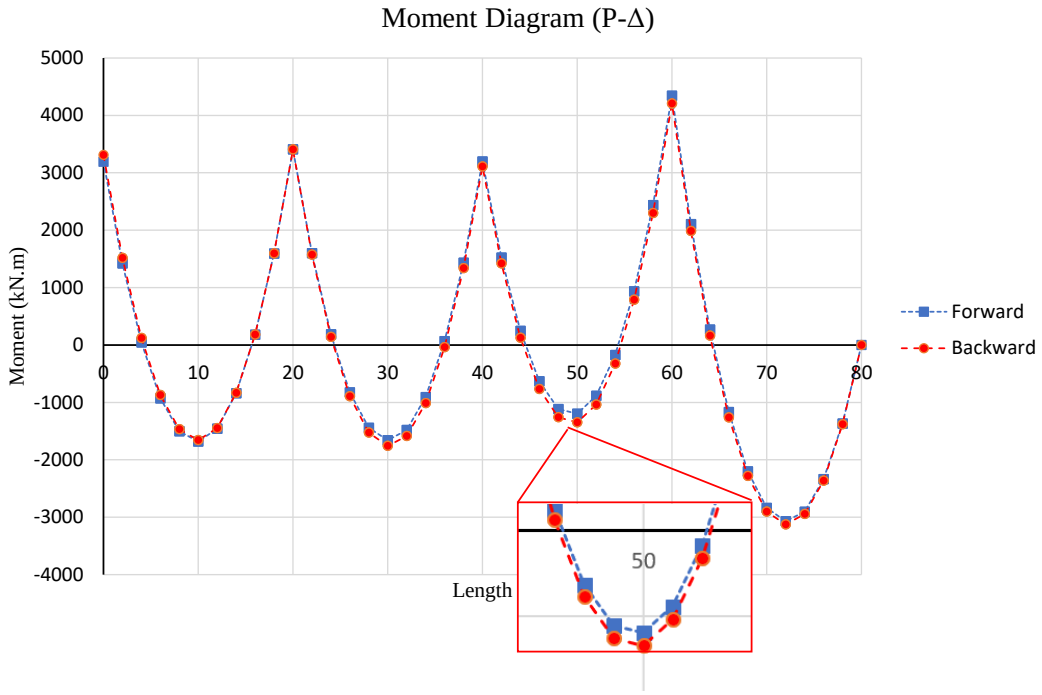

Figure 4.13 Backward and Forward Analysis Moment Diagram (P-Δ) (Truss Element)

4.4.3.2 Comparison of Analysis Methods Results (With Time-Dependent Material Properties) (Linear Truss Element)

In this part of the thesis, time-dependent material properties will be considered, and results will be re-evaluated. In backward construction stage analysis, it is not possible to consider these effects because they can only be calculated in the increasing time steps. However, in the backward analysis, creep and shrinkage strains will be calculated from time t=1 to t=25000 days, converted into positive temperature increases, and subsequently applied to the beam elements as positive temperature loading. This is because these strains have already resulted in shortening in the girder. Calculation of creep coefficient, shrinkage strain, modulus of elasticity, and development of strength can be found in Appendix B. For the calculation of temperature loading, Appendix C can be followed.

In forward construction stage analysis, time-dependent material properties will be taken into account in small time steps (1 day) and added to each other. If time steps are chosen in small intervals more accurate results will be obtained. CEB- FIP Model Code 1990 was used for this analysis. In both backward and forward analysis P-Δ effect was taken into account. Cable Forces for both methods and change in tension in each cable can be found in Figure 4.14 to 4.17.

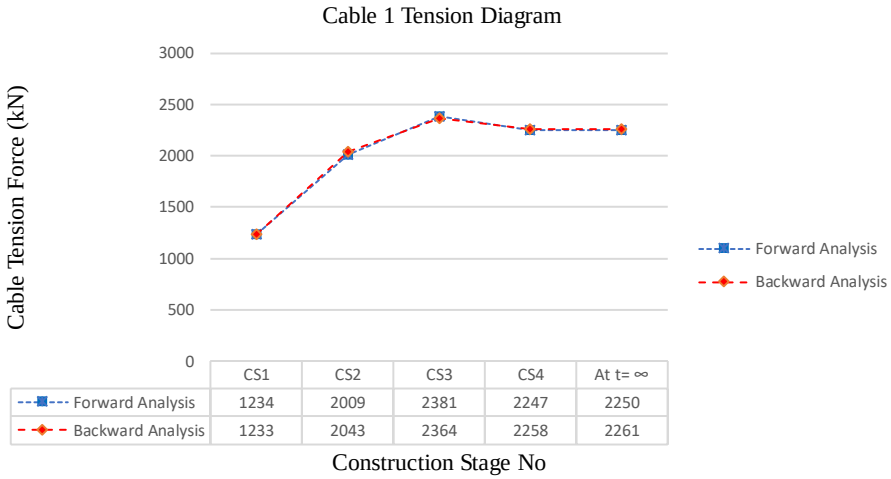

Figure 4.14 Cable 1 Tension Force Change with Time-Dependent Material (Truss Element)

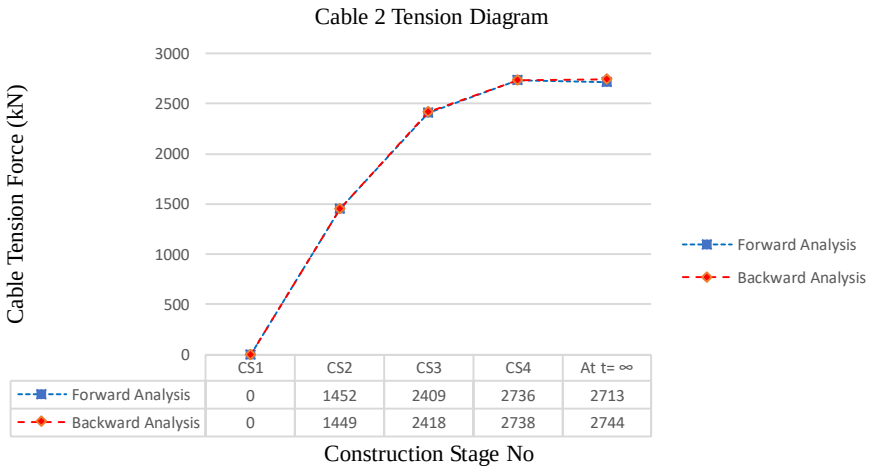

Figure 4.15 Cable 2 Tension Force Change with Time-Dependent Material (Truss Element)

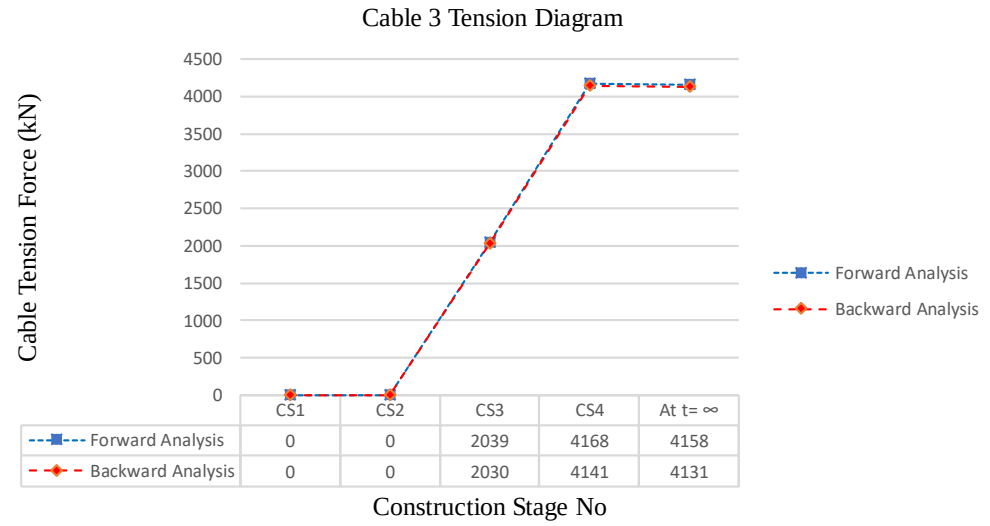

Figure 4.16 Cable 3 Tension Force Change with Time-Dependent Material (Truss Element)

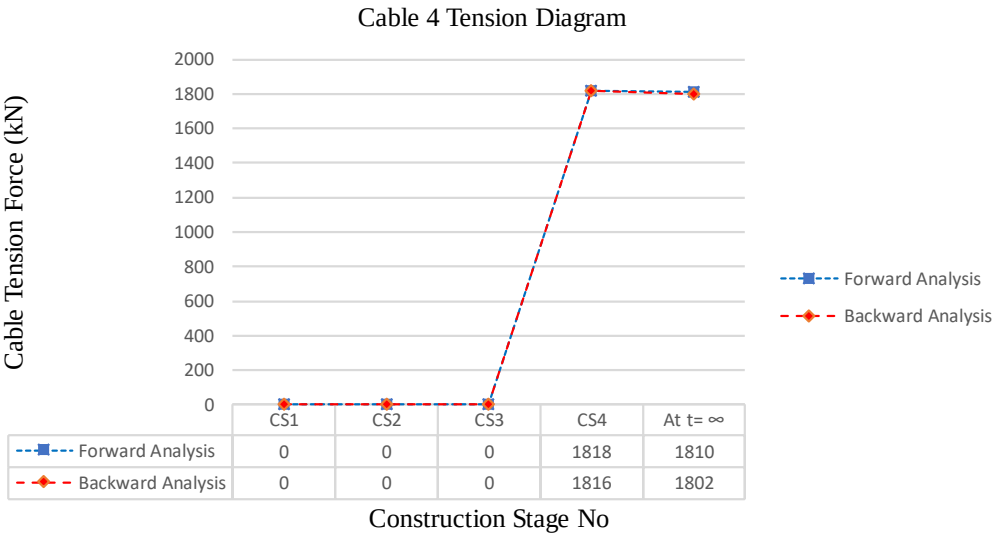

Figure 4.17 Cable 4 Tension Force Change with Time-Dependent Material (Truss Element)

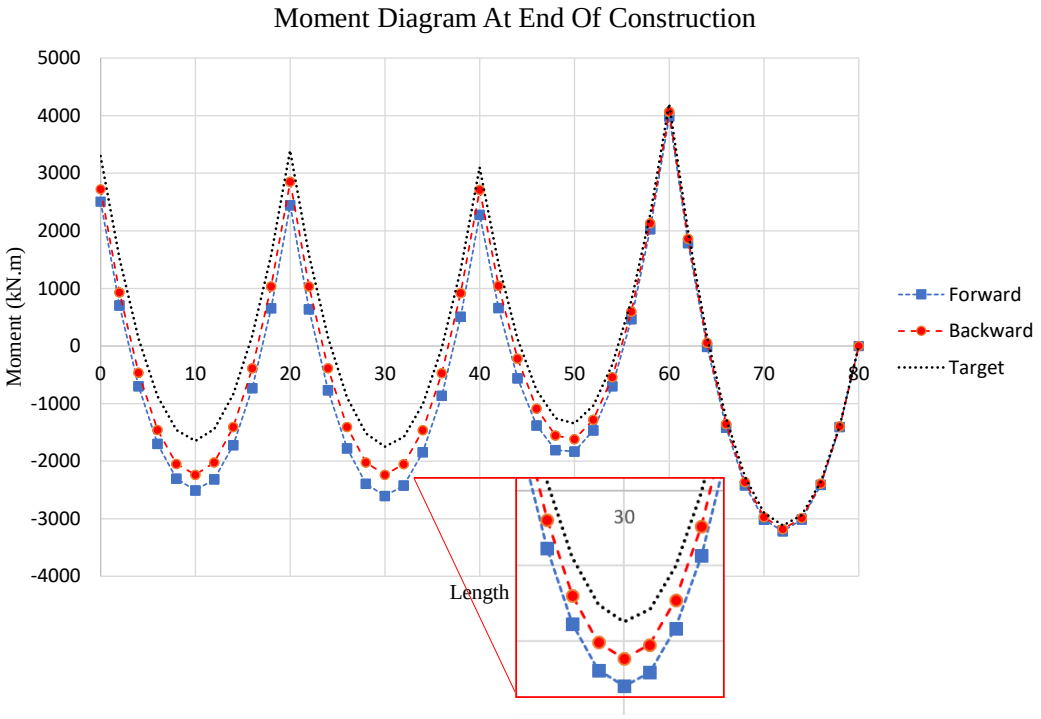

Figure 4.18 Backward, Forward Analysis and Target Moment Diagram with Time-Dependent Material (Truss Element)

As can be seen from cable force graphs, values are very close to each other but not exactly the same (max. difference, %1.6). In the moment diagram, when the construction process has just finished, there is a difference in values (approx. %15), especially in 1,2, and 3 numbered mid-spans and at cable support points. In Figure 4.12, which does not consider the time-dependent effects, the backward and forward analysis moment diagram has the same values. Apart from this situation, Figure 4.18 clearly shows how time-dependent material properties can change cable forces and bending moments. In this analysis, there was a one-day step for time-dependent material effects to take place; if this duration is increased, the difference between the moment diagram of forward and backward analysis cases is expected to increase. When the construction is finished, moment diagrams for both analysis types are far apart from the target moment diagram. But in Figure 4.19, it is seen that both forward and backward analysis moment diagrams have creeped to the target moment diagram. If cable forces have not been adjusted according to the beam on rigid

support approach, this bending moment will creep to different values and desired displaced shape would not have been reached. Between time when construction has just finished and until time infinity where all creep and shrinkage have taken place, moment diagram and also internal forces have changed significantly (approx. %50) as going from Figure 4.18 to Figure 4.19. Therefore, design engineers should carefully check the structure with other loadings like temperature, temperature gradient, moving loads and etc. where the superstructure internal forces and cable tension values during this time interval is changing significantly.

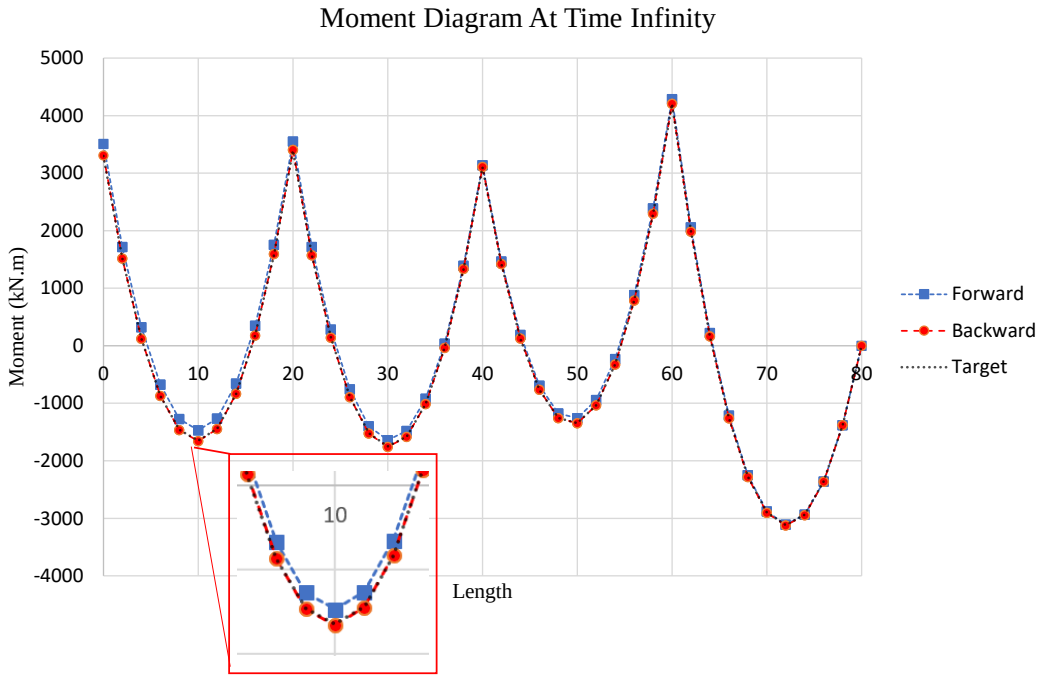

Figure 4.19 Backward, Forward Analysis and Target Moment Diagram with Time-Dependent Material at Time Infinity t=25000 days (Truss Element)

4.4.4 Ernst Truss Element

In this part, instead of linear truss element, Ernst truss element will be used for cable elements. This type of element is commonly used among bridge engineers because it is easy to implement compared to catenary element which is nonlinear. Ernst truss is a linear cable like truss element as explained in Section 3.5. The elasticity modulus

will always be changed to mimic the cable sag behavior which effects the cable stiffness.

4.4.4.1 Comparison of Analysis Methods Results (Without Time-Dependent Material Properties) (Ernst Truss Element)

Time dependent material properties were not taken into consideration at this stage. As shown from Figure 4.20 to 4.23 cable forces do not deviate from each other except Cable 2 and 3 at construction stage 4. This change in values for forward and backward analysis occurs because of the chosen cable element type as Ernst truss. When Cable 4 was tensioned, there occurred change in sag values in the remaining three cables but this change is greater at the two Cables called 2 and 3 which are closer to Cable 4. Cable 2 tension force decreases but Cable 3 tension force increases compared to the backward analysis. This effect caused decrease in moment diagram of the girder where Cable 2 is attached and increase in moment diagram of the girder where Cable 3 is attached in Figure 4.24.

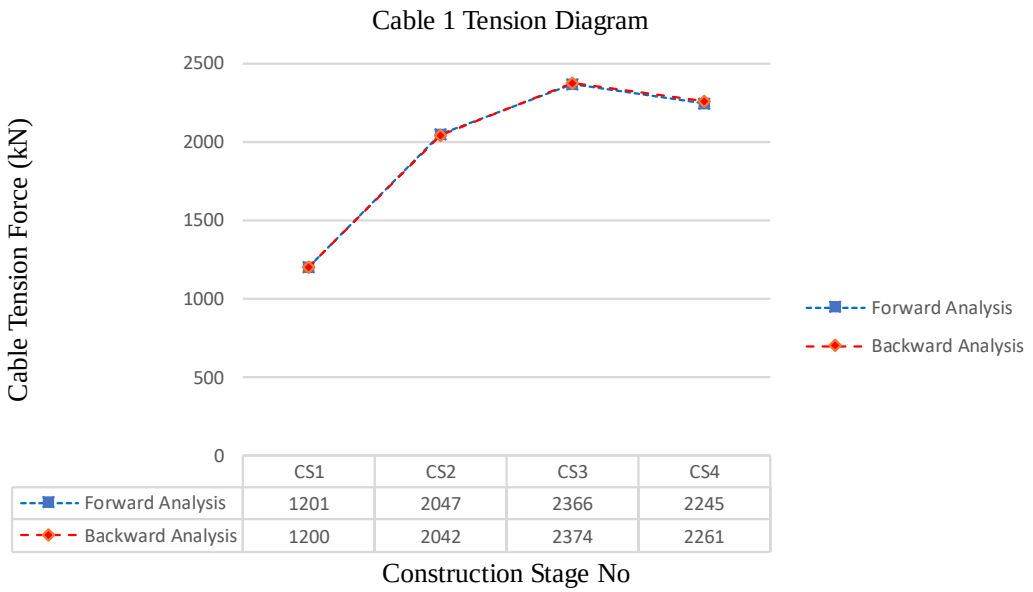

Figure 4.20 Cable 1 Tension Force Change (Ernst Truss Element)

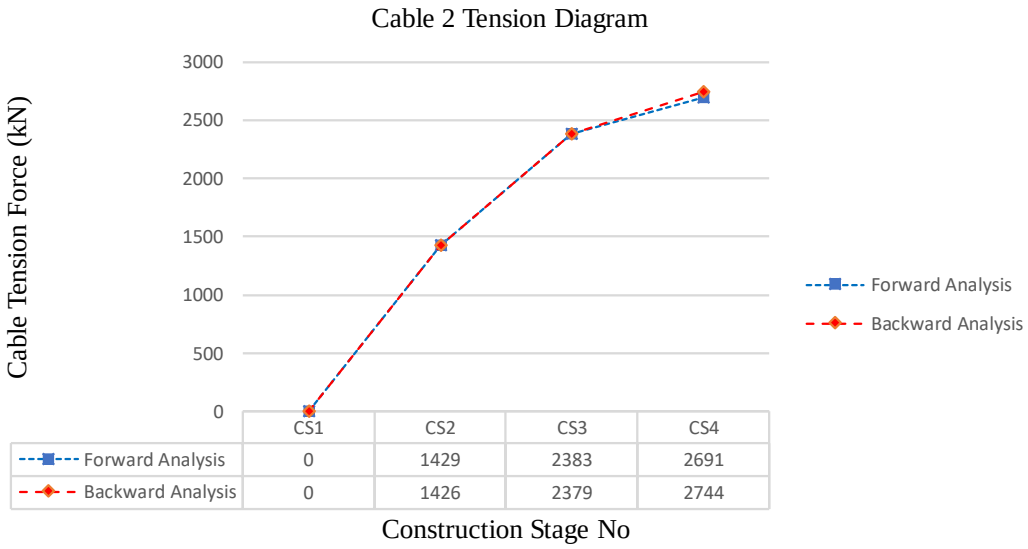

Figure 4.21 Cable 2 Tension Force Change (Ernst Truss Element)

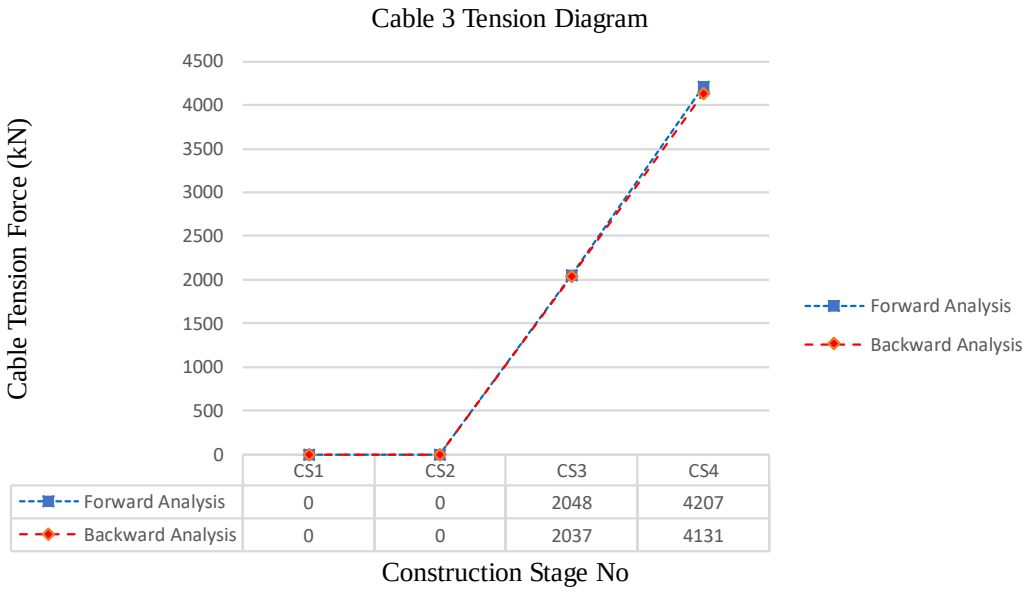

Figure 4.22 Cable 3 Tension Force Change (Ernst Truss Element)

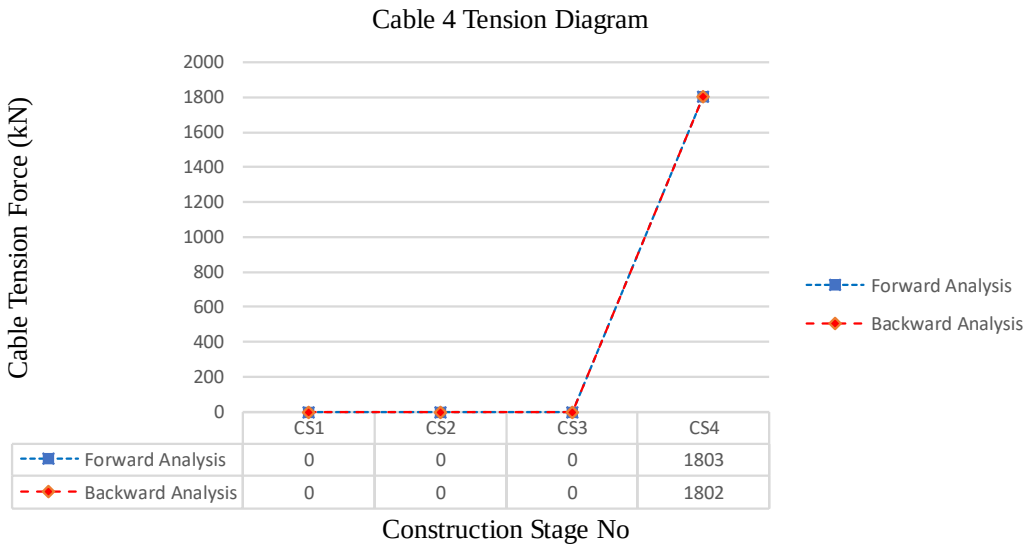

Figure 4.23 Cable 4 Tension Force Change (Ernst Truss Element)

According to the results both for cable tension forces and girder moment diagram, backward and forward analysis can be used in the design if time dependent material properties are not considered in the analysis. Compared to the previous analysis that were done using linear truss element in section 3.4.1 results are close to each other but because Ernst truss element was considered in this part, there occurred some changes in the cable forces (%2) and bending moment diagram (%11) as shown in Figure 4.24. These are caused by the change in stiffness of the cable elements during construction stages. Results showed that if elements that consider the cable nonlinearity are used in the analysis there will definitely be change in cable and girder internal forces unlike linear truss elements, because these elements consider the sag which affected the axial rigidity of the cable. In the following section time-dependent material properties will be defined and results will be compared to each other.

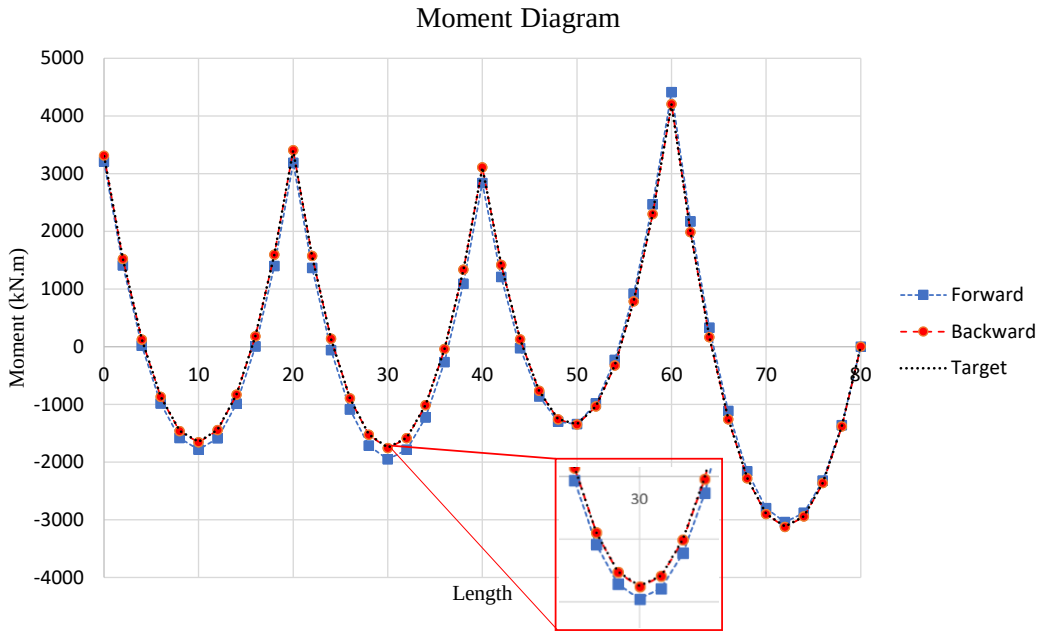

Figure 4.24 Backward and Forward Analysis Moment Diagram (Ernst Truss Element)

4.4.4.2 Comparison of Analysis Methods Results (With Time-Dependent Material Properties) (Ernst Truss Element)

In this section, material time dependent effects were taken into account. In the backward analysis, these effects were considered as positive temperature loading and applied to the girder elements because they have already caused shortening in the axial direction of the girder. For the time-dependent material properties and their detailed calculations Appendix B can be followed. For the calculation of thermal loading Appendix C can be investigated. For the forward analysis time-dependent material properties were taken into account as in the real order and calculated by using small time steps and accumulated as explained. From Figure 25 to Figure 28 it is clear that there is little difference in Cable 1 and Cable 4 forces (%1.5) but there is more difference in Cable 2 and Cable 3 forces (%3.2) when the construction process has just finished.

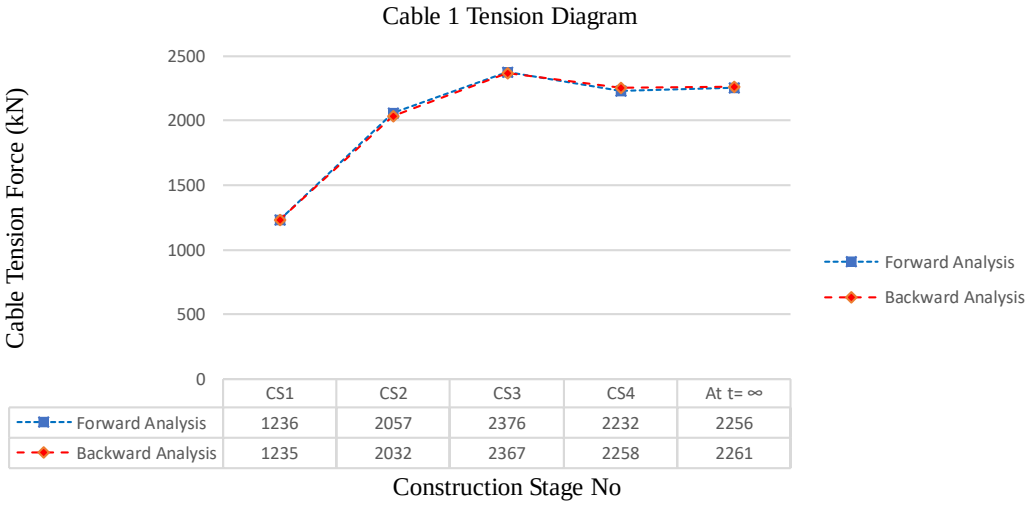

Figure 4.25 Cable 1 Tension Force Change with Time-Dependent Material (Ernst Truss Element)

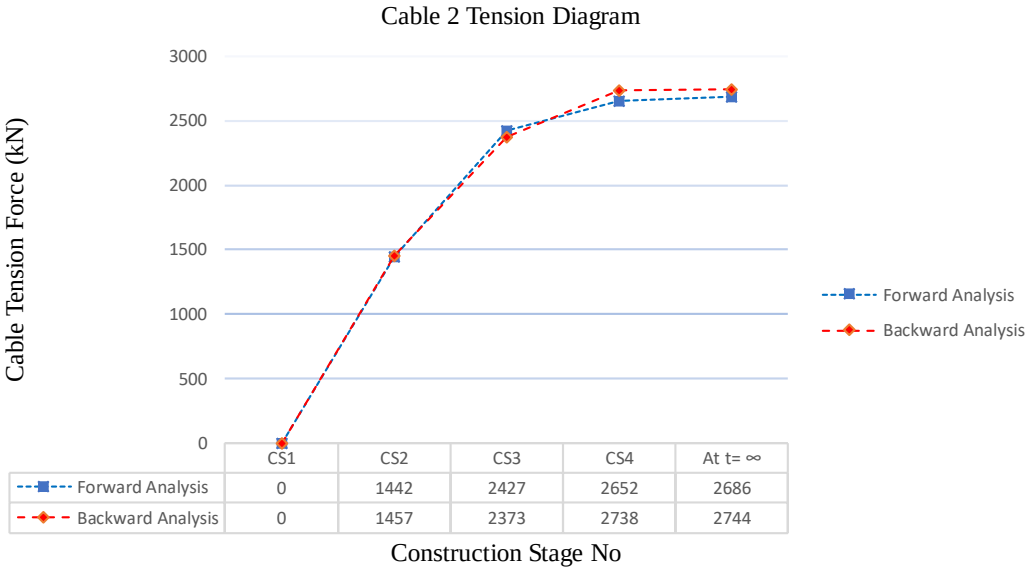

Figure 4.26 Cable 2 Tension Force Change with Time-Dependent Material (Ernst Truss Element)

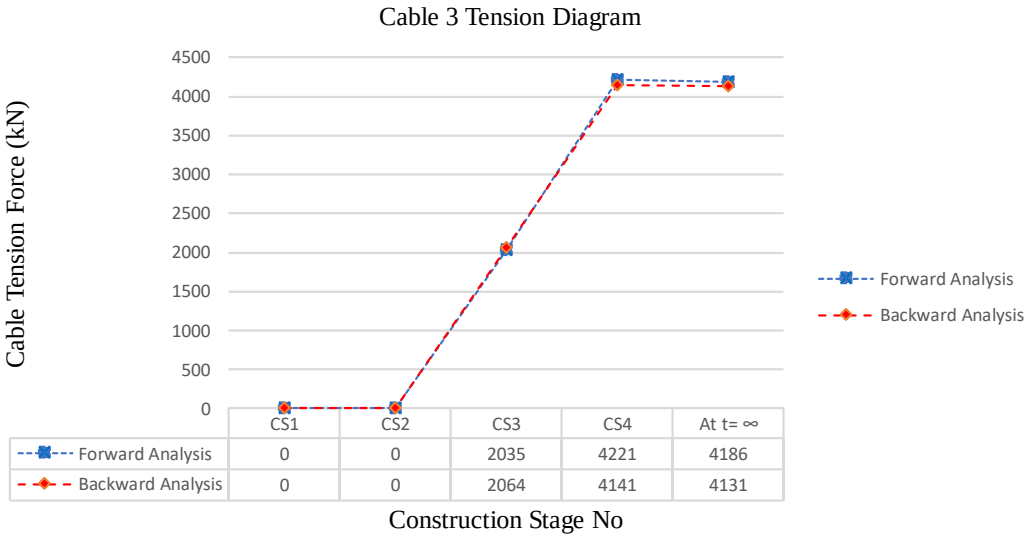

	CS1	CS2	CS3	CS4	At t= ∞
Forward Analysis	0	0	2035	4221	4186
Backward Analysis	0	0	2064	4141	4131

Figure 4.27 Cable 3 Tension Force Change with Time-Dependent Material (Ernst Truss Element)

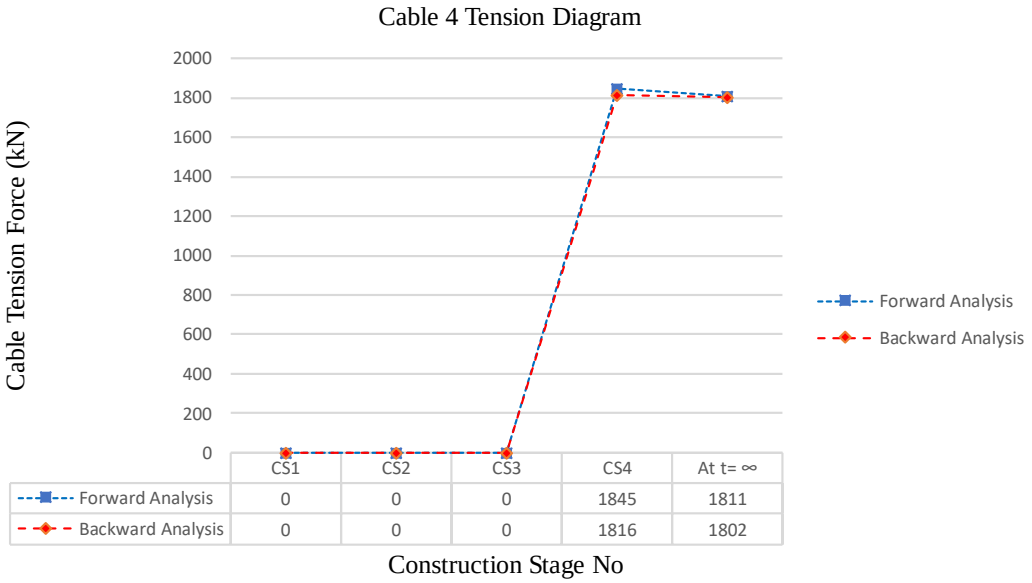

	CS1	CS2	CS3	CS4	At t= ∞
Forward Analysis	0	0	0	1845	1811
Backward Analysis	0	0	0	1816	1802

Figure 4.28 Cable 4 Tension Force Change with Time-Dependent Material (Ernst Truss Element)

This situation, difference in cable forces between forward and backward construction stage analyses, caused Span1-2-3 sagging moments to increase in the forward

analysis compared to the backward analysis. Also, this change affected the overall bending moment distribution. As a result, it can be concluded that although there is a change in cable forces between two analysis methods this difference is small (approx. %3) and does not affect the stay cable design. But this difference caused big amount of difference (%28) in bending moment, in time where the construction has just finished and bridge was opened to the traffic Figure 4.29. If only the backward analysis were used for construction stage calculations, sagging moments would have been underestimated compared to the ones obtained in the forward analysis, but hogging moments were overestimated. This situation can cause design problems when especially moving load analysis are added to the moment diagram that was obtained at the end of the construction stage analysis. Therefore, when time dependent material properties were taken into consideration, backward analysis could issue design problems.

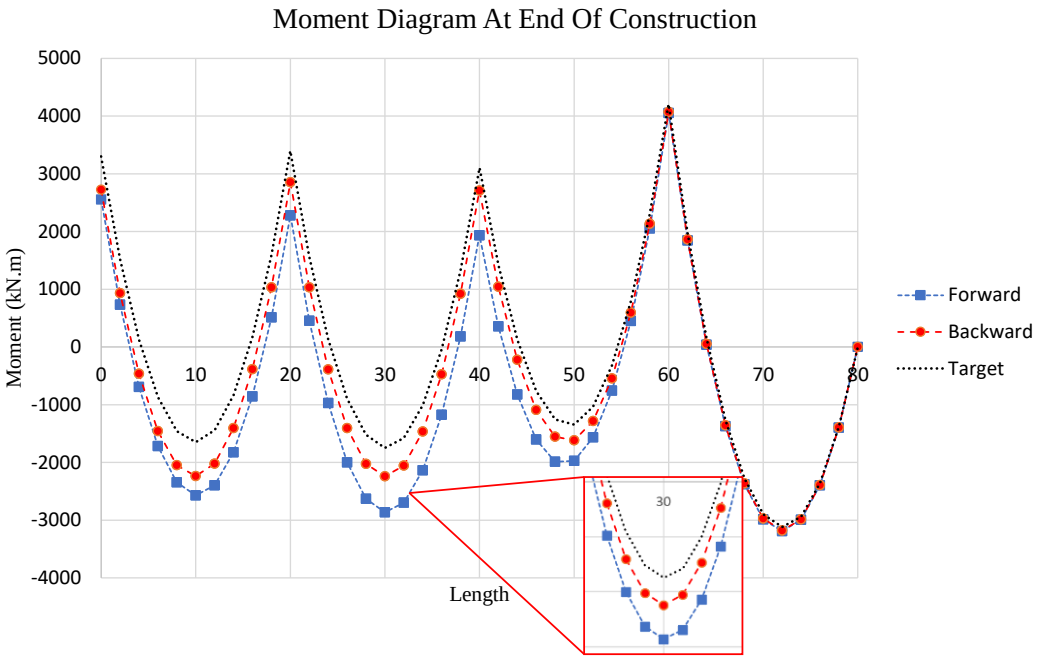

Figure 4.29 Backward, Forward Analysis and Target Moment Diagram with Time-Dependent Material Effects (Ernst Truss Element)

As can be followed from the cable tension diagrams at time infinity all cable forces reached almost to the same values for both analysis methods. This effected the

moment distribution both in span and cable anchor points. Moment diagram changed and reached to the target moment diagram values at time infinity as expected Figure 4.30. This situation shows how important to use beam on rigid supports approach in the design and analysis of cable stayed bridges. Only in this way the desired moment diagram and cable forces can be achieved and all uncertainties that are caused by time dependent affects can be minimized.

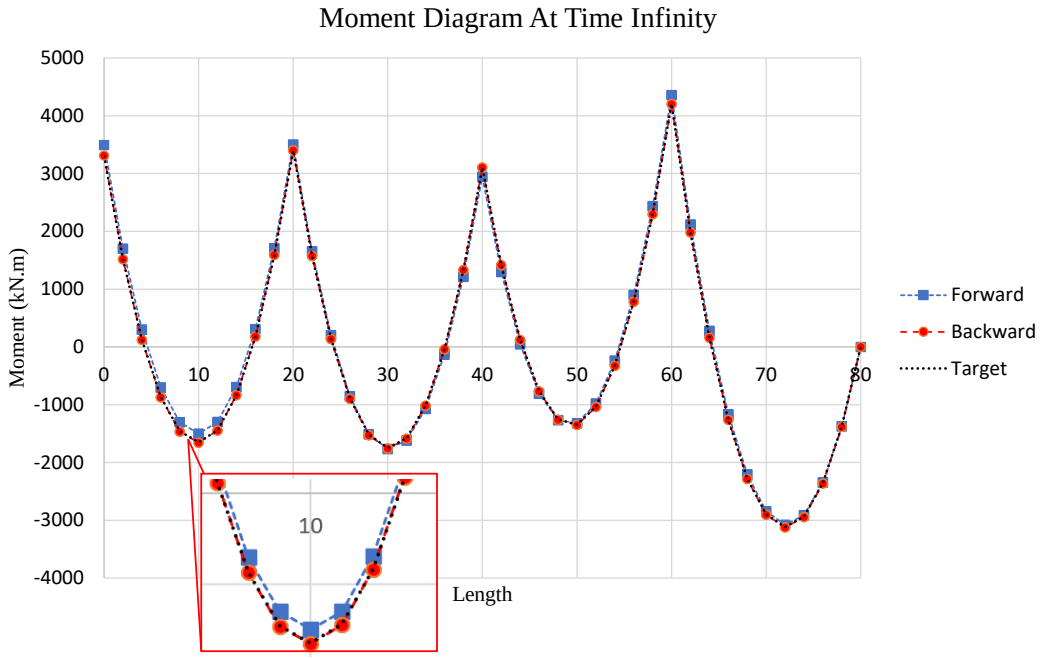

Figure 4.30 Backward, Forward Analysis and Target Moment Diagram with Time-Dependent Material at Time Infinity t=25000 days (Ernst Truss Element)

4.4.5 Cable Element

In this section, nonlinear cable elements were used in the analysis. Firstly, Midas Civil and Larsa 4D cable element formulations will be explained. In Midas Civil, the elastic catenary element was used in the analysis, and its formulation can be followed from the Analysis Reference. In Larsa 4D Manual, the cable element is defined as follows; “The cable element is identical to the truss element except a cable element cannot resist compressive force. The cable element can only be used in a nonlinear

analysis. If, during the analysis, the axial force in a cable element becomes compressive, then the cable element is assumed to have no axial stiffness and cannot carry any load. It is kept in the model as an inactive element with no contributing stiffness. During the loading process of a nonlinear analysis, if the element can become tensile again, it is included in the model with contributing stiffness to the system. This element has geometric nonlinearity and stress-stiffening in all nonlinear analysis types. The Super Cable Element has multiple internal Gaussian points that simplifies cable modeling. Self-weight and other types of distributed and concentrated loads imposed within the element are analyzed as equivalent concentrated loads at internal Gaussian points. While simplifying the modeling of cables, the element provides a realistic and reliable solution considering geometric nonlinearity due to the sagging effect under arbitrary loading."

4.4.5.1 Comparison of Analysis Methods Results (Without Time-Dependent Material Properties) (Catenary Cable Element)

Although nonlinear catenary elements were used in the analysis, cable forces in both analysis methods resulted nearly the same values (~%1.2). Larsa 4D and Midas Civil showed that their cable formulations gave almost the same cable forces (approx. %0.3), and by this way, obtained moment diagrams were very close to each other (~%2.5).

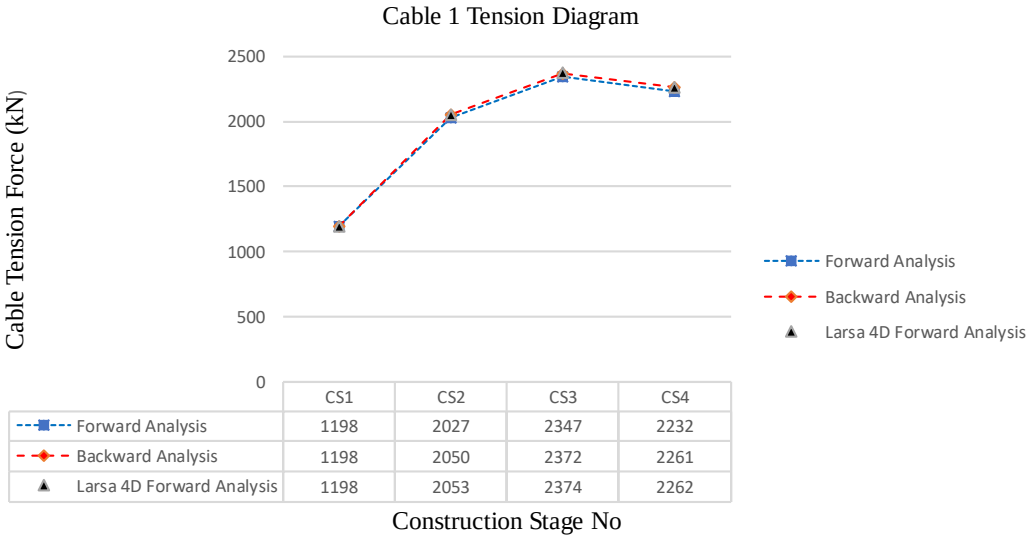

	CS1	CS2	CS3	CS4
Forward Analysis	1198	2027	2347	2232
Backward Analysis	1198	2050	2372	2261
Larsa 4D Forward Analysis	1198	2053	2374	2262

Figure 4.31 Cable 1 Tension Force Change (Catenary Cable Element)

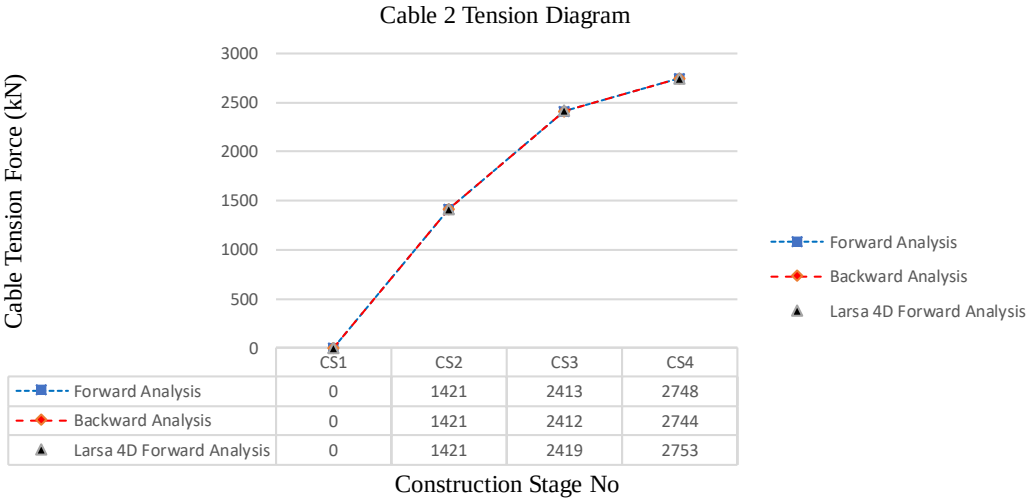

	CS1	CS2	CS3	CS4
Forward Analysis	0	1421	2413	2748
Backward Analysis	0	1421	2412	2744
Larsa 4D Forward Analysis	0	1421	2419	2753

Figure 4.32 Cable 2 Tension Force Change (Catenary Cable Element)

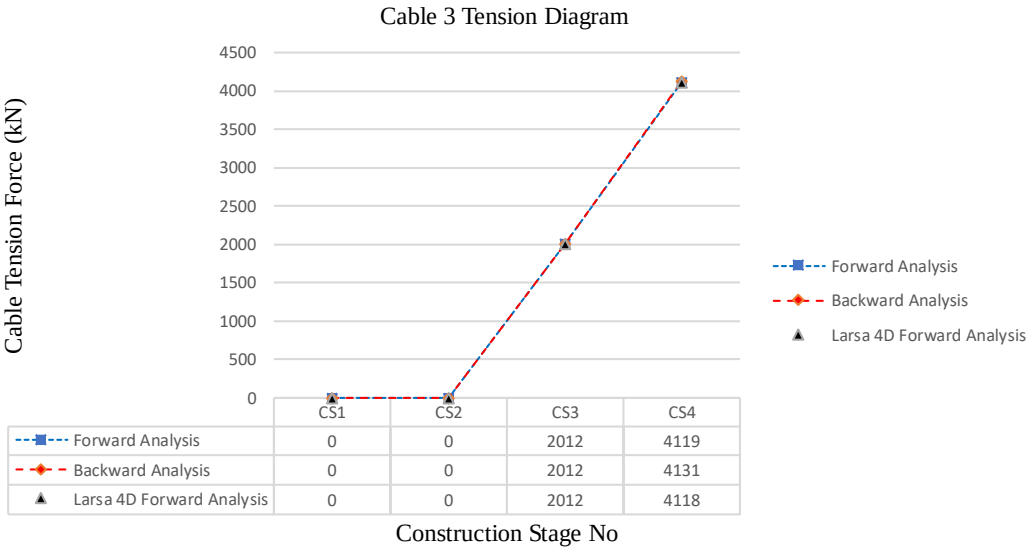

Figure 4.33 Cable 3 Tension Force Change (Catenary Cable Element)

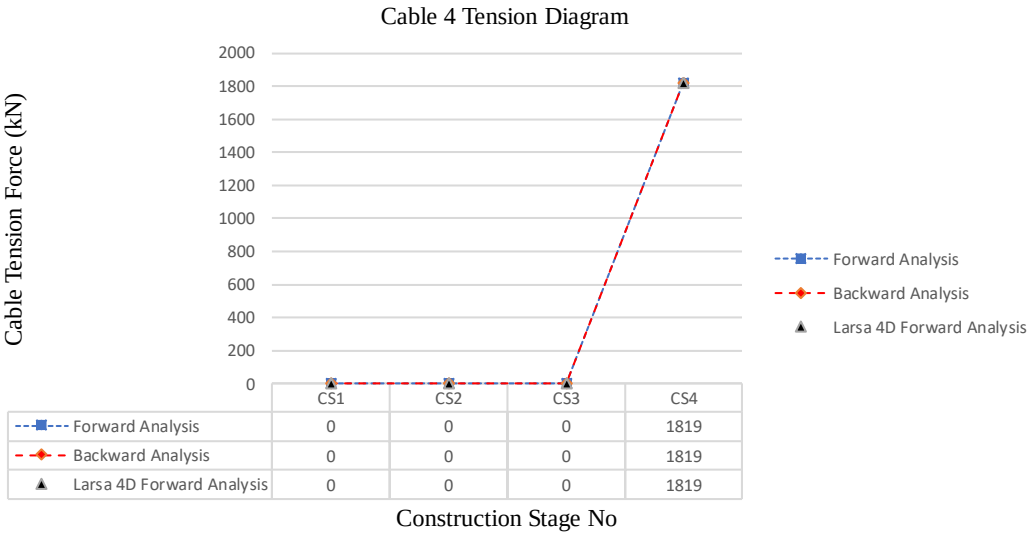

Figure 4.34 Cable 4 Tension Force Change (Catenary Cable Element)

There are minor differences in the moment values of the girder. These were the results of how the P-Δ effects were considered in both analysis programs. Also, when casting the new segment, matched cast approach was applied in both programs. Although, it was not explained in the manuals of both analysis programs deeply, it is evident that there are differences in how this analysis was handled and how the

new segments were attached to the last part. But it is clear that if time-dependent material properties were not taken into account, results of both analysis methods and analysis software were close enough (~%2.5) to use in the analysis and in the design process. If the bridge superstructure was chosen as an orthotropic steel section, using backward or forward analysis as a design tool does not make any difference. But as it was shown in the following paragraphs, when time dependent material effects were considered, differences occurred both in cable tension forces and in internal force values.

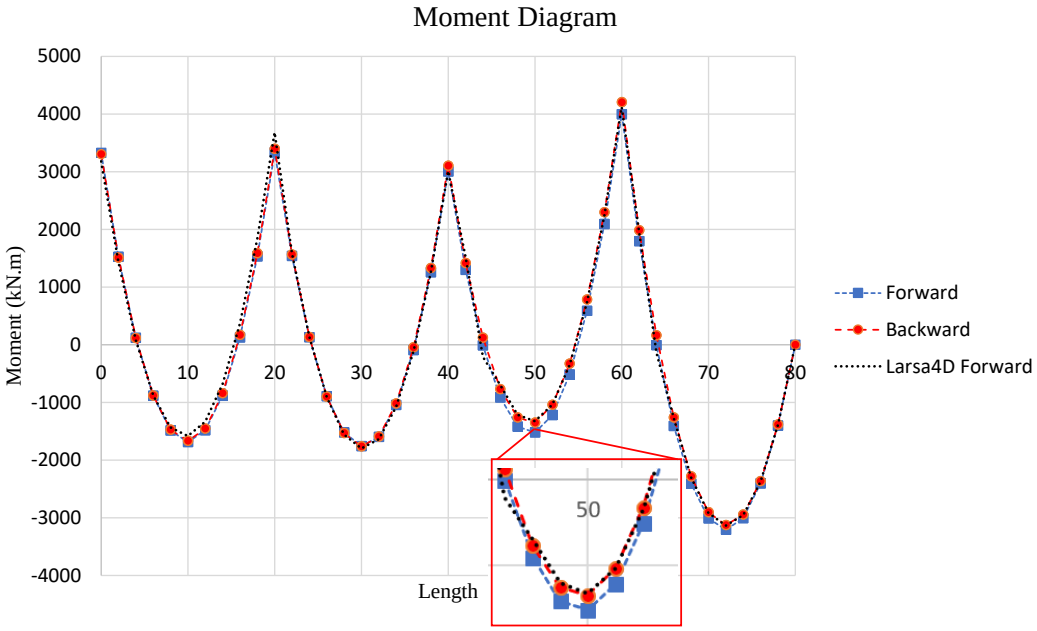

Figure 4.35 Backward and Forward Analysis Moment Diagram (Catenary Cable Element)

4.4.5.2 Comparison of Analysis Methods Results (With Time-Dependent Material Properties) (Catenary Cable Element)

When time-dependent material properties were considered, as in the previous analysis, cable tension forces changed in small amounts (approx.%2.3), as seen in Figures 4.36 to 4.39. These small changes resulted in differences in internal forces. At construction stage 4, where the construction operations have just finished, slight

differences occurred in cable tensions (~%2.5). But at time infinity, as expected, cable forces came close to the desired tension forces. Also, it can be concluded that time-dependent material calculations ended with similar results (%1.2). in both computer programs from a cable tension point of view.

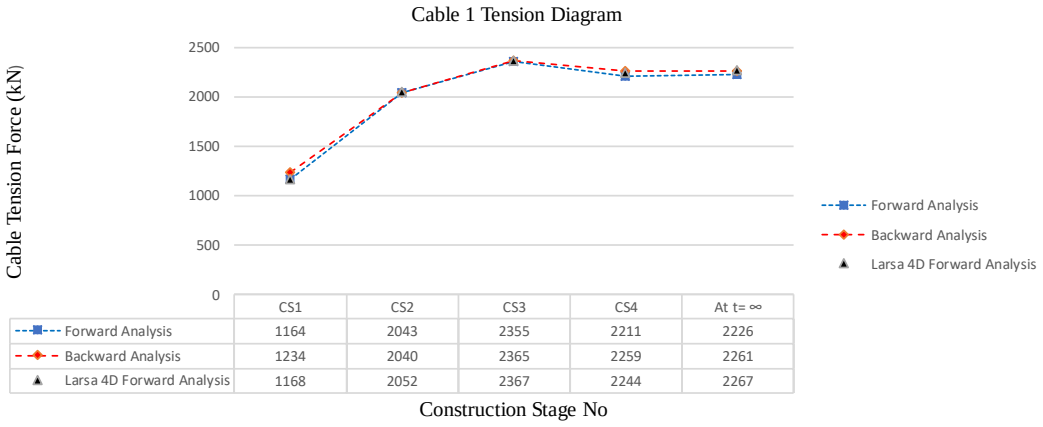

	CS1	CS2	CS3	CS4	At t= ∞
Forward Analysis	1164	2043	2355	2211	2226
Backward Analysis	1234	2040	2365	2259	2261
Larsa 4D Forward Analysis	1168	2052	2367	2244	2267

Figure 4.36 Cable 1 Tension Force Change with Time-Dependent Material (Catenary Cable Element)

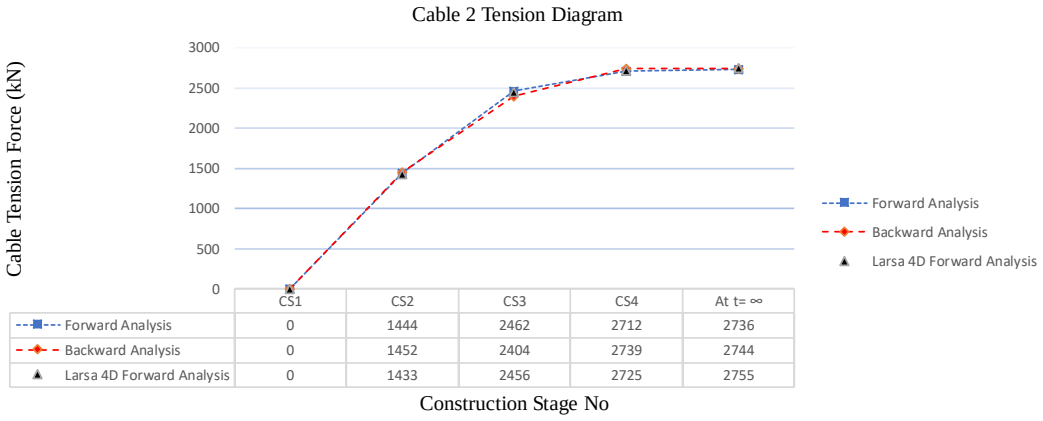

	CS1	CS2	CS3	CS4	At t= ∞
Forward Analysis	0	1444	2462	2712	2736
Backward Analysis	0	1452	2404	2739	2744
Larsa 4D Forward Analysis	0	1433	2456	2725	2755

Figure 4.37 Cable 2 Tension Force Change with Time-Dependent Material (Catenary Cable Element)

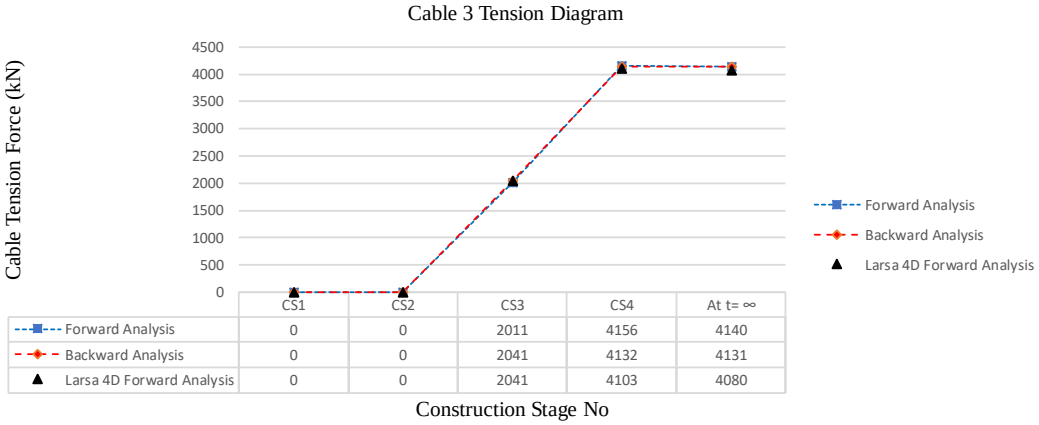

Figure 4.38 Cable 3 Tension Force Change with Time-Dependent Material (Catenary Cable Element)

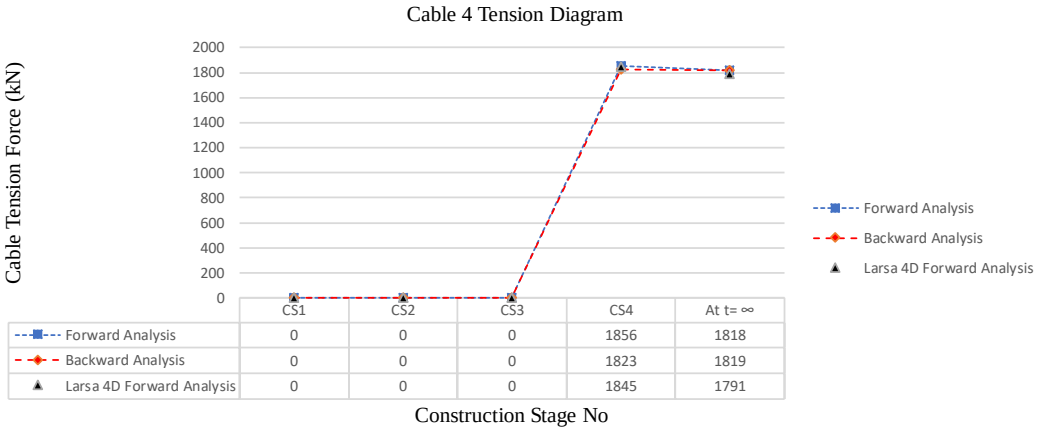

Figure 4.39 Cable 4 Tension Force Change with Time-Dependent Material (Catenary Cable Element)

The moment diagrams of both Midas Civil and Larsa 4D are very close (%3.7) to each other in the forward analysis method, as shown in Figure 4.40. Forward analysis is slightly different (~%5) from backward analysis, which resulted from accumulations of internal forces during forward analysis, time-dependent material effects, and how the newly erected segment was attached to the previous one by using matched cast approach. It is again important to note that there are scatters in the internal forces between the two analysis methods, and as explained previously

backward analysis method should be used cautiously in design when other loadings, such as traffic loads, are taken into consideration and when the construction processes have just finished.

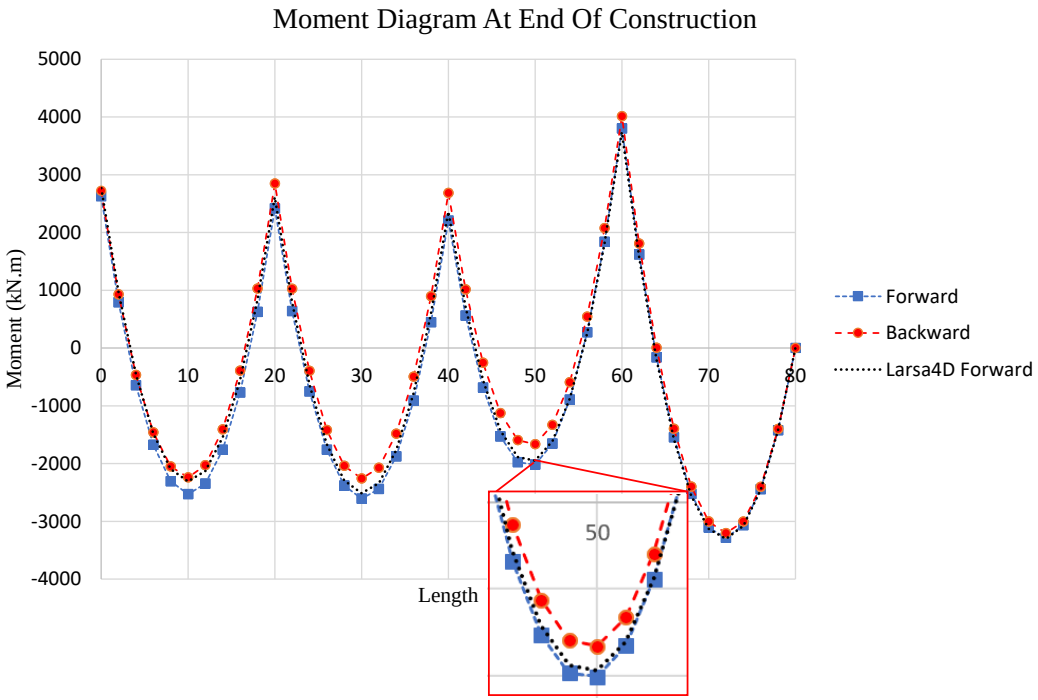

Figure 4.40 Backward, Forward Analysis Moment Diagram with Time-Dependent Material (Catenary Cable Element)

At time infinity, when time passes and reaches 25000 days, the moment diagrams creep to the values obtained from the beam on rigid supports approach. In all analyses conducted until now, all moment diagram values and cable tension forces reached to the calculated target values. Again, emphasis should be given to the beam on rigid supports approach because only in this way desired cable forces and moment diagrams were obtained, as shown in Figure 4.41. Minor differences (%6.8) in values between moment diagrams occurred between the two analysis programs because of how the P-Δ and large displacement effects were taken in to account in the analysis. But forward analysis results for both computer programs reached nearly the same values.

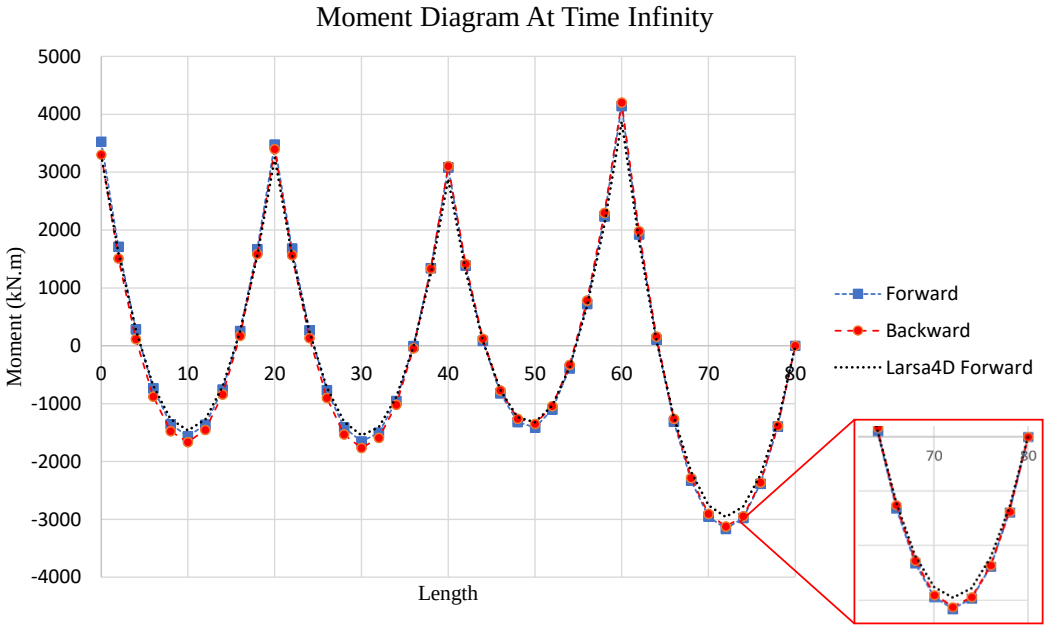

Figure 4.41 Backward, Forward Analysis and Target Moment Diagram with Time-Dependent Material at Time Infinity t=25000 days (Catenary Cable Element)

As seen from Figure 4.42 and Figure 4.43, backward and forward analysis deformation graphs are different. The reason behind this was the construction procedure and how the segments were connected to each other by using matched cast approach. Because in this procedure, the new segment was attached to the previous one tangentially and in a deformed shape which is not applicable in the backward analysis method. If the results in Figure 4.42 are correctly applied to the model, the desired profile level in Figure 4.43 is obtained, as shown in red. Results obtained from forward analysis using both analysis programs show the real displacement values at the end of the construction and at time infinity. These results could be used to produce manufacturing camber in a factory in stress free situation.

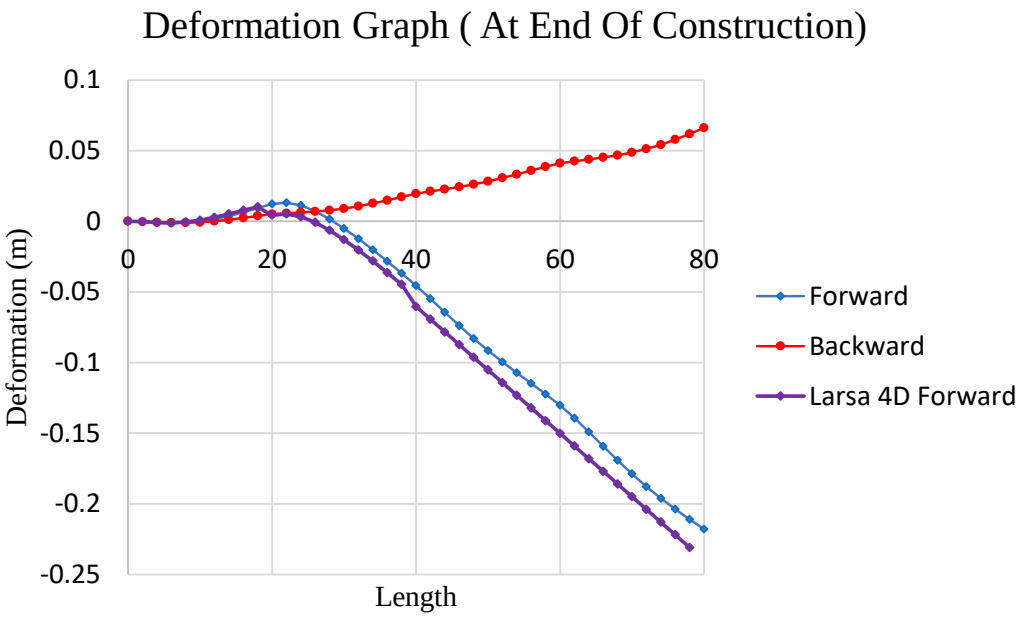

Figure 4.42 Backward, Forward Analysis Deformation Graph at Construction Finish (Catenary Cable Element)

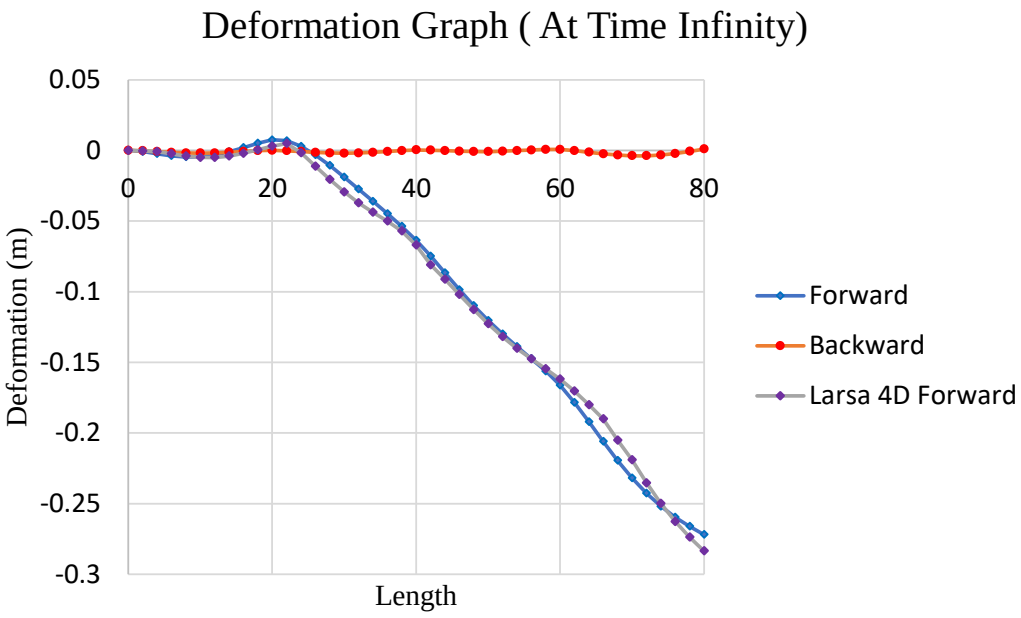

Figure 4.43 Backward, Forward Analysis Deformation Graph at Time Infinity (Catenary Cable Element)

4.5 Effects of Time Step Size on Time-Dependent Material Properties and Their Impact on the Results

This part delved into the effects of the time step size on time-dependent material properties and their impact on the analysis results. The consideration of time-dependent material properties is critical in capturing real-world behavior, particularly in situations where materials exhibit changes over time due to factors such as creep and shrinkage.

Initially, the creep coefficient and shrinkage strain values for 0.5 day and 1 day were compared, as illustrated in Figures 4.44 and 4.45, respectively. It can be inferred that utilizing either 0.5 day or 1 day in calculating the values does not significantly impact the analysis, as the obtained values are the same for both time steps.

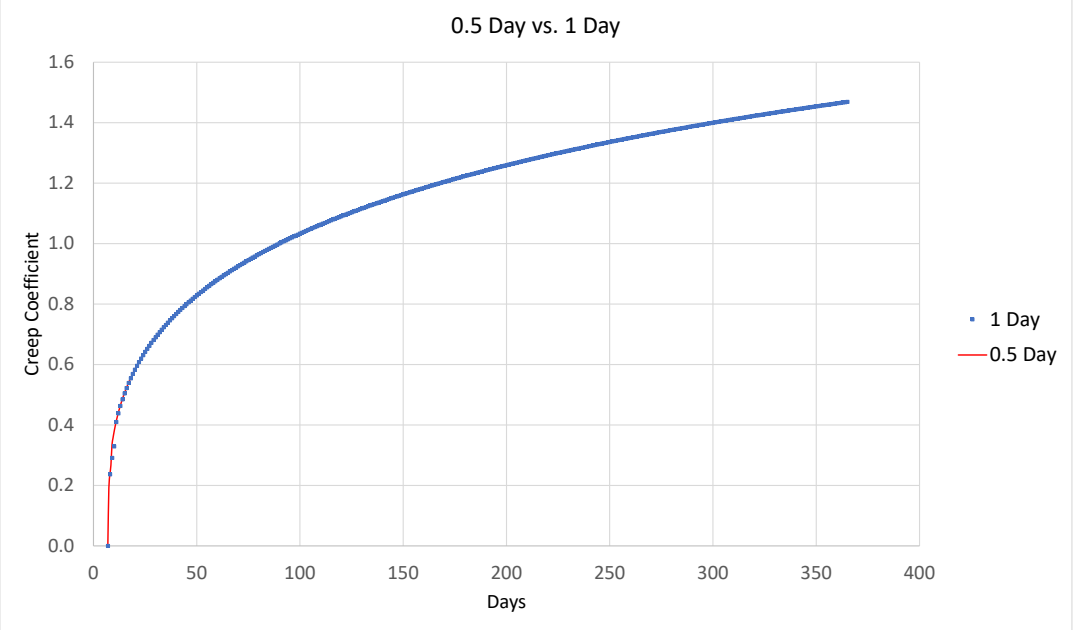

Figure 4.44 Creep Coefficient For 0.5 day and 1 day

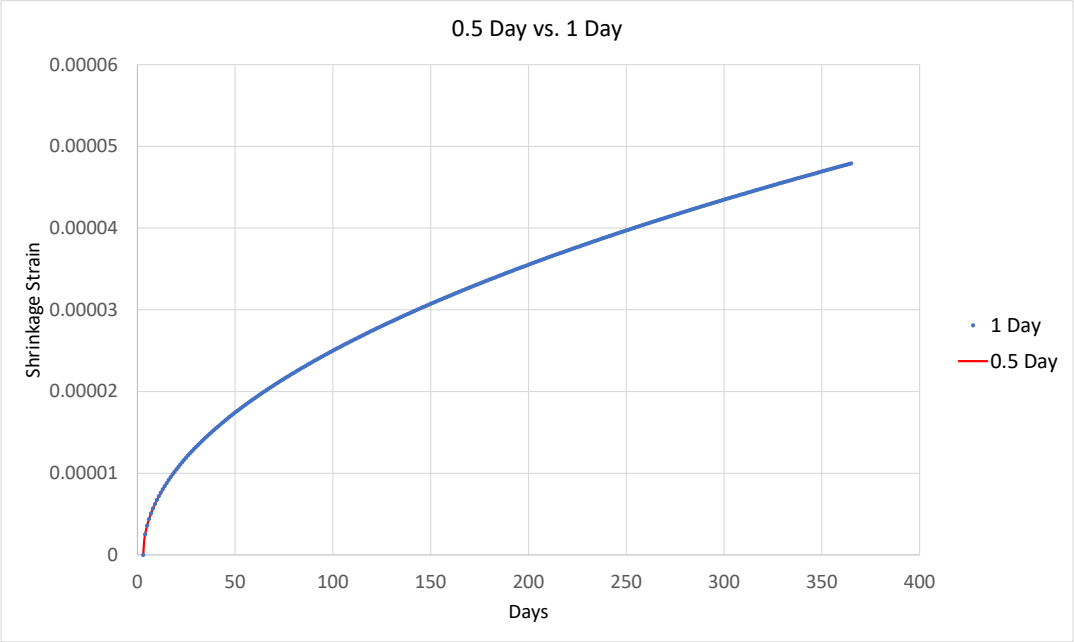

Figure 4.45 Shrinkage Strain For 0.5 day and 1 day

Secondly, the impact of decreasing the calculation time steps in the analysis was thoroughly examined by reducing the time steps from 1 day to 0.5 day. As seen in Figure 4.46, there is no difference between time steps of 0.5 to 1 day. However, for a 10-day time step, the significance becomes apparent, with differences ranging from 0.0101% to 5.85%. Therefore, selecting smaller time steps for calculating time-dependent material effects yields more accurate results than larger time steps.

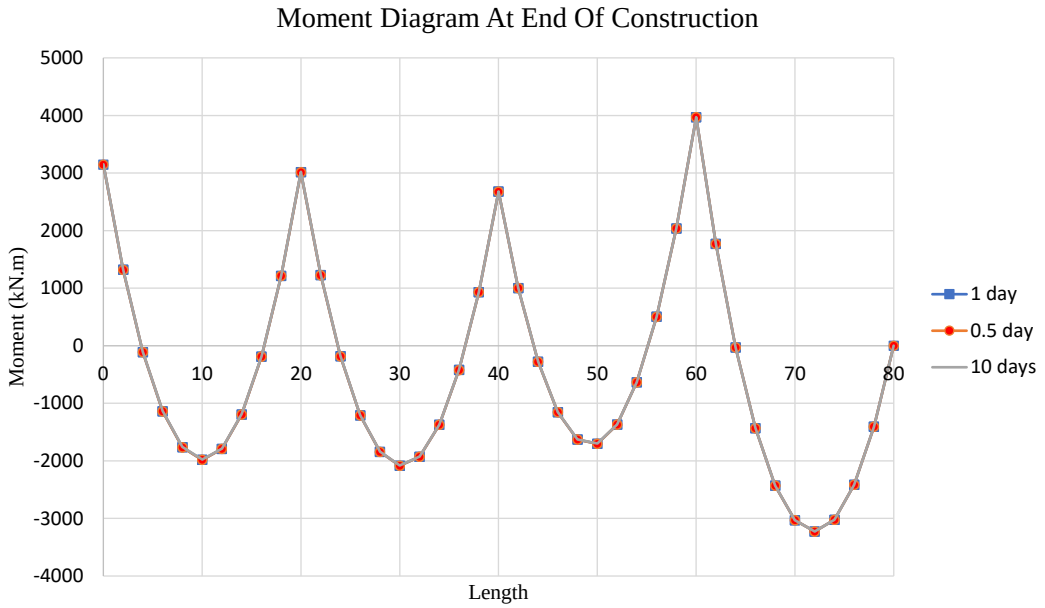

Figure 4.46 Moment Diagrams For 0.5 Day, 1 Day and 10 Days' Time Steps

4.6 Comparison of Different Cable Element Type Results

In the previous sections, different cable element types such as linear truss, Ernst truss and catenary cable elements were used for the backward and forward analysis. All the results were obtained, and in this section results of these three elements were compared taking into consideration time dependent material properties at finish of construction and at time infinity, when all creep and shrinkage took place by using the forward analysis method.

Investigating Figure 4.44, at time, when the construction has just finished, catenary cable element and Ernst truss almost gave the same moment diagram (%9 difference). But there was quite a big (%27) difference among linear truss and the other two elements. This difference occurred because in linear truss element sag of the cable element could not be taken into consideration in the analysis. Although Ernst truss is a linear element, it can take into account the effect of sag on the cable stiffness, by this way it gave close results to the most advanced catenary cable element.

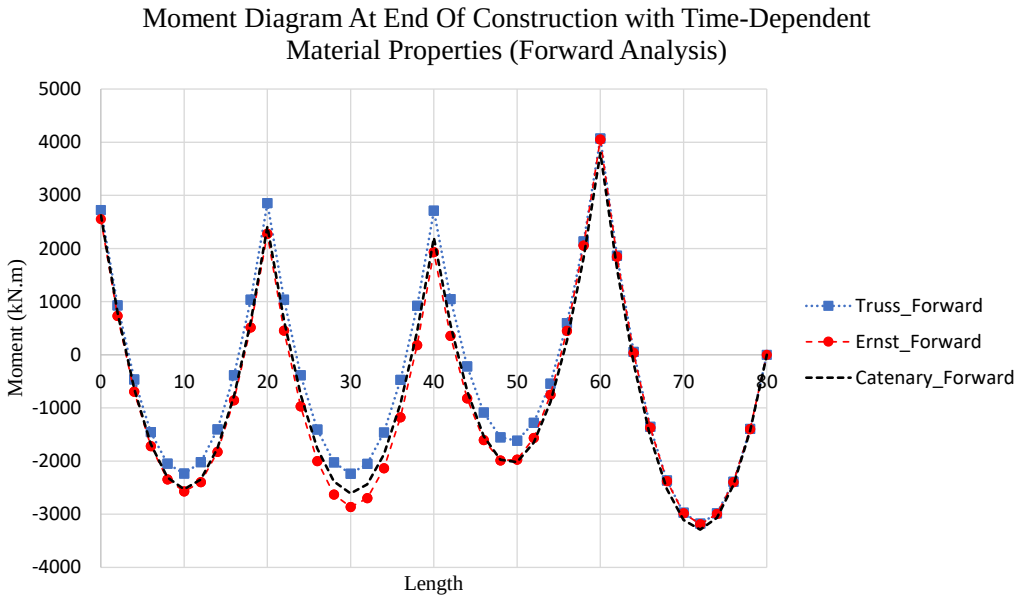

Figure 4.47 Forward Analysis with Time-Dependent Material Properties at Finish of Construction, for Linear Truss, Ernst Truss and Elastic Catenary Element

Interestingly, at time infinity all three models with different type of elements almost reached to the target moment diagram as seen in Figure 4.45. Backward analysis results were not considered in this section because their results were same as the target moment diagram.

It was concluded that choosing cable forces at the beginning of the analysis based on beam on rigid supports approach gave very good results at time infinity. It is advised that using linear truss element could generate problems especially just at time when the construction just finished. Therefore, it is advised to use either catenary cable element or Ernst truss element in the construction stage analysis because both type of elements could take into account the cable sag effect and reflect the real behavior.

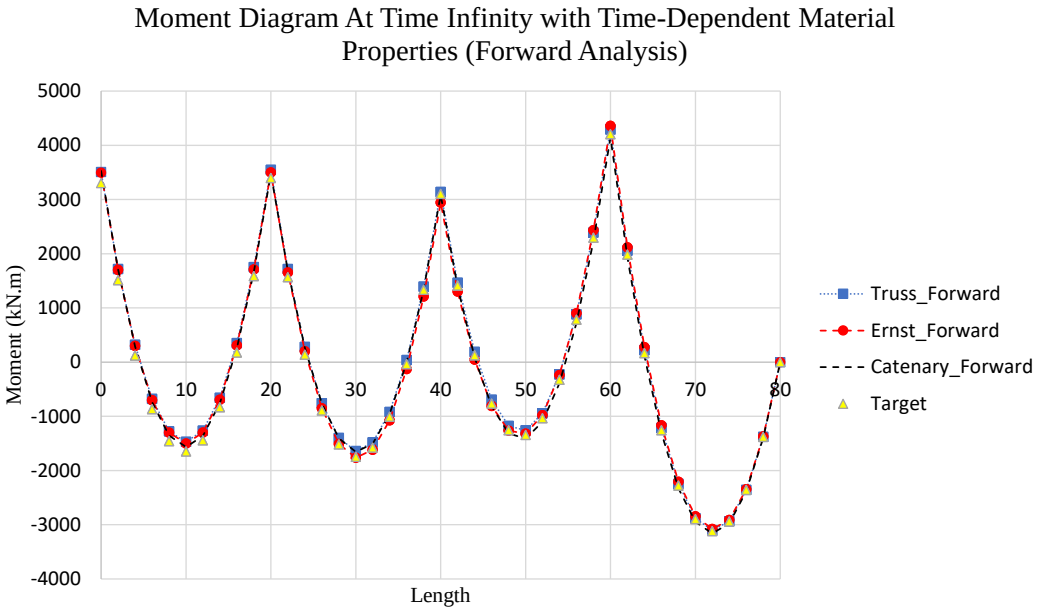

Figure 4.48 Forward Analysis and Target Moment Diagram with Time-Dependent Material Properties at Time Infinity t=25000 days, for Linear Truss, Ernst Truss and Elastic Catenary Element

CHAPTER 5

CONCRETE CABLE-STAYED BRIDGE

In this chapter, a concrete cable-stayed bridge with a concrete box superstructure will be analyzed, and the results will be evaluated. As in the previous section, two computer programs called Midas Civil and Larsa 4D were used for the analysis. The results of these programs were also compared to each other and assessed by considering only the most advanced analysis type with catenary elements as cables and considering the time-dependent material properties and large deformations.

5.1 Information About the Structure

The main dimensions of the structure and cables were taken from a real bridge designed in Turkey, as seen in Figure 5.1. The system has three spans with side spans lengths of 204m each, with a main span of 423m and a total length of 831m. There are 136 cables in the bridge, 34 at each side span and 68 at the main span, as seen in Figure 5.2. The total height of the tower is 196m. These dimensions generally satisfy the proportions described in Chapter 2 for the cable-stayed bridges.

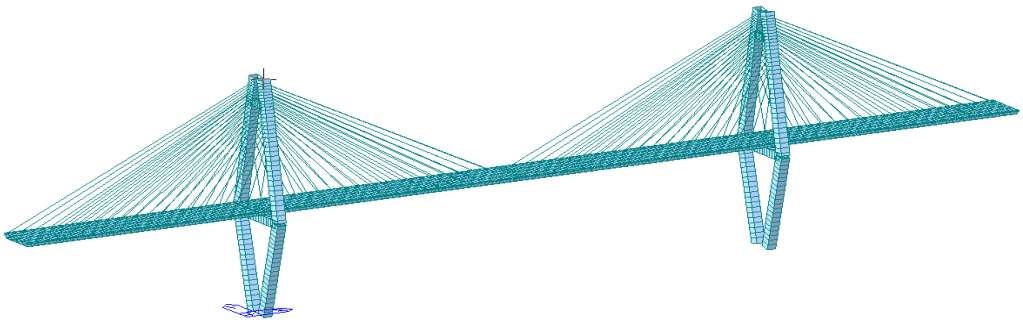

Figure 5.1 General View of the Bridge

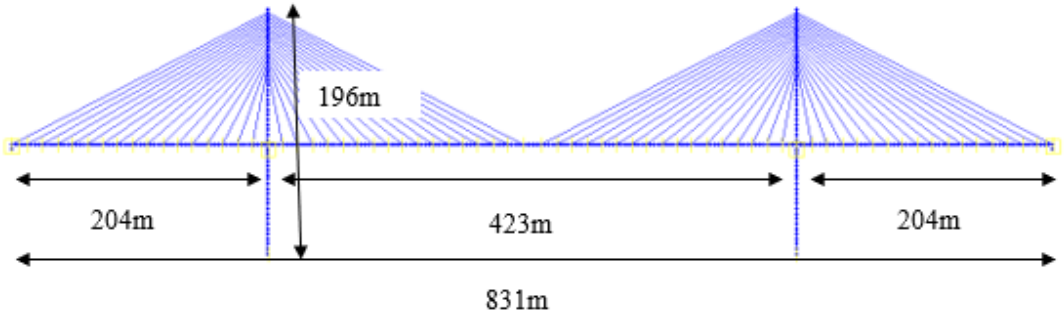

Figure 5.2 General Dimensions of the Structure

There are 17 segments in the side spans, 34 segments and a key segment in the main span. Each segment has a length of 12m. The bridge is considered to be built by the balanced cantilever method of construction using a floating crane approach in which the weight of the construction equipment does not act on the bridge. In this method, concrete segments of lengths 12m were produced at each side of the pylon, and the cables were stressed simultaneously.

Pylon was designed as a diamond shape. There are pot bearings in the side spans and at the pylons. Pylons were considered to be built totally in one step without time-dependent material properties. A small part of the construction process is shown in Figure 5.3. Main spans were defined with the abbreviation M, and side spans with S.

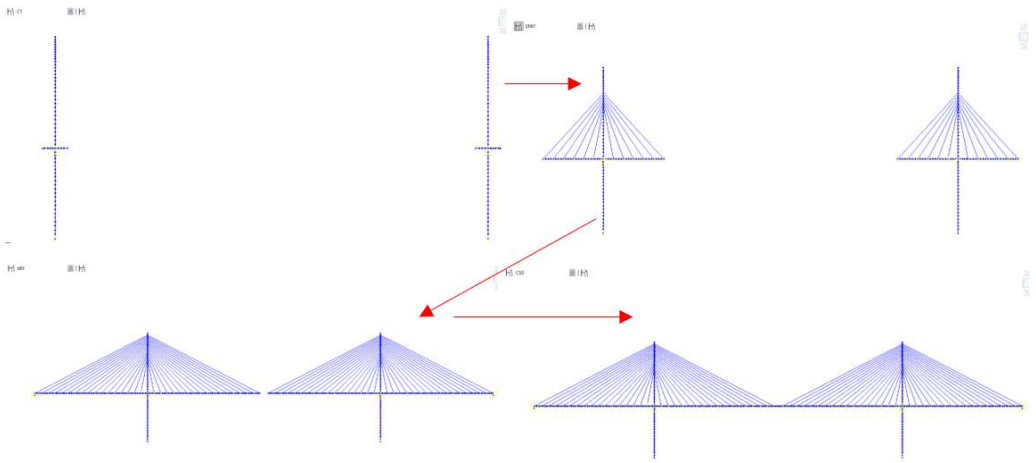

Figure 5.3 Balanced Cantilever Construction of the Bridge

The bridge's cross-section consists of a 4-cell concrete box girder with sectional properties, as presented in Appendix D in addition to pylon and cable cross sectional properties. The pylon and superstructure consist of C50 class concrete. Material properties of the sections and cables can be found in Table 5.1.

Table 5.1 Material Properties of Pylon, Superstructure and Cable

	Unit Weight (kN/m3)	*Elasticity Modulus (kN/m2)*	*Poisson's Ratio*	*Thermal Coefficient (1/C)*
Pylon & Girder	25	33941000	0.2	1e-5
Cable	78	200000000	0.3	1e-5

5.2 Desired Final Configuration of the Structure

As explained in Section 3.3.1, cable-stayed bridges with concrete decks are usually and preferably designed as at time infinity so that the girder would have a moment distribution like at cable anchor points; there are roller supports that are fixed in the gravity direction. This way, creep in that direction is eliminated, and no additional forces are expected because of time-dependent material properties. The target bending moment diagram is shown in Figure 5.4. In this figure, half of the whole moment diagram of the bridge girder was demonstrated because of clarity.

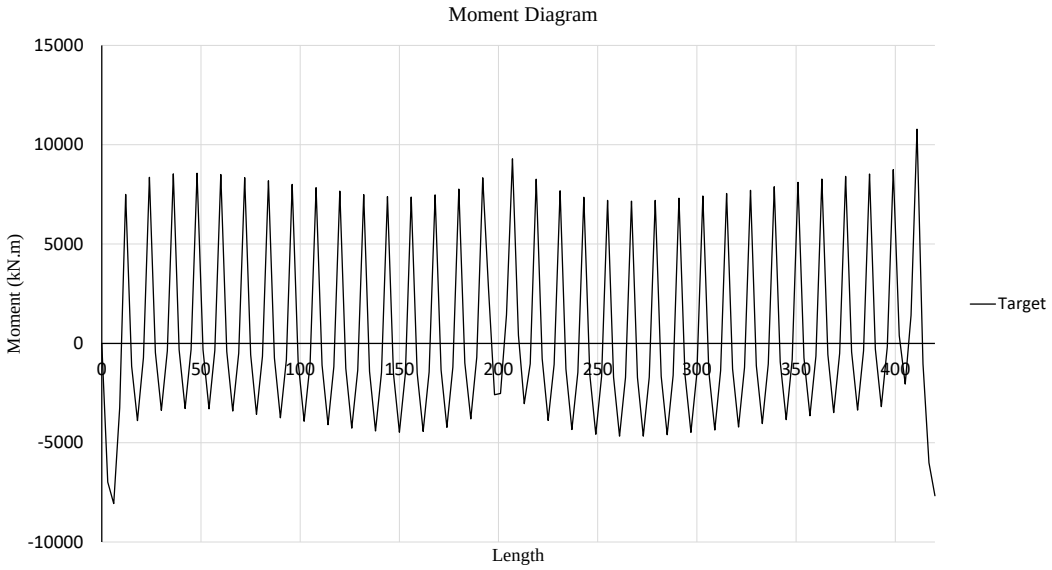

Figure 5.4 Target Moment Diagram of the Bridge Superstructure

5.3 Analysis of the Structure

The structure was analyzed by using Catenary cable element with time-dependent material effects. Two-time dependent analyses were conducted with one-day and seven days duration and compared to each other.

5.3.1 Backward Construction Stage Analysis

Backward procedure was used in the cable-stayed bridge construction stage analysis. As explained in 3.4.1, this type of analysis consists of dismantling the finished structure in the backward direction. The process is shown in Figure 5.5. Only symmetric dismantling was considered in the analysis. The cable forces were determined and used in the forward analysis as first tension estimates. This analysis was conducted solely using Midas Civil since the primary comparison of the two programs was carried out through forward analysis, which accounted for all nonlinearities and time-dependent effects.

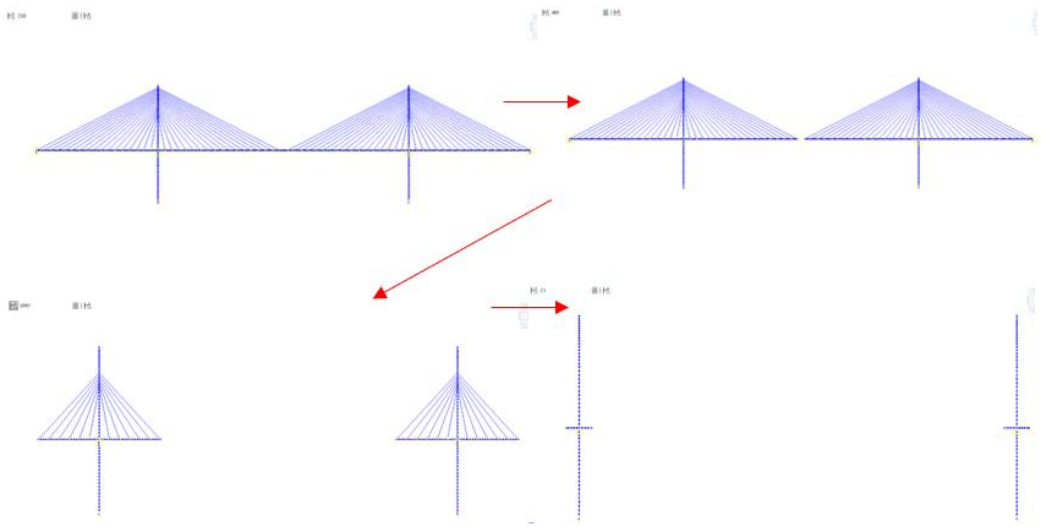

Figure 5.5 Backward Construction Stage Analysis Procedure

First of all, the creep coefficient and shrinkage strain were calculated as explained in Appendix E. Then, using the creep coefficient and shrinkage strain, an equivalent temperature was obtained to simulate the creep and shrinkage effects in the bridge and given to the bridge superstructure as positive temperature loading. Calculation of the temperature value in degrees can be found in Appendix F. After all creep and shrinkage were given to the superstructure in the reverse direction, moment diagram becomes as in Figure 5.6. This situation also demonstrates the moment diagram in the bridge when the construction just finished.

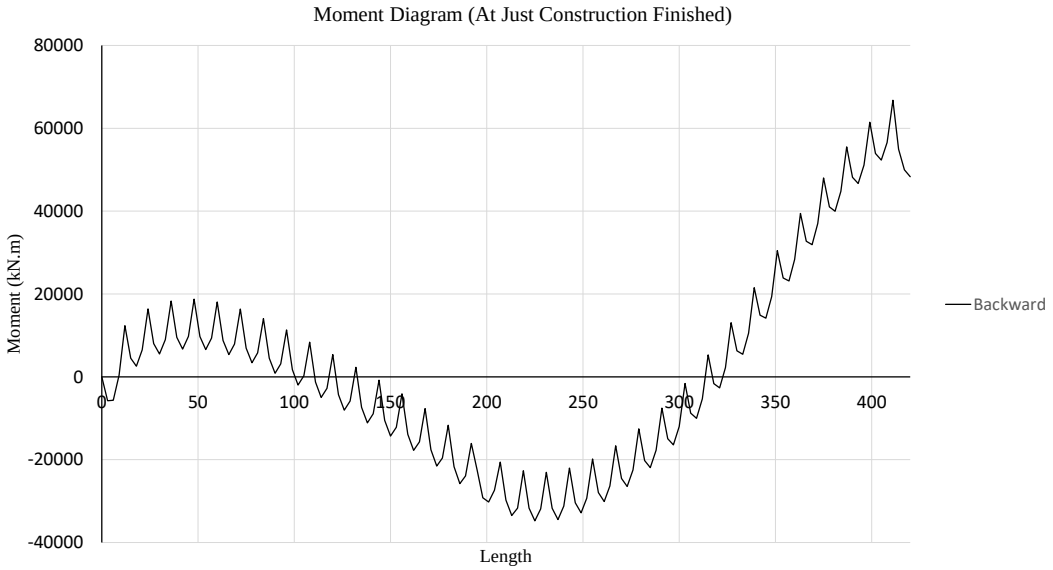

Figure 5.6 Moment Diagram at Which Temperature Given in Backward Direction

After this step, the most crucial part of the analysis came into the picture; dismantling the key segment was done by de-stressing the cables that were anchored to the left and right of the key segment, named M17, M16, and M15. These cable forces were stressed as, at the beginning and end of the element, moment, shear, and axial force effects all became zero, as shown in Figure 5.7. In this way, the key segment can be dismantled. After this critical operation, cables and segments were dismantled in the backward direction one by one. At each process, cable tension forces were obtained. These forces are the forces that should be applied to the cables in the forward direction. Again, not to repeat in this section at the beginning, the moment diagram values are same as the target values, as shown in Figure 5.4.

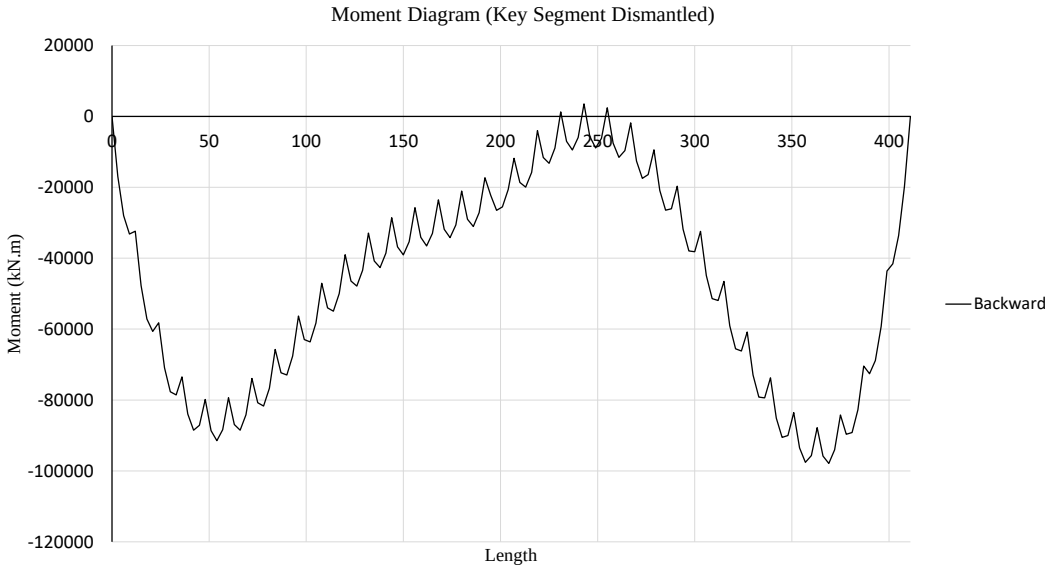

Figure 5.7 Moment Diagram at which Key Segment Was Dismantled in Backward Direction

5.3.2 Forward Construction Stage Analysis

Forward construction stage analysis follows the same sequence as the bridge is constructed at the site, as shown in Figure 5.3. The general and technical explanations of the procedure can be found in Section 4.3.2. In this analysis, cable forces were obtained from the backward analysis, and at each critical step, cable forces were tuned as close to the backward ones as possible. These critical steps are just before and after the key segment was mantled, lowering support at the side span and at time infinity when all creep and shrinkage have occurred. The most important difference between backward and forward analysis comes from the difference in the accumulation of forces and displacements. In backward analysis, all steps are independent of each other, which means the steps do not affect each other and do not have a memory as they should be in the real construction sequence. Contrary to backward analysis, forward analysis has memory which means, as in the real case, forces and displacements are all affected by the previous one at each step until the construction ends, and each of them accumulates in the real-time sequence. This

analysis summed the time-dependent effects of creep and shrinkage as described in CEB- FIP Model Code 1990. In the analysis, these time steps were kept as small as possible to take into effects more realistically and accurately.

5.3.3 Comparison of Backward and Forward Construction Stage Analysis

The bridge system is highly indeterminate, and its indeterminacy can be closely estimated with the number of cables. Therefore, it is very time-consuming to converge to the desired cable forces at the desired time of construction. Up to the point where the support has been jacked, the cable forces were tried to be as close to the backward analysis cable forces, and the moment diagram obtained is shown in Figure 5.8 with the backward moment diagram by using the Larsa 4D verification.

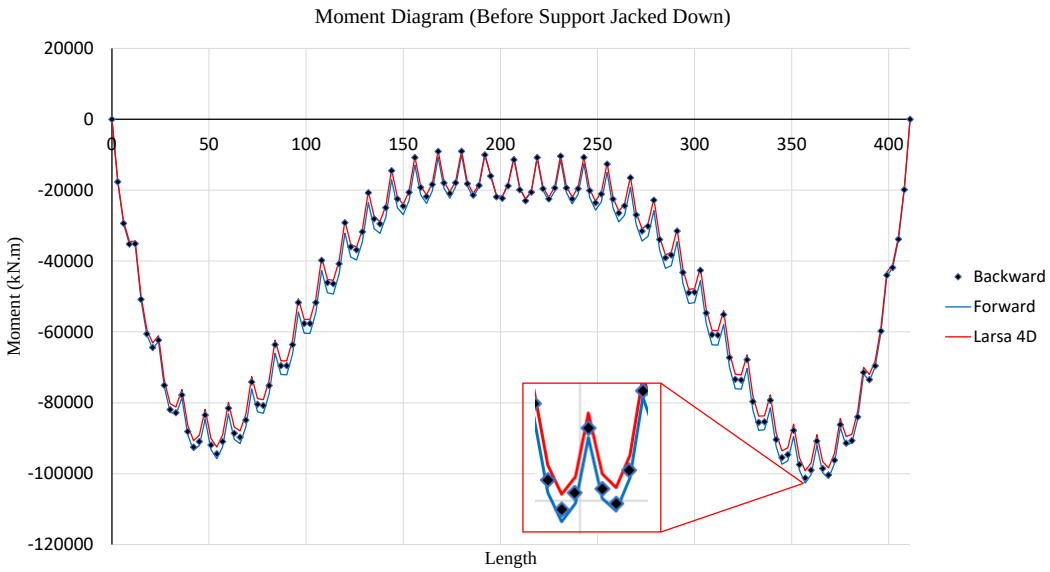

Figure 5.8 Moment Diagram Before Support Was Jacked Down

These results show that both forward analysis results are very close (%8.5) to the backward analysis results, but Larsa 4D has converged very well to the target values. This difference between the two programs can result from how the match casting was achieved, how the time-dependent material properties converged, and how the

geometric nonlinearities were adopted in the analyses. But to conclude, in designing this kind of concrete bridge up to the point where the support has settled down, both backward and forward analysis results can be used safely based on the engineer's judgement.

In the next step, the support at the side span should be installed at the actual place where the construction finished as zero coordinate in the gravity direction. To achieve this target, supports were given support settlement, and the bearings were transferred to the original positions. If this condition was not satisfied, force had been locked in the superstructure, and the system would not converge to the desired values. The resulting moment diagrams of this case can be seen in Figure 5.9.

Figure 5.9 Moment Diagram After Support Was Jacked Down

As seen from these results, it is apparent that both analyses have converged very well to the backward results, but there are small differences (%8.2) in the side span moment. One reason for this is that it stems from the nature of the two different analysis approaches. The accumulation of the moment diagram occurred in the forward analysis, while in the backward analysis, this was not the case, and all results were independent of each other.

In the next step key segment closure forces were calculated such that there would not be any kink at the attached key segment with the previous sections and became tangentially connected. The results can be seen in Figure 5.10.

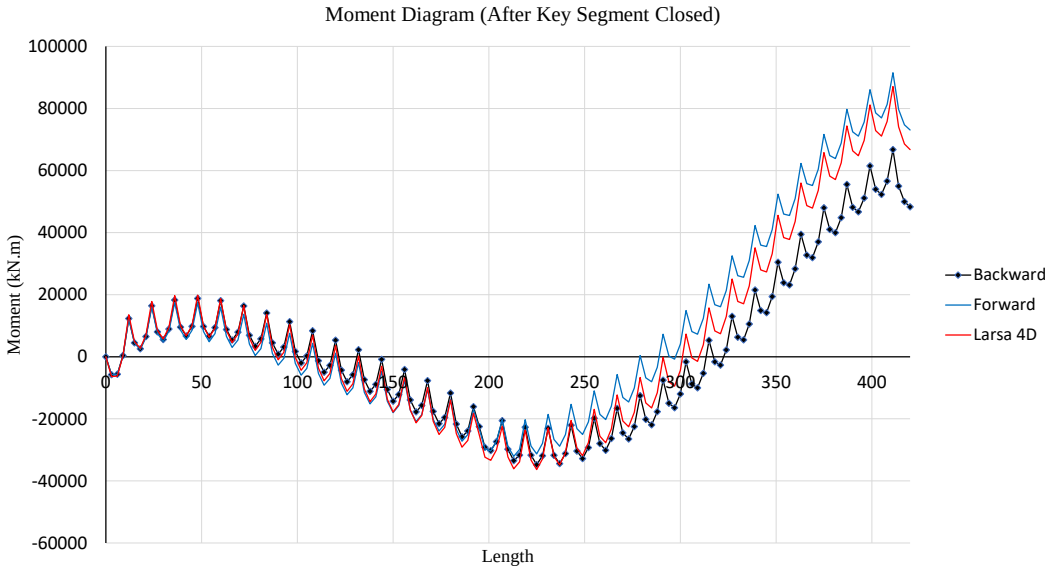

Figure 5.10 Moment Diagram After Key Segment Closed

As expected from the results of Chapter 4, it is seen that after key segment closure, especially in the main span, backward and forward analysis were not exactly matched, but in the side span results are very close (%6) to each other and for each analysis software. This difference occurred, because of indeterminacy, large displacements and accumulation of results in the forward analysis. It is important that especially at the closure of key segment, design engineer should be very careful in designing the cross section, because results especially in the main span scattered considerably despite the cable forces were same in both analysis methods.

In the next step, 25000 days passed from the construction finish time, and all-time dependent effects occurred. As obtained from the results of Chapter 4, it was expected to converge to the results of the beam on rigid supports approach. In the main span, results were closely matched to the target moment diagram, but in the pylon region where sliding bearings were and at the side span, results scattered from the target values.

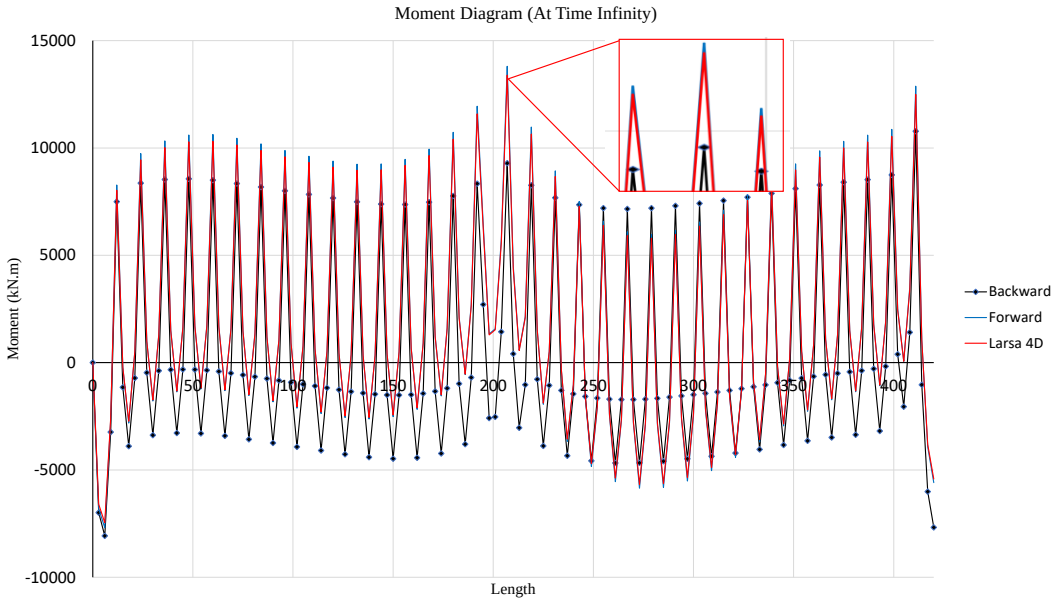

Figure 5.11 Moment Diagram at Time Infinity

The reasons for these differences mainly resulted from the high indeterminacy of the bridge compared to the simple structures investigated in Chapter 4. Other reasons of this difference originated from the philosophy of the analysis methods. In the backward analysis, as stated before, there is no accumulation of the results compared to the forward analysis. Also, P-Δ effects increased the creep deflections which in turn magnified the moments. Another possibility of this difference can be caused by how the time-dependent properties were converted into temperature loading in order to mimic the behavior in the backward analysis.

There are also minor differences (%3) between the results of Midas Civil and Larsa 4D. The main difference arose from the geometric nonlinearity calculation algorithms, as the same time steps were chosen for time-dependent material property calculations, as discussed and approved in Chapter 4.

In order to better investigate how the duration affected the moment diagram at time infinity, 7 days duration for construction time was assumed and applied at the computer model. Results can be seen in Figure 5.12.

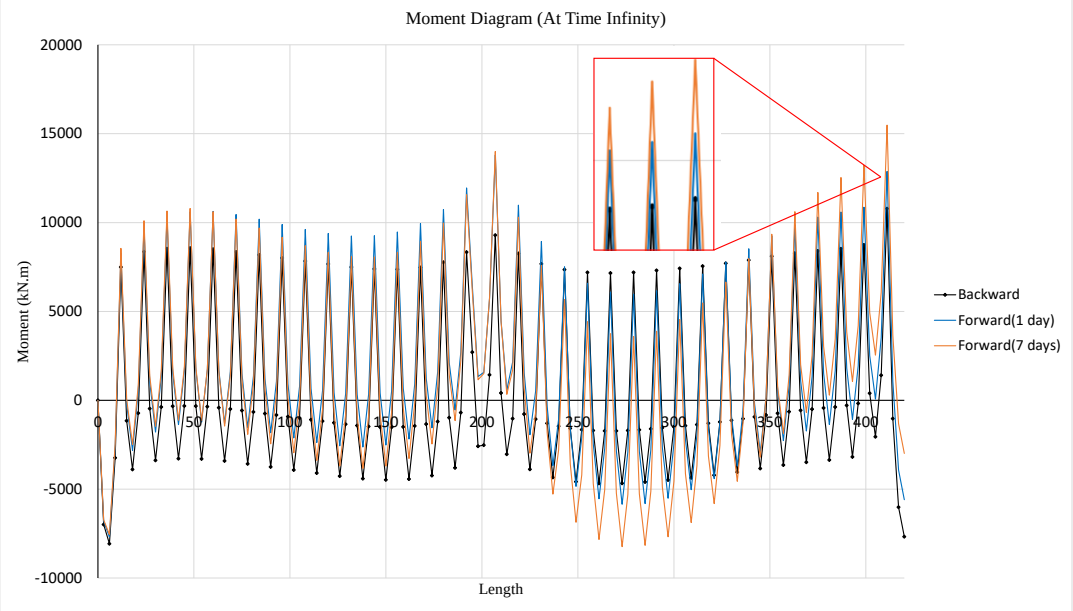

Figure 5.12 Moment Diagram at Time Infinity for 1 Day and 7 Days

Results changed considerably when the duration of the construction between segments was increased from 1 day to 7 days. In 1 day duration time, when using exactly the same cable forces obtained from the backward analysis, moment diagram shown in blue line was close in the side span but scattered from the target values in the main span. In regions close to the pylon, cable forces seemed slightly lower, but in the region close to mid-span, it seemed higher. Therefore, they did not match exactly to each other. When the duration was increased, these differences increased, and the creep effects were observed to be dominant in the analysis. The moment diagram came down in the regions close to the pylon and went up in the regions close to mid-span compared to target moment diagram because of creep. If the same cable forces, obtained in the backward analysis, are used in the cable-stayed bridge design without tuning them, it is not possible to reach the target moment diagram at the end. In the systems in Chapter 4, the system indeterminacy was low compared to the real bridge; therefore, the influences of time-dependent properties were low.

Time-dependent effects can lead to the deformation of a bridge from its intended alignment, disturbing the comfort of passengers and vehicles. To counteract this issue, precamber values must be incorporated during the construction process. These

values need to be carefully calculated; otherwise, the desired outcomes may remain unattainable. Another form of camber, known as the manufacturing camber, comes into play in steel girder bridges. In this analysis, once the bridge is fully constructed, its deflections are mirrored using the desired alignment as a baseline. The mirrored deflection diagram is then utilized as camber values during the manufacturing process in a stress-free environment at the factory.

One of the most critical parameters in cable-stayed bridge construction is the variation in cable forces over time. The shortest and closest cable to the pylon numbered 460 was used for the comparison purposes. As shown in Figure 5.14, the difference in cable forces between two analysis programs is only 0.5%, indicating a high degree of similarity in cable element formulations used by both software. The detailed analysis, which assesses the closeness of the cable element formulations, was explored in Chapter 4.

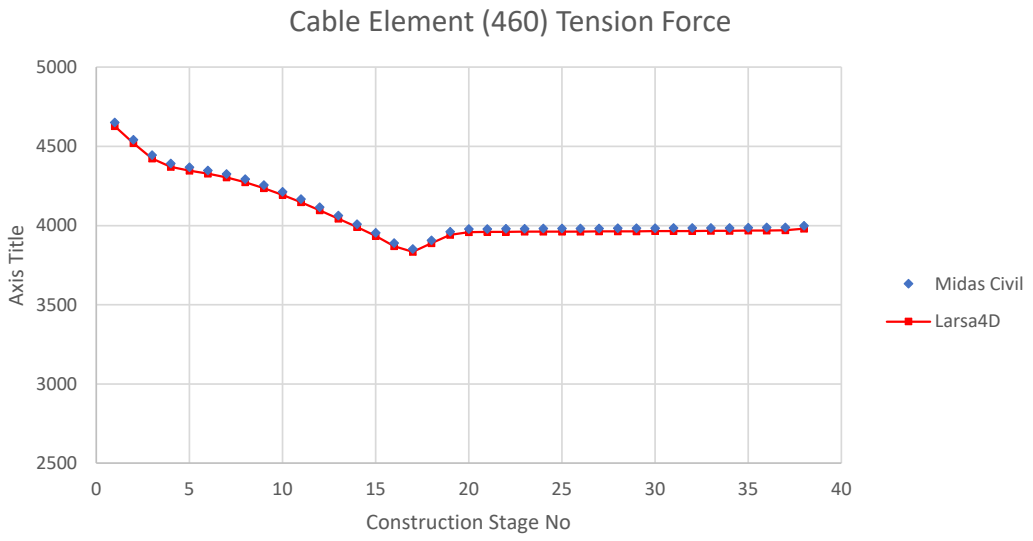

Figure 5.13 Change of Tension Force in Cable (460) During Construction Stages

One of the most crucial parameters that should be monitored during construction is the deflections at the top of the pylon in the horizontal direction. This can provide valuable information regarding whether the cables have been shortened to the correct lengths. Therefore, this comparison offers another method for evaluating cable

formulations in Larsa4D and Midas Civil. In Figure 5.14, it can be concluded that the cable element formulations do not significantly differ from each other; only a 1.1% difference was observed. But accumulation of these small differences caused more scattered moment diagram.

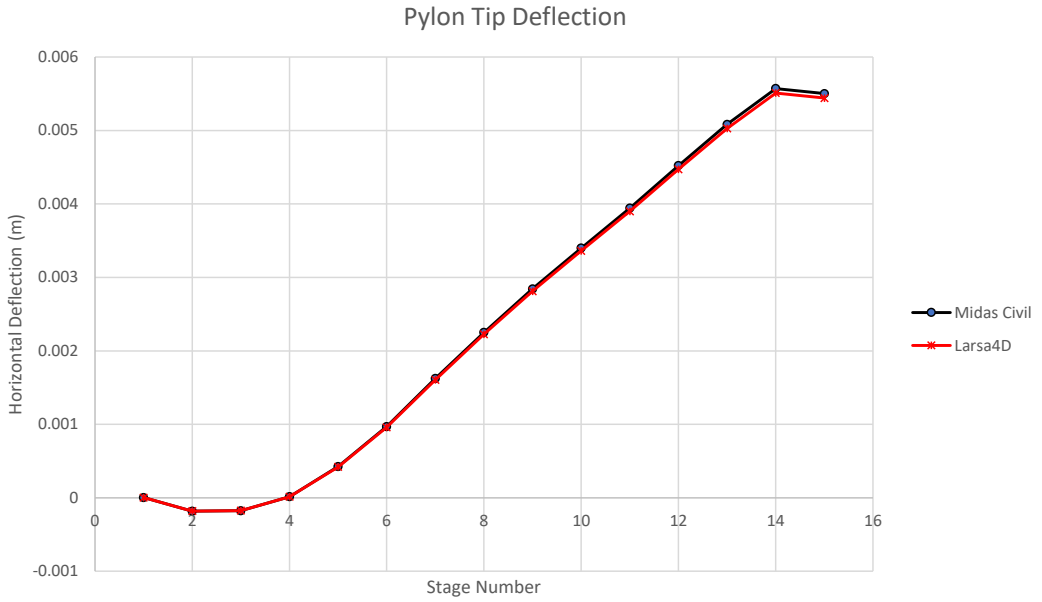

Figure 5.14 Change of Deflection At The Tip of The Pylon During Construction Stages

CHAPTER 6

SUMMARY AND CONCLUSIONS

The main objective of this thesis is to perform a comparative analysis of construction stage results using two distinct approaches: backward and forward analysis. This focus on a comparative assessment sets the current study apart from Svensson's (2012) work, as it directly compares these two approaches. By evaluating and contrasting the outcomes of backward and forward analyses, the thesis seeks to offer insights into the strengths and weaknesses of each method within the context of construction stage analysis for cable-stayed bridges. The ultimate goal is to equip engineers with essential knowledge for applying these two distinct methods in practical bridge projects and interpreting their results accurately.

Firstly, bridges were evaluated according to the spans they pass, and the cable-stayed bridge load transfer mechanism was briefly discussed as the pylon and bridge girder were mainly in compression and bending, and stay cables were in tension.

Then, different types of cable-stayed bridges were introduced. Essential components in all cable-stayed bridges were represented and explained in detail, like pylon shapes, cable anchorages, cables, etc.

In addition, general dimensioning rules for cable-stayed bridges were explained in detail. In order to give a better understanding, flow of forces in this kind of bridge system was investigated. Preliminary basic hand calculations were provided for explanatory purposes. The design strategy of the bridge deck according to different materials was presented. Backward and forward analysis types were introduced, and deeply explained how to conduct construction stage analysis. Lastly, static analysis of cables was presented to cover the topic thoroughly.

Furthermore, as two computer programs, namely Larsa 4D and Midas Civil, were employed in the analysis, a comparison of their capabilities was conducted, focusing

on cable element formulation, geometric nonlinearity, and match casting approaches. Through this comparison, it was noted that the cable element formulation and match casting approaches exhibited consistency with each other. However, discrepancies were identified in the results related to geometric nonlinearity, as explained in the relevant chapter. This disparity is the primary reason why the main bridge bending moment diagrams exhibit variations between the two software applications.

A thorough investigation was conducted on a basic cable-stayed-like structure, intentionally choosing a concrete bridge deck similar to the main bridge. Initially, time-dependent material analyses were omitted to demonstrate that backward and forward analysis results were identical under these conditions. Subsequently, in all following analyses, cable forces were determined through backward analysis based on the target moment diagram at the finished state. These cable forces were then directly applied in the forward analysis. Three types of cable elements were utilized: Linear Truss, Ernst Truss, and Catenary element. The analysis results indicated that all cable elements exhibited similar behavior, and the bending moment diagrams were closely aligned, with a difference of approximately 1.5%.

Following this, time-dependent effects were incorporated. At the completion of the structure, small differences (approximately 6.5%) were observed between the moment diagrams of backward and forward analyses. As expected, with the passage of time and the occurrence of creep and shrinkage, the bending moment diagram gradually approached the target values, consistent with the beam on rigid supports approach. It is essential to note that this investigation was based on a relatively small cable-stayed structure with fewer degrees of indeterminacy compared to real structures.

Based on the results, it was observed that due to the high tension in cable elements, all element types behaved similarly, closely resembling the behavior of catenary elements. Additionally, it was confirmed that the beam on rigid support approach for concrete structures yielded consistent results, as elucidated in the analysis. Therefore, it can be inferred that by adjusting the cable forces to match their vertical

force component with the force that would exist if a roller support were present at that joint, any additional moments due to the effects of creep would likely be mitigated.

Moreover, when the cable tension force is sufficiently high, all types of cable elements exhibit similar behavior in terms of axial rigidity. In the analysis, particularly Ernst and catenary cable elements yielded results close to the target moment diagram for time infinity, with a deviation of approximately 9.8%. The reason the linear truss element did not provide close results was its inability to account for the sag effect, unlike the other two types of elements.

Furthermore, when incorporating time-dependent material effects through temperature loading in backward analysis, the results closely aligned with those obtained using the time step method in forward construction stage analysis for this cable-stayed structure. Additionally, minor variations were observed in moment diagram values (approximately 6.9%) and cable forces (approximately 1.8%) between the Midas Civil and Larsa 4D structural analysis programs. These differences primarily stemmed from how large displacement effects were considered between the two programs.

In summary, the analysis suggests that engineers should exercise caution when employing backward analysis immediately after the construction has finished. The two analysis types may yield different results, which might be intolerable in the design process.

Finally, a real cable-stayed bridge system was selected to validate the results obtained in the previous section. Once again, the target moment diagram based on the beam on rigid supports approach was chosen for the completeness of the analysis. Unlike the structure defined in the previous chapter, the analysis of the real bridge involves some considerations. These include how the end support is lowered to avoid generating additional locked-in forces in the bridge and how the key segment is closed to prevent any kinks in the finished alignment.

In the backward analysis, aiming to simulate the time-dependent material effects from the completion of construction until time infinity, a temperature loading was applied to the superstructure. Until the closure of the key segment with the same cable forces, both backward and forward analyses yielded close results. However, after the key segment was closed, even though the cable forces remained constant, the moment diagrams of forward and backward analyses scattered due to the accumulation of results. Up to this point, forward analysis can be utilized as an upper-bound solution if the bridge is designed using both analysis types simultaneously..

After all time-dependent material effects had occurred, the moment diagram of the forward analysis closely approached the backward analysis moment diagram. However, when the time step between the casting of segments was increased from 1 day to 7 days, the differences between the moment diagrams increased considerably (up to 30%), even with the same cable forces. Therefore, in comparison to a simple system analysis, if a real bridge design is to be conducted, relying solely on backward analysis as a design tool could yield different results from the actual situation.

These results also indicate that as the number of redundancies (indeterminacy) increases, time-dependent effects become more pronounced in the analysis. Hence, it underscores the importance of carefully considering time-dependent material effects and choosing appropriate time steps in the analysis of complex structures, especially in the design of real cable-stayed bridges.

To summarize, it is advisable to use backward analysis to obtain initial estimates of stay cable forces and then perform forward analysis to better consider time-dependent material effects, both in member forces and in calculating camber values. It's worth noting that in small cable-stayed structures, internal forces tend not to deviate significantly from each other, as explained in the relevant chapter. However, as demonstrated in the main bridge example, these differences could increase considerably in the larger scale.

Applying the beam on rigid supports approach helps mitigate additional moments caused by creep effects to a great extent. Engineers should exercise caution when using backward analysis immediately after construction has finished, as the two analysis types can yield different results, which may not be tolerable in the design.

Until key segment closure, both backward and forward analyses yielded very close results. However, due to the accumulation of results, moment diagrams in forward and backward analyses may diverge. Up to this point, forward analysis can serve as an upper-bound solution if the bridge is designed using both analysis types simultaneously. As demonstrated in the real bridge example, an increase in the number of redundancies (indeterminacy) increases the impact of time-dependent effects in the analysis.

For large-scale cable-stayed bridges, it is advisable to use backward analysis for initial estimates of stay cable forces and conduct forward analysis to better account for time-dependent material effects. If the construction duration lengthens, the effects of time-dependent material on girder moments increase considerably. Although Midas and Larsa results were close to each other, obtaining identical results may not be possible due to the different approaches to geometric nonlinearity effects in the two programs. For this reason, in the design of large-scale cable-stayed bridges, using two structural analysis software simultaneously is recommended to ensure comprehensive consideration of details.

The analysis focused exclusively on concrete balanced cantilever cable-stayed bridges, with a comprehensive examination of this specific type. Future studies may explore other bridge superstructures, including composite (steel and concrete) girder types, employing different construction methods, and examining unsymmetric construction for a more comprehensive understanding.

REFERENCES

Arici, M., Granata, M. F., Margiotta, P., & Recupero, A. (2010, January). Creep effects and stress adjustments in cable-stayed bridges with concrete deck. In Proceedings of 3rd fib Conference.

Comité Euro-International du Béton. (1993). CEB-FIP model code 1990: Design code. Thomas Telford Publishing.

Elbadry, M. M., & Ghali, A. (2001). Analysis of time-dependent effects in concrete structures using conventional linear computer programs. Canadian Journal of Civil Engineering, 28(2), 190-200.

El Shenawy, E. A. (2013). Form finding for cable-stayed and extradosed bridges.

Gimsing, N. J., & Georgakis, C. T. (2011). Cable supported bridges: Concept and design. John Wiley & Sons.

Janjic, D., Pircher, M., & Pircher, H. (2003). Optimization of cable tensioning in cable-stayed bridges. Journal of bridge engineering, 8(3), 131-137.

Leonhardt, F., & Zellner, W. (1980). Cable-stayed bridges. IABSE Survey, AIPC Review, IVBH Berichte, 80(S-13/80).

Pipinato, A., Pellegrino, C., & Modena, C. (2012). Structural analysis of the cantilever construction process in cable-stayed bridges. Periodica Polytechnica. Civil Engineering, 56(2), 141.

Roark, R. J. (1975). Young, wc: Formulas for stress and strain.

Schlaich, M. (2001). Erection of cable-stayed bridges having composite decks with precast concrete slabs. Journal of Bridge engineering, 6(5), 333-339.

Song, C., Xiao, R., & Sun, B. (2018). Optimization of cable pre-tension forces in long-span cable-stayed bridges considering the counterweight. Engineering Structures, 172, 919-928.

Svensson, H. S., Christopher, B. G., & Saul, R. (1986). Design of a cable-stayed steel composite bridge. Journal of Structural Engineering, 112(3), 489-504.

Svensson, H. (2013). Cable-stayed bridges: 40 years of experience worldwide. John Wiley & Sons.

Troitsky, M. S. (1977). Cable-stayed bridges. Theory and design (No. Monograph).

Wang, P. H., Tang, T. Y., & Zheng, H. N. (2004). Analysis of cable-stayed bridges during construction by cantilever methods. Computers & Structures, 82(4-5), 329-346.

Virlogeux, M. (2001). Bridges with multiple cable-stayed spans. Structural Engineering International, 11(1), 61-82.

Vu, T. V., Lee, H. E., & Bui, Q. T. (2012). Nonlinear analysis of cable-supported structures with a spatial catenary cable element. Structural Engineering and Mechanics, 43(5), 583-605.

APPENDICES

A. Node Numbering of Basic Concrete Cable-Stayed Structure

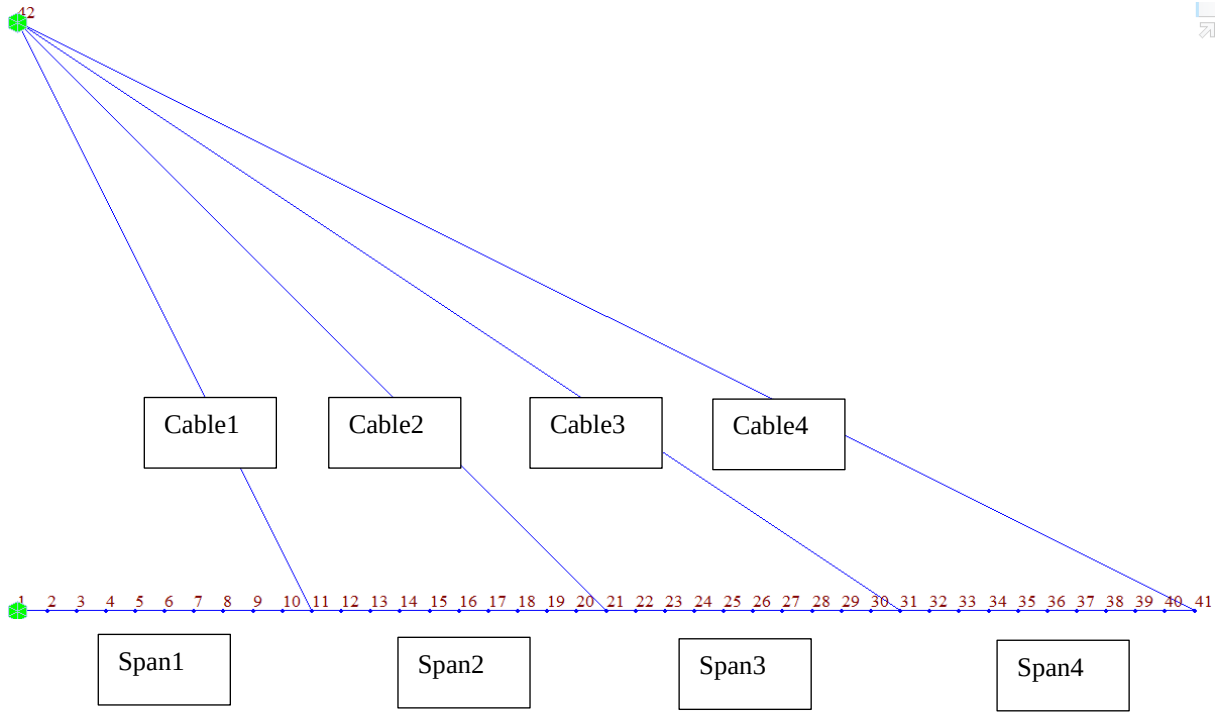

B. Calculation of Modulus of Elasticity, Development of Strength and Modulus of Elasticity with Time, Creep Coefficient and Shrinkage Strain of Concrete Cable-Stayed Structure

Modulus of Elasticity
(CEB-FIP Model Code 1990)

fck =	30	MPa
Δf =	8	MPa
f_{cm0} =	10	MPa
E_{c0} =	2.15E+04	MPa

E_{ci} is the modulus of elasticity (Mpa) at a concrete age of 28 days
f_{ck} is the characteristic strength (Mpa)

$E_{ci} = E_{c0} [(f_{ck} + \Delta f) / f_{cmo}]^{1/3}$ = **3.36E+04 MPa**

Development of Strength with Time
(CEB-FIP Model Code 1990)

s =	0.25	
t =	28	day
f_{ck} =	30	MPa
f_{cm} =	38	MPa
t_1 =	1	day
Δ_f =	8	MPa
$\beta_{cc}(t)$=	1.00	

$f_{cm} = f_{ck} + \Delta f$

$f_{cm}(t) = \beta_{cc}(t) f_{cm}$

$\beta_{cc}(t) = \exp\{s[1 - (28 / (t/t_1)^{1/2}]\}$

$f_{cm}(t)$ is the mean concrete compressive strength at an age ot t days

f_{cm} is the mean compressive strength after 28 days

$\beta_{cc}(t)$ is a coefficient which depends on the age of concrete t

t is the age of concrete

s is a coefficient which depends on the type of cement

0.2 for rapid hardening high strength cements RS

0.25 for normal and rapid hardening cements N and R

0.38 for slowly hardening cements SL

$f_{cm}(t)$ = **38 MPa**

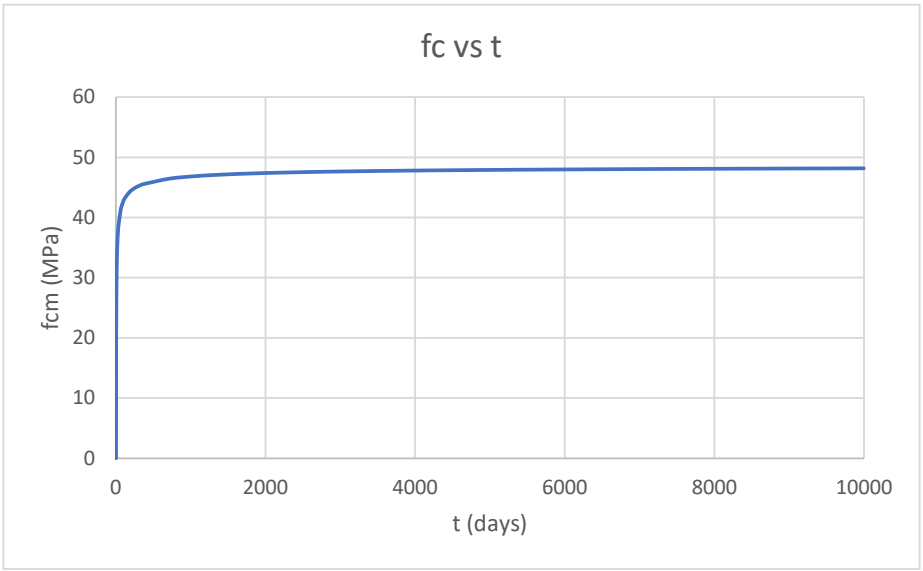

Development of Modulus of Elasticity with Time
(CEB-FIP Model Code 1990)

$\beta_E(t) = [\beta_{cc}(t)]^{0.5}$

$E_{ci}(t) = \beta_E(t)E_{ci}$

$E_{ci}(t)$ is the modulus of elasticity at an age of t days

E_{ci} is the modulus of elasticity at an age of 28 days

$\beta_E(t)$ is a coefficient which depends on the age of concrete t days

$\beta_E(t) =$ 1.00

$E_{ci}(t) =$ **3.36E+04** **MPa**

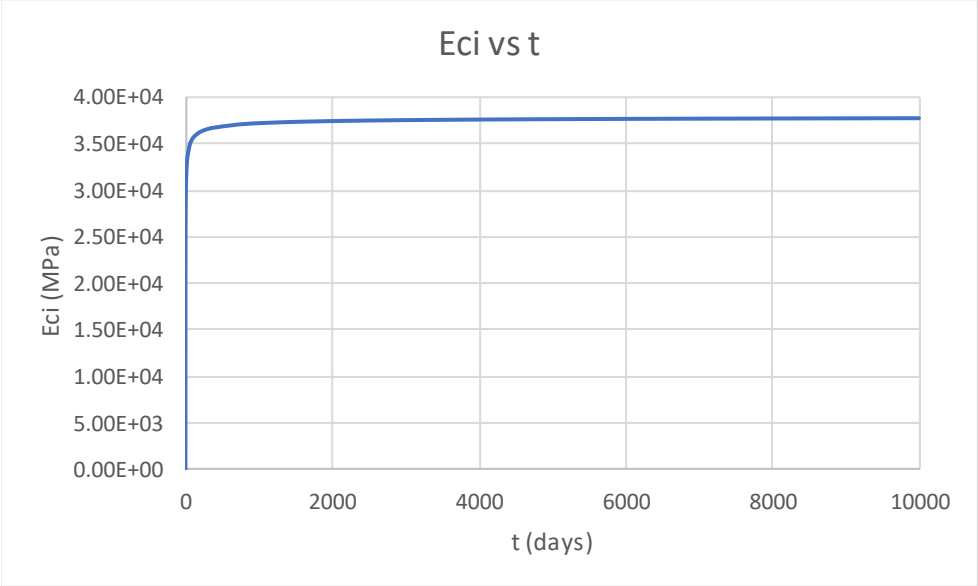

Creep
(CEB-FIP Model Code 1990)

A_c=	2.00E+06	mm^2
u =	6.00E+03	mm
t=	25000	days
RH=	80	%
t_0 =	7	days
$h=2A_c/u$ =	667	mm
f_{cm0} =	10	MPa
RH_0 =	100	%
h_0 =	100	mm
t_1 =	1	day
f_{cm}=	38	MPa

$\phi_{RH} = 1+ (1-RH/RH_0) / (0.46(h/h_0)^{1/3} =$ 1.2310

$\beta(f_{cm}) = 5.3/(f_{cm}/f_{cm0})^{0.5} =$ 2.7188

$\beta(t_0) = 1/ (0.1+(t_0/t_1)^{0.2}) =$ 0.6346

$\beta_c(t-t_0) = [((t-t_o)/t_1)/(\beta_H+(t-t_0)/t_1)]^{0.3} =$ 0.9827

$\beta_H = 150 \{ 1+ (1.2\ RH/RH_0)^{18}\} h/h_0+250 =$ 1500 <=1500

$\varphi_0 = \varphi_{RH}\beta(f_{cm})\beta(t_0) =$ 2.12

$\varphi(t,t_0) = \varphi_0\beta_c(t-t0) =$ **2.1**

φ_0 is the notional creep coefficient

β_c is the coefficient to describe the development of creep with time after loading

t is the age of concrete at the moment in days

t_0 is the age of concrete at loading in days

f_{cm} is the mean compressive strength of concrete at age 28 days in MPa

RH is the relative humidity of the ambient environment (%)

h is the notional size of member in mm where A_c is the cross section and u is the perimeter of the member in contact with the atmosphere

Shrinkage
(CEB-FIP Model Code 1990)

t=	25000	days
t_s =	3	days
β_{sc} =	5	
RH=	80	%
h=$2A_c/u$ =	666.66667	mm
f_{cm0} =	10	MPa
RH_0 =	100	%
h_0 =	100	mm
t_1 =	1	day
f_{cm}=	38	MPa
f_{cm0} =	10	MPa

ε_{cs0} is the notional shrinkage coefficient
β_s is the coefficient to describe the development of shrinkage with time
t is the age of concrete in days
t_s is the age of concrete at the beginning of shrinkage in days
RH is the relative humudity of the ambient atmosphere (%)
f_{cm} is the mean compressive strength of concrete
at the age of 28 days in MPa
β_{sc} is a coefficient which depends on the cement type
β_{sc} = 4 for slowly hardening cements SL
β_{sc} = 5 for normal or rapid hardening cements N and R
β_{sc} = 8 for rapid hardening cements RS

$\beta_{sRH} = 1- (RH/RH_0)^3$ = 0.488

$\beta_{RH} = -1.55\ \beta_{sRH}$ for 40%<=RH<99% = -0.756

β_{RH} = 0.25 for RH >= 99%

$\varepsilon_s(f_{cm}) = [160 + 10\beta_{sc}(9 - f_{cm}/f_{cm0})] \times 10^{-6} =$ 0.000420

$\beta_s(t-t_s) = [((t-t_s)/t_1) / (350(h/h_0)^2 + (t-t_s)/t_1)]^{0.5} =$ 0.78512

$\varepsilon_{cs0} = \varepsilon_s(f_{cm})\beta_{RH} =$ -0.000318

$\varepsilon_{cs}(t,t_s) = \varepsilon_{cs0}\beta_s(t-t_s) =$ **-0.000249**

C. Calculation of Temperature Loading Values of Concrete Cable-Stayed Structure To Take into Account Time-Dependent Material Properties

	Span1	Span2	Span3	Span4
Duration of Construction (days)	1	1	1	1
N (kN)	8043	7026	5076	1620
A (m2)	2	2	2	2
E (kPa)	3.50E+07	3.50E+07	3.50E+07	3.50E+07
$\sigma = N / A$ (kPa)	4021.5	3513	2538	810
$\varepsilon = \sigma / E$	0.000115	0.000100	0.000073	0.000023
φ	2.1	2.1	2.1	2.1
$\varphi \times \varepsilon$	0.000241	0.000211	0.000152	0.000049
ε shrinkage	0.000249	0.000249	0.000249	0.000249
$\Sigma \varepsilon$	0.000490	0.000460	0.000401	0.000298
α	1.00E-05	1.00E-05	1.00E-05	1.00E-05
$\Delta T = \Sigma \varepsilon / \alpha$ (degree)	49.03	45.98	40.13	29.76

N = Axial load in the corresponding span
A = Area of the girder cross section
E = Modulus of elasticity
σ = Axial stress in the girder of the corresponding span
ε = Axial strain in the girder of the corresponding span
φ = Creep coefficient (Appendix C)
ε shrinkage = shrinkage strain
α = Coefficient of thermal expansion
ΔT = Equivalent temperature increase in order to take into account time-dependent material properties

D. Cross Sectional Properties of Girder and Cables

	H(m)	B(m)	Area (m^2)	Asy(m^2)	Asz(m^2)	Ixx(m^4)	Iyy(m^4)	Izz(m^4)
Girder	3,5	38	26,25	18,68	3,84	1,83E+02	5,78E+01	2,85E+03
Pylon (1 leg)	7	8	32,24	20,8	18,2	3,06E+02	1,90E+02	2,41E+02
CableM1	-	-	1,20E-02	-	-	-	-	-
CableM2	-	-	1,01E-02	-	-	-	-	-
CableM3	-	-	1,01E-02	-	-	-	-	-
CableM4	-	-	1,01E-02	-	-	-	-	-
CableM5	-	-	1,20E-02	-	-	-	-	-
CableM6	-	-	1,20E-02	-	-	-	-	-
CableM7	-	-	1,46E-02	-	-	-	-	-
CableM8	-	-	1,46E-02	-	-	-	-	-
CableM9	-	-	1,46E-02	-	-	-	-	-
CableM10	-	-	1,73E-02	-	-	-	-	-
CableM11	-	-	1,52E-02	-	-	-	-	-
CableM12	-	-	1,73E-02	-	-	-	-	-
CableM13	-	-	1,73E-02	-	-	-	-	-
CableM14	-	-	1,73E-02	-	-	-	-	-
CableM15	-	-	1,79E-02	-	-	-	-	-
CableM16	-	-	1,79E-02	-	-	-	-	-
CableM17	-	-	1,79E-02	-	-	-	-	-
CableS1	-	-	1,01E-02	-	-	-	-	-
CableS2	-	-	1,01E-02	-	-	-	-	-
CableS3	-	-	1,01E-02	-	-	-	-	-
CableS4	-	-	1,01E-02	-	-	-	-	-
CableS5	-	-	1,20E-02	-	-	-	-	-
CableS6	-	-	1,20E-02	-	-	-	-	-
CableS7	-	-	1,46E-02	-	-	-	-	-
CableS8	-	-	1,46E-02	-	-	-	-	-
CableS9	-	-	1,46E-02	-	-	-	-	-
CableS10	-	-	1,52E-02	-	-	-	-	-
CableS11	-	-	1,52E-02	-	-	-	-	-
CableS12	-	-	1,73E-02	-	-	-	-	-
CableS13	-	-	1,73E-02	-	-	-	-	-
CableS14	-	-	1,73E-02	-	-	-	-	-
CableS15	-	-	1,79E-02	-	-	-	-	-
CableS16	-	-	1,79E-02	-	-	-	-	-
CableS17	-	-	1,79E-02	-	-	-	-	-

Girder and Pylon were modeled by using beam elements each divided into 4 elements. Cables were modeled as catenary elements which took into account full nonlinearity in the analysis. Coordinates of one Pylon was shown in the below table. Other pylon is the symmetric of these coordinates.

Node Number	X (m)	Y (m)	Z (m)
290	8.5	16.86943	139.024
291	8.5	16.07225	143.024
294	8.5	14.6396	150.2193
295	8.5	13.99047	153.4693
296	8.5	12.04307	163.2193
297	8.5	11.39394	166.4693
298	8.5	9.746142	174.7193
299	8.5	9.266783	177.1193
300	8.5	7.828704	184.3193
301	8.5	7.369318	186.6193
302	8.5	6.011214	193.4189
303	8.5	5.429857	196.424
406	8.5	-6.01121	193.4189
407	8.5	-6.46053	191.1693
414	8.5	-7.8287	184.3193
415	8.5	-8.30577	181.9193
416	8.5	-9.74614	174.7193
417	8.5	-10.2455	172.2193
418	8.5	-12.0431	163.2193
419	8.5	-12.6922	159.9693
420	8.5	-14.6396	150.2193
424	8.5	-16.0723	143.024
425	8.5	-16.8694	139.024
426	8.5	-19.1091	127.786
427	8.5	-19.9063	123.786
428	8.5	-22.2979	111.786
429	8.5	-23.095	107.786
430	8.5	-25.4866	95.786
431	8.5	-26.2838	91.786
432	8.5	-28.3312	81.51
433	8.5	-26.5396	74.5
434	8.5	-28.0825	80.53692
435	8.5	-27.4563	78.087
436	8.5	-23.8562	64
437	8.5	-22.9617	60.5
438	8.5	-19.8949	48.5

Node Number	X (m)	Y (m)	Z (m)
439	8.5	-18.8727	44.5
440	8.5	-15.8059	32.5
441	8.5	-14.7836	28.5
442	8.5	-11.7168	16.5
443	8.5	-10.6946	12.5
444	8.5	-7.5	0
497	8.5	14.78362	28.5
499	8.5	17.8504	40.5
503	8.5	21.93945	56.5
504	8.5	27.45634	78.087
505	8.5	26.53963	74.5
506	8.5	25.48658	95.786
507	8.5	23.09504	107.786
508	8.5	19.10912	127.786
548	8.5	15.80588	32.5
549	8.5	16.82814	36.5
552	8.5	19.89493	48.5
553	8.5	20.91719	52.5
554	8.5	23.85619	64
555	8.5	24.75067	67.5
556	8.5	28.08246	80.53692
558	8.5	27.87813	83.786
559	8.5	27.08095	87.786
560	8.5	24.6894	99.786
561	8.5	23.89222	103.786
562	8.5	21.50067	115.786
563	8.5	20.70349	119.786
564	8.5	18.38408	131.424
565	8.5	17.5869	135.424
566	8.5	15.27507	147.024
568	8.5	9.715251	174.874
570	8.5	13.34134	156.7193
571	8.5	12.69221	159.9693
572	8.5	10.79474	169.4693
573	8.5	10.24548	172.2193
574	8.5	8.787423	179.5193

Node Number	X (m)	Y (m)	Z (m)
575	8.5	8.30577	181.9193
576	8.5	6.909932	188.9193
577	8.5	6.460532	191.1693
579	8.5	10.69457	12.5
617	8.5	-5.42986	196.424
620	8.5	-6.90993	188.9193
621	8.5	-7.36932	186.6193
622	8.5	-8.78742	179.5193
623	8.5	-9.26678	177.1193
624	8.5	-10.7947	169.4693
625	8.5	-11.3939	166.4693
626	8.5	-13.3413	156.7193
627	8.5	-13.9905	153.4693
629	8.5	-9.71525	174.874
631	8.5	-15.2751	147.024
632	8.5	-17.5869	135.424
633	8.5	-18.3841	131.424
634	8.5	-20.7035	119.786
635	8.5	-21.5007	115.786
636	8.5	-23.8922	103.786
637	8.5	-24.6894	99.786
638	8.5	-27.081	87.786
639	8.5	-27.8781	83.786
642	8.5	-25.6452	71
643	8.5	-24.7507	67.5
644	8.5	-21.9395	56.5
645	8.5	-20.9172	52.5
646	8.5	-17.8504	40.5
647	8.5	-16.8281	36.5
648	8.5	-13.7614	24.5
649	8.5	-12.7391	20.5
650	8.5	-9.67231	8.5
651	8.5	-8.65005	4.5
673	8.5	7.5	0
674	8.5	18.87267	44.5
678	8.5	22.96171	60.5
679	8.5	25.64515	71

Node Number	X (m)	Y (m)	Z (m)
680	8.5	28.33122	81.51
681	8.5	26.28377	91.786
682	8.5	22.29785	111.786
683	8.5	19.9063	123.786
684	8.5	11.71683	16.5
685	8.5	12.73909	20.5
686	8.5	13.76136	24.5
687	8.5	9.672307	8.5
688	8.5	8.650045	4.5

E. Calculation of Modulus of Elasticity, Development of Strength and Modulus of Elasticity with Time, Creep Coefficient and Shrinkage Strain of Concrete Cable-Stayed Bridge

Modulus of Elasticity
(CEB-FIP Model Code 1990)

fck =	50	MPa
Δf =	8	MPa
f_{cm0} =	10	MPa
E_{c0} =	2.15E+04	MPa

E_{ci} is the modulus of elasticity (Mpa) at a concrete age of 28 days
f_{ck} is the characteristic strength (Mpa)

$E_{ci} = E_{c0} [(f_{ck} + \Delta f) / f_{cmo}]^{1/3}$ = **3.86E+04 MPa**

Development of Strength with Time
(CEB-FIP Model Code 1990)

s =	0.25	
t =	28	day
f_{ck} =	50	MPa
f_{cm} =	58	MPa
t_1 =	1	day
Δ_f =	8	MPa
$\beta_{cc}(t)$=	1.00	

$f_{cm} = f_{ck} + \Delta f$

$f_{cm}(t) = \beta_{cc}(t) f_{cm}$

$\beta_{cc}(t) = \exp\{s[1 - (28 / (t/t_1)^{1/2}]\}$

$f_{cm}(t)$ is the mean concrete compressive strength at an age ot t days

f_{cm} is the mean compressive strength after 28 days

$\beta_{cc}(t)$ is a coefficient which depends on the age of concrete t

t is the age of concrete

s is a coefficient which depends on the type of cement

0.2 for rapid hardening high strength cements RS

0.25 for normal and rapid hardening cements N and R

0.38 for slowly hardening cements SL

$f_{cm}(t)$ = **58 MPa**

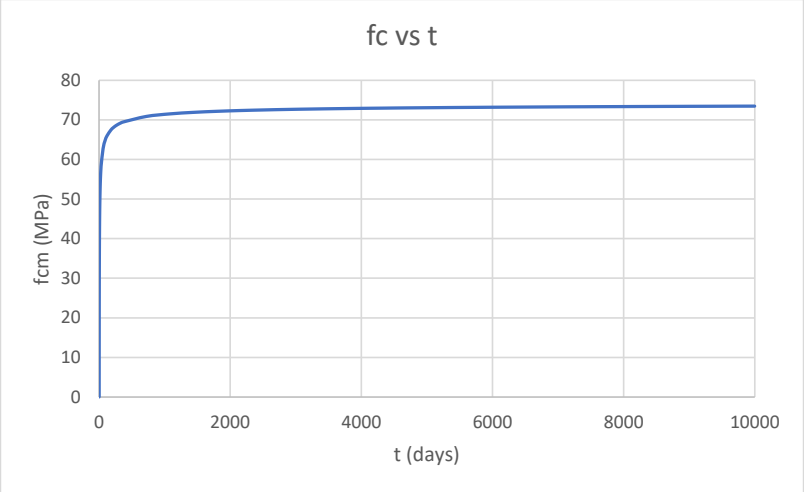

Development of Modulus of Elasticity with Time
(CEB-FIP Model Code 1990)

$\beta_E(t) = [\beta_{cc}(t)]^{0.5}$

$E_{ci}(t) = \beta_E(t)E_{ci}$

$E_{ci}(t)$ is the modulus of elasticity at an age of t days
E_{ci} is the modulus of elasticity at an age of 28 days
$\beta_E(t)$ is a coefficient which depends on the age of concrete t days

$\beta_E(t) =$ 1.00
$E_{ci}(t) =$ **3.86E+04** **MPa**

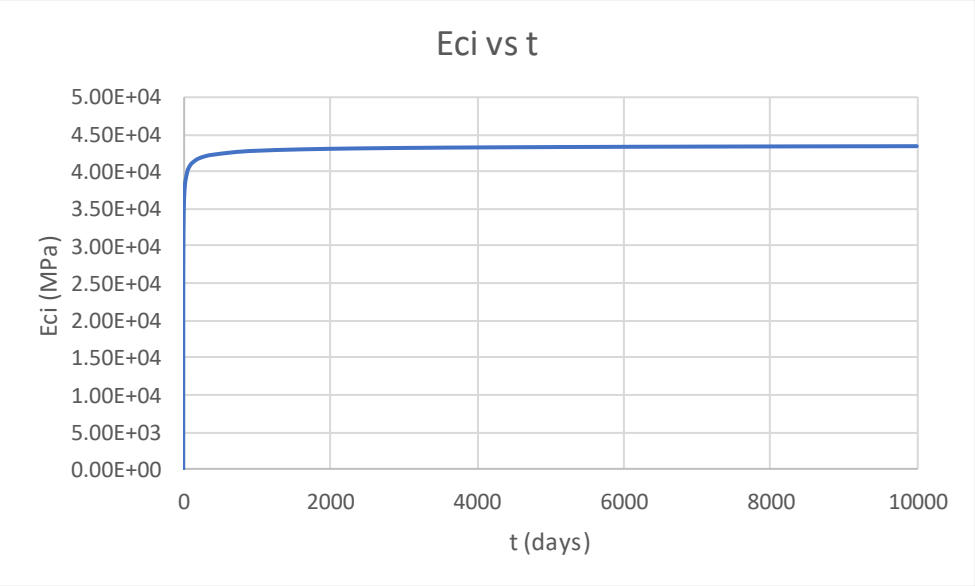

Creep
(CEB-FIP Model Code 1990)

A_c=	2.63E+07	mm^2
u =	8.16E+04	mm
t=	25000	days
RH=	80	%
t_0 =	7	days
$h=2A_c/u$ =	643	mm
f_{cm0} =	10	MPa
RH_0 =	100	%
h_0 =	100	mm
t_1 =	1	day
f_{cm}=	58	MPa

$\phi_{RH} = 1+ (1-RH/RH_0) / (0.46(h/h_0)^{1/3}$ = 1.2338

$\beta(f_{cm}) = 5.3/(f_{cm}/f_{cm0})^{0.5}$ = 2.2007

$\beta(t_0) = 1/ (0.1+(t_0/t_1)^{0.2})$ = 0.6346

$\beta_c(t-t_0) = [((t-t_o)/t_1)/(\beta_H+(t-t_0)/t_1)]^{0.3}$ = 0.9827

$\beta_H = 150 \{ 1+ (1.2\ RH/RH_0)^{18}\} h/h_0+250$ = 1500 <=1500

$\varphi_0 = \varphi_{RH}\beta(f_{cm})\beta(t_0)$ = 1.72

$\varphi(t,t_0) = \varphi_0\beta_c(t-t0)$= **1.7**

φ_0 is the notional creep coefficient

β_c is the coefficient to describe the development of creep with time after loading

t is the age of concrete at the moment in days

t_0 is the age of concrete at loading in days

f_{cm} is the mean compressive strength of concrete at age 28 days in MPa

RH is the relative humidity of the ambient environment (%)

h is the notional size of member in mm where A_c is the cross section and u is the perimeter of the member in contact with the atmosphere

Shrinkage
(CEB-FIP Model Code 1990)

t=	25000	days
t_s =	3	days
β_{sc} =	5	
RH=	80	%
h=2A_c/u =	643.41139	mm
f_{cm0} =	10	MPa
RH_0 =	100	%
h_0 =	100	mm
t_1 =	1	day
f_{cm}=	58	MPa
f_{cm0} =	10	MPa

ε_{cs0} is the notional shrinkage coefficient
β_s is the coefficient to describe the development of shrinkage with time
t is the age of concrete in days
t_s is the age of concrete at the beginning of shrinkage in days
RH is the relative humudity of the ambient atmosphere (%)
f_{cm} is the mean compressive strength of concrete
at the age of 28 days in MPa
β_{sc} is a coefficient which depends on the cement type
β_{sc} = 4 for slowly hardening cements SL
β_{sc} = 5 for normal or rapid hardening cements N and R
β_{sc} = 8 for rapid hardening cements RS

$\beta_{sRH} = 1- (RH/RH_0)^3$ = 0.488

$\beta_{RH} = -1.55\ \beta_{sRH}$ for 40%<=RH<99% = -0.756

β_{RH} = 0.25 for RH >= 99%

$\varepsilon_s(f_{cm}) = [160 + 10\beta_{sc}(9 - f_{cm}/f_{cm0})] \times 10^{-6} =$ 0.000320

$\beta_s(t-t_s) = [((t-t_s)/t_1) / (350(h/h_0)^2 + (t-t_s)/t_1)]^{0.5} =$ 0.79565

$\varepsilon_{cs0} = \varepsilon_s(f_{cm})\beta_{RH} =$ -0.000242

$\varepsilon_{cs}(t,t_s) = \varepsilon_{cs0}\beta_s(t-t_s) =$ **-0.000193**

F. Calculation of Temperature Loading Values of Concrete Cable-Stayed Bridge To Take into Account Time-Dependent Material Properties in Backward Analysis for One Day Duration

	SpanM1	SpanM2	SpanM3	SpanM4	SpanM5	SpanM6	SpanM7	SpanM8	SpanM9	SpanM10	SpanM11	SpanM12	SpanM13	SpanM14	SpanM15	SpanM16	SpanM17
Duration of Construction (days)	1	1	1	1	1	1	1	1	1	1	1	1	1	1	1	1	1
N (kN)	164436	162911	160010	155857	150562	144210	136893	128632	119486	109481	98637	87003	74562	61398	47527	32978	0
A (m2)	26.3	26.3	26.3	26.3	26.3	26.3	26.3	26.3	26.3	26.3	26.3	26.3	26.3	26.3	26.3	26.3	26.3
E (kPa)	3.39E+07	3.39E+07	3.39E+07	3.39E+07	3.39E+07	3.39E+07	3.39E+07	3.39E+07	3.39E+07	3.39E+07	3.39E+07	3.39E+07	3.39E+07	3.39E+07	3.39E+07	3.39E+07	3.39E+07
σ = N / A (kPa)	6263.7	6205.6	6095.1	5936.9	5735.2	5493.2	5214.5	4899.8	4551.4	4170.3	3757.3	3314.1	2840.2	2338.8	1810.4	1256.2	0.0
ε = σ / E	0.000185	0.000183	0.000180	0.000175	0.000169	0.000162	0.000154	0.000144	0.000134	0.000123	0.000111	0.000098	0.000084	0.000069	0.000053	0.000037	0.000000
φ	1.7	1.7	1.7	1.7	1.7	1.7	1.7	1.7	1.7	1.7	1.7	1.7	1.7	1.7	1.7	1.7	1.7
φ x ε	0.000314	0.000311	0.000305	0.000297	0.000287	0.000275	0.000261	0.000245	0.000228	0.000209	0.000188	0.000166	0.000142	0.000117	0.000091	0.000063	0.000000
ε shrinkage	0.000193	0.000193	0.000193	0.000193	0.000193	0.000193	0.000193	0.000193	0.000193	0.000193	0.000193	0.000193	0.000193	0.000193	0.000193	0.000193	0.000193
Σ ε	0.000507	0.000504	0.000498	0.000490	0.000480	0.000468	0.000454	0.000438	0.000421	0.000402	0.000381	0.000359	0.000335	0.000310	0.000284	0.000256	0.000193
α	1.00E-05	1.00E-05	1.00E-05	1.00E-05	1.00E-05	1.00E-05	1.00E-05	1.00E-05	1.00E-05	1.00E-05	1.00E-05	1.00E-05	1.00E-05	1.00E-05	1.00E-05	1.00E-05	1.00E-05
ΔT = Σ ε / α (degree)	50.7	50.4	49.8	49.0	48.0	46.8	45.4	43.8	42.1	40.2	38.1	35.9	33.5	31.0	28.4	25.6	19.3

	SpanS1	SpanS2	SpanS3	SpanS4	SpanS5	SpanS6	SpanS7	SpanS8	SpanS9	SpanS10	SpanS11	SpanS12	SpanS13	SpanS14	SpanS15	SpanS16	SpanS17
Duration of Construction (days)	1	1	1	1	1	1	1	1	1	1	1	1	1	1	1	1	1
N (kN)	164435	162913	160012	155860	150566	144214	136898	128636	119489	109480	98631	86992	74544	61371	47481	32812	16553
A (m2)	26.3	26.3	26.3	26.3	26.3	26.3	26.3	26.3	26.3	26.3	26.3	26.3	26.3	26.3	26.3	26.3	26.3
E (kPa)	3.39E+07	3.39E+07	3.39E+07	3.39E+07	3.39E+07	3.39E+07	3.39E+07	3.39E+07	3.39E+07	3.39E+07	3.39E+07	3.39E+07	3.39E+07	3.39E+07	3.39E+07	3.39E+07	3.39E+07
σ = N / A (kPa)	6263.6	6205.7	6095.2	5937.0	5735.3	5493.4	5214.7	4900.0	4551.6	4170.3	3757.0	3313.7	2839.5	2337.7	1808.6	1249.9	630.5
ε = σ / E	0.000185	0.000183	0.000180	0.000175	0.000169	0.000162	0.000154	0.000144	0.000134	0.000123	0.000111	0.000098	0.000084	0.000069	0.000053	0.000037	0.000019
φ	1.7	1.7	1.7	1.7	1.7	1.7	1.7	1.7	1.7	1.7	1.7	1.7	1.7	1.7	1.7	1.7	1.7
φ x ε	0.000314	0.000311	0.000305	0.000297	0.000287	0.000275	0.000261	0.000245	0.000228	0.000209	0.000188	0.000166	0.000142	0.000117	0.000091	0.000063	0.000032
ε shrinkage	0.000193	0.000193	0.000193	0.000193	0.000193	0.000193	0.000193	0.000193	0.000193	0.000193	0.000193	0.000193	0.000193	0.000193	0.000193	0.000193	0.000193
Σ ε	0.000507	0.000504	0.000498	0.000490	0.000480	0.000468	0.000454	0.000438	0.000421	0.000402	0.000381	0.000359	0.000335	0.000310	0.000284	0.000256	0.000225
α	1.00E-05	1.00E-05	1.00E-05	1.00E-05	1.00E-05	1.00E-05	1.00E-05	1.00E-05	1.00E-05	1.00E-05	1.00E-05	1.00E-05	1.00E-05	1.00E-05	1.00E-05	1.00E-05	1.00E-05
ΔT = Σ ε / α (degree)	50.7	50.4	49.8	49.0	48.0	46.8	45.4	43.8	42.1	40.2	38.1	35.9	33.5	31.0	28.4	25.6	22.5